Hydration of C$_3$A with Calcium Sulfate Alone and in the Presence of Calcium Silicate

THÈSE N^O 5035 (2011)

PRÉSENTÉE LE 20 MAI 2011
À LA FACULTÉ SCIENCES ET TECHNIQUES DE L'INGÉNIEUR
LABORATOIRE DES MATÉRIAUX DE CONSTRUCTION
PROGRAMME DOCTORAL EN SCIENCE ET GÉNIE DES MATÉRIAUX

ÉCOLE POLYTECHNIQUE FÉDÉRALE DE LAUSANNE

POUR L'OBTENTION DU GRADE DE DOCTEUR ÈS SCIENCES

PAR

Alexandra QUENNOZ

acceptée sur proposition du jury:

Prof. M. Rappaz, président du jury
Prof. K. Scrivener, directrice de thèse
Dr P. Bowen, rapporteur
Dr S. Garrault, rapporteur
Dr E. Gartner, rapporteur

EPFL

ÉCOLE POLYTECHNIQUE
FÉDÉRALE DE LAUSANNE

Suisse
2011

ABSTRACT

Tricalcium aluminate (C_3A) is one of the main constituents of Portland cement. Even though it represents less than 10% of the total composition, its strong reaction with water can lead to a rapid setting, called flash set. Gypsum is added to regulate this reaction and preserves the workability of the cement paste at early ages. The understanding of the C_3A-gypsum reaction is therefore crucial for the comprehension of the early hydration of cement. The role of the amount of C_3A and the sulfate balance o cement hydration are of major interest since two important routes for the development of new cementitious materials are the increasing rate of substitution materials and the increasing level of aluminate in clinker.

This thesis aimed to investigate the C_3A – gypsum reaction alone and in the presence of alite in order to provide basic knowledge on the C_3A-gypsum reactions and study the interactions that occur between the cement phases when hydration occurs in alite-C_3A-gypsum systems. Alite and C_3A as well as clinkers of controlled composition were synthesized. Model systems composed of C_3A with different gypsum additions and alite-C_3A-gypsum systems were studied in terms of hydration kinetics, phase assemblage and microstructural development.

This work confirmed the findings of previous works on the mechanism that controls C_3A-gypsum hydration when sulfate ions are present in solution and gave new results on the reaction when gypsum is depleted. It was shown that AFm phases do not crystallize only as platelets that fill the space between the C_3A grains but also form an "inner" product within the original C_3A grain boundaries and that hydrogarnet (for which the presence depends on the gypsum addition) crystallizes as a rim around C_3A grains. Moreover the influence of the gypsum addition on the morphology of the AFm platelets and the role of their morphology on the hydration rate were highlighted. In the presence of alite the hydration kinetics of C_3A-gypsum systems was subject to change due to the adsorption of sulfate ions on C-S-H and the reduction of the space available for the reaction. In addition, with the correlation of calorimetric, XRD and SEM analyses it was possible to observe a second formation of ettringite from C_3A and sulfate ions released from C-S-H after the depletion of gypsum. Finally, the rate of alite hydration related to the growth of C-S-H was shown to be modified in the presence of C_3A and gypsum.

Keywords: phase synthesis; C_3A; gypsum; model cements; hydration kinetics; microstructure

RÉSUMÉ

L'aluminate tricalcique (C$_3$A) est l'un des constituants principaux du ciment. Bien qu'il ne corresponde qu'à 10% de la composition totale du ciment, sa forte réactivité avec l'eau peut conduire à une prise trop rapide de l'ouvrage. Des sulfates de calcium, dont le gypse, sont ajoutés au clinker pour réguler la réaction du C$_3$A et préserver l'ouvrabilité. L'étude de la réaction C$_3$A-gypse est donc fondamentale pour la compréhension de l'hydratation du ciment à jeune âge. De plus, le rôle de la teneur en C$_3$A du ciment et de la balance des sulfates dans l'hydratation du ciment présente un intérêt majeur car deux perspectives de développement de nouveaux matériaux cimentaires sont l'augmentation des additions minérales et de la teneur en aluminates du clinker.

Ce travail de thèse s'est intéressé dans un premier temps à l'étude de la réaction C$_3$A-gypse. Dans un second temps, cette même réaction a été étudiée dans des mélanges modèles composés d'alite, C$_3$A et gypse afin d'identifier les diverses interactions qui ont lieu entre les différentes phases du ciment lors de l'hydratation.

Ce travail a confirmé les conclusions d'études précédentes sur les mécanismes qui contrôlent la cinétique d'hydratation des systèmes C$_3$A-gypse lorsque les ions sulfates sont présents en solution et a apporté de nouveaux résultats sur la réaction après la consommation du gypse. Il a été observé que les phases AFm ne cristallisent pas seulement dans l'espace entre les grains de C$_3$A mais qu'un produit d'hydratation « inner » se forme également. De plus, lorsque l'hydrogrenat est présent cette phase a été observée formant une couche d'hydrate à la surface des grains de C$_3$A. Par ailleurs, il a été démontré que la morphologie des feuillets d'AFm dépend de la quantité de gypse initial du mélange et que cette même morphologie influence la cinétique de la réaction. En présence d'alite, la cinétique d'hydratation du mélange C$_3$A-gypse est modifiée de manière importante en raison de l'adsorption des ions sulfates sur les C-S-H et de la diminution de l'espace disponible pour la réaction. Grâce à la corrélation des résultats obtenus par calorimétrie, XRD et SEM, il a été possible de mettre en évidence une formation secondaire d'ettringite après la consommation du gypse par la réaction du C$_3$A avec les ions sulfates provenant des C-S-H. Finalement, il a été observé que la présence de C$_3$A-gypse affecte également la cinétique d'hydratation de l'alite dans les systèmes multi-phasés. Une accélération de la vitesse de réaction de cette phase lors de la période de croissance des C-S-H a été démontrée.

Mots clés: synthèse de phases; C$_3$A; gypse; ciments modèles; cinétique d'hydratation; microstructure

RIASSUNTO

L'alluminato tricalcio (C_3A) è uno dei costituenti principali del cemento Portland. Anche se rappresenta meno del 10% della composizione totale, la sua forte reazione con l'acqua può portare a una presa rapida, chiamata "flash set". Del gesso è quindi aggiunto per regolare questa reazione e preservare la lavorabilità della pasta di cemento. Le richerche sulla reazione C_3A-gesso sono fondamentali per la comprensione dell'idratazione del cemento. L'aumento del tasso di materiali di sostituzzione e l'aumento del livello degli alluminati nel clinker saranno due importanti vie di sviluppo di nuovi materiali cementizi ed è per questo che al giorno d'oggi c'è un interrese crescente per il ruolo del C_3A nell' idratazione del cemento e del'equilibrio dei solfati.

Questa tesi si è concentrata inizialmente sullo studio della reazione C_3A-gesso. In un secondo tempo questa stessa reazione è stata studiata in miscele costituite da alite, C_3A e gesso per identificare le varie interazioni che si possono verificare fra le principali fasi del cemento durante l'idratazione.

Questo lavoro ha confermato le conclusioni di precedenti studi sui meccanismi che controllano la cinetica di idratazione dei sistemi C_3A-gesso quando gli ioni solfati sono presenti in soluzione e ha portato nuovi risultati concernenti la reazione dopo il consumo del gesso. E 'stato mostrato che le fasi AFm non cristallizzano solo nello spazio presente tra i grani di C_3A ma che un prodotto d'idratazione "inner" si forma. Inoltre, quando l'idrogranato è presente, questa fase forma uno strato di idrato sulla superficie dei grani di C_3A. Inoltre, è stato dimostrato che la morfologia della fase AFm dipende della quantità iniziale di gesso della miscela e che questa stessa morfologia influenza la cinetica di reazione. In presenza di alite, la cinetica di idratazione del sistema C_3A-gesso è modificata in modo significativo a causa del adsorbimento degli ioni solfati sul C-S-H e della riduzione dello spazio disponibile per la reazione. Grazie ad una correlazione dei risultati ottenuti con la calorimetria, XRD e SEM, è stato possibile evidenziare una formazione secondaria di ettringite dopo il consumo di gesso per reazione del C_3A con gli ioni solfati provenienti dal C-S-H. Infine, è stato osservato che la presenza di C_3A e gesso modifica la cinetica di idratazione dell'alite accelerando il tasso di reazione di questa fase durante la fase di nucleazione e crescita.

Parole chiavi: sintesi di fasi; C_3A, gesso; cinetica d'idratazione; microstruttura

REMERCIEMENTS

Je souhaite remercier sincèrement toutes les personnes qui ont contribué de près ou de loin à ce travail :

- En premier lieu ma directrice de thèse Karen Scrivener pour m'avoir ouvert les portes de son laboratoire idéalement équipé, pour son soutient et ses conseils scientifiques. Je lui suis également reconnaissante de m'avoir fait confiance en me permettant de présenter mon travail dans de nombreuses conférences.

- Emmanuel Gallucci pour m'avoir fait découvrir l'univers du ciment. Ses encouragements et nos nombreuses discussions scientifiques au début de ma thèse ont été très précieux.

- Les membres de mon jury de thèse : Dr Paul Bowen, Dr Sandrine Garrault et Dr Ellis Gartner pour la relecture attentive de mon travail et la pertinence de leurs commentaires, ainsi que le Prof. Michel Rappaz, président du jury.

- Les collaborateurs du LTP, LC et CIME et en particulier Carlos Morais, Jacques Castano, Danièle Laub et Marco Cantoni pour leur accueil dans leurs locaux et leur aide avec les différentes machines.

- Tous mes collègues du LMC, dans l'ordre et le désordre: Lionel, Antonino, M. Simonin, M. Vulliemin, M. Dizerens, Amor, Janine, Sandra et Anne-Sandra pour régler tous les petits et grand problèmes techniques et administratifs. Mercedes, Patrick, Shashank, Cyrille, Aditya et Christophe pour les heures passées à parler de courbes de calo. Steve Feldman, Gwenn Le Saoût et Silke Ruffing pour leur aide avec la DX. Mes collègues de bureau: Mercedes (re!), Ines, Carolina, Aude, Théo, et Cheng pour leur bonne humeur et leur soutient au quotidien. Ainsi qu'à Vanessa, Olga, Rodrigo, Hui, Thomas, Julien, Mathieu, Arnaud, John, Cédric, Elise, Amélie, Tony, Kyle, Gaurav, Hossam, Victor, Ruzena, Alain, Mohamad, Quang Huy, Julien, Mohsen, Quentin, Marie-Alix, Homeira, … et tous ceux qui ont été de passage et qui ont fait partie de la grande

famille LMC durant ces quatre années, pour l'agréable atmosphère de travail et tous les moments partagés au labo et en dehors.

- Les étudiants qui ont participé activement à ce travail lors de projets de semestre ou durant l'été: Nadja Marxer, Julien Ston, Amaël Cohades, Jean-Côme Chardonnens et Joël Porret.

- Mes amis pour leurs encouragements et tout particulièrement Catherine, qui soumet sa thèse au moment où j'écris ces lignes, pour avoir patiemment répondu "courage tu vas y arriver" à tous mes mails qui commençaient par "ahhhhhhggggggrrrr".

- Mon père pour m'avoir toujours soutenue, quels qu'aient été mes choix.

J'aimerais finalement adresser un clin d'œil à mes grand –pères qui ont travaillé avec du ciment sur les chantiers pendant des années pour qu'un jour l'un de leurs petits enfants puisse se permettre le luxe de faire une thèse sur ce matériaux.

TABLE OF CONTENTS

GLOSSARY

Cementitious notation

C	Free lime -CaO
S	Silica – SiO_2
A	Alumina – Al_2O_3
F	Iron oxide - Fe_2O_3
H	Water – H_2O
\$ or $\overline{S}$	Sulfur trioxide – SO_3
C_3S	Tricalcium silicate – alite – $3CaO.SiO_2$
C_2S	Dicalcium silicate – belite – $2CaO.SiO_2$
C_3A	Tricalcium aluminate – $3CaO.Al_2O_3$
C_4AF	Calcium alumino- ferrite phase
$C\$H_2$	Gypsum – $CaSO_4.2H_2O$
$C\$$ and $C\$H_{0..5}$	Anhydrite and Hemihydrate
CH	Calcium hydroxide – portlandite – $Ca(OH)_2$
C-S-H	Calcium silicate hydrate gel
AFt	Ettringite - $C_6A\$H_{32}$
AFm	$C_3A.CaX_2.yH_2O$ where X may be OH^- (Hydroxy-AFm), SO_4^{2-} (monosulfoaluminate), and CO_3^{2-} (monocarboaluminate)

Other abbreviations

PC – OPC	Portland cement – ordinary Portland cement
w/c – w/s	water to cement ratio – water to solid ratio
PSD	particle size distribution
XRD	x-ray diffraction
SEM	scanning electron microscopy
SE	secondary electrons
BSE	backscattered electrons
EDS	energy dispersive spectroscopy

CHAPTER 1   INTRODUCTION

Cement is mainly composed of calcium silicate, calcium aluminate and calcium sulfate phases. When mixed with water all these phases react to form products that lead to the setting of the cement paste; these reactions are called hydration. Understanding the chemical reactions that cause this material to harden is of interest for both academia and industry.

From an industrial standpoint, there is a growing wish for the development of more sustainable materials. Indeed, concrete is by far the most used material in the world (more than $1m^3$ or 2 tons being produced per person per year worldwide). On a unit basis the associated CO_2 emissions are lower than alternative materials [1], but due to the huge volumes, cement production accounts for some 5-8% of manmade CO_2. Since there is no satisfactory alternative to cementitious materials, improvements in sustainability of these materials must be made. Therefore to lower CO_2 emissions it will be necessary in the future to use an increasingly wide range of cementitious materials optimized according to locally available ingredients. This is a great challenge, as concrete is a complex material, currently relying on largely empirical knowledge for use. More complete understanding of the basic mechanisms of hydration is needed to provide a rational basis for new mix design as well as the selection of mineral additions and the development of chemical admixtures.

From an academic point of view the complexity of the hydration reactions of the cement phase offers interesting challenges in experimental techniques and modeling methods. One of the main centers of interest is the development of numerical models than can predict properties from the microstructure. For examples, one of the core projects of the Laboratory of Construction Materials at EPFL aims to determine the kinetics and microstructural development of the hydration reactions to simulate a microstructure from which behavior can be predicted using an integrated modeling and experimental approach. The model μic (pronounced MIKE) has been developed by Bishnoi [2] based on the experimental work of Costoya [3] on alite hydration. Even though alite does not completely represent the hydration of Portland cement, it has often been studied in a first approach to simplify the investigation of cement hydration as it is the major compound of clinker and dominates the early reactions.

However the calcium aluminate and calcium sulfate phases have an important role in the early hydrations and their reactions need to be understood in order to be further integrated in numerical models or taken into account in the development of new cementitious material.

The aim of this thesis is therefore to generate basic knowledge on the tricalcium aluminate (C_3A) – gypsum reaction and in a second time to study the interactions that can occur between C_3A-gypsum and alite when hydration occurs in multi-phase systems such as alite-C_3A-gypsum which is the most basic model cement that react as a Portland cement.

Even though C_3A represent less than 10% of the Portland cement its high reactivity can influence the rheology and the setting time of the cement [4]. In order to regulate its reaction calcium sulfate is added. The understanding of the C_3A-gypsum reaction is therefore crucial for the comprehension of the early hydration of cement. However, it has to be kept in mind that cement hydration is not only the simple sum of the reactions of its constituents, but the result of multiple interactions between all the phases. The comprehension of the interactions that occur between alite and C_3A-gypsusm when hydration occurs in multi-phase systems is also necessary for the improvement of models such as µic and the development of more sustainable cementitious materials. The influence of the cement composition on the hydration kinetics and microstructural development, in particular the amount of C_3A and the sulfate balance are of special interest since two very important routes for the development of new materials are increasing levels of addition and increasing level of aluminate in clinker.

In this work, pure clinker phases were synthesized and model systems of different compositions were prepared and their hydration studied in terms of kinetics, phase assemblage and microstructural development. The data generated by this thesis were also used for the development and the validation of µic as developed in the thesis of A.Kumar at EPFL (in progress).

This document is structured as follow:

Chapter 2 presents the protocols used for the synthesis of the cement phases as well as the characterization of the powders produced. Furthermore, the techniques used to investigate the hydration of the model systems are described.

In **Chapter 3** the study of hydration of C_3A-gypsum systems is presented. The influence of the gypsum content on the kinetics, the phase assemblage and the microstructural development are described.

2

Important key points such as possible mechanisms that control the hydration rate during the first days of hydration are detailed. Moreover, the microstructural development is carefully described up to 28 days of hydration. The influence of the gypsum content on the microstructure and the chemical composition of the hydrates is discussed.

Chapter 4 presents the study on alite-C_3A-gypsum systems. The nature and the effects of the interactions that occur between the cement phases when hydration take place in multi-phase systems are investigated. The influence on the hydration of the individual cement phases of the relative time of occurrence of aluminate and silicate reactions, which is determined by the sulfate content, as well as the influence of the C_3A content and the distribution of the anhydrous phases are described. The differences and similarities observed in the microstructural development of systems composed of the individual phases and multi-phase systems are also highlighted.

Finally in **Chapter 5** the most important findings of this work are summarized and some perspectives for future work are given.

References

1. *Inventory of carbon and energy, ICE version 1.6a.* Available from: http://wiki.bath.ac.uk/display/ICE/Home+Page.

2. Bishnoi, S. and K.L. Scrivener, *μic: A new platform for modelling the hydration of cements.* Cement and Concrete Research, 2009. 39(4): p. 266-274.

3. Costoya, M., *Synthesis and Hydration Mechanism Study of Tricalcium Silicate* Thèse de Doctorat, Ecole Polytechnique Fédérale de Lausanne, 2008.

4. Taylor, H.F.W., *Cement Chemistry 2nd edition.* Thomas Telford ed. 1997.

CHAPTER 2   SYNTHESIS OF PURE PHASES AND TECHNIQUES

This chapter describes the protocols for the synthesis of pure phases and pure clinker, followed by a description of the techniques used for the hydration study.

2.1 Alite synthesis

Tricalcium silicate is an orthosilicate containing discrete SiO_4^{4-} tetrahedra and O^{2-} ions as anions. Three triclinic (T), three monoclinic (M) and one rhombohedral (R) forms exist. C_3S is stable, with respect to C_2S + C, between 1250°C and 1800°C, but, it can be stabilized at room temperature by quenching. In clinker C_3S is usually impure and referred to as alite. The impurities have a strong influence on the polymorph that can be obtain. In cement clinker, the most frequent impurities are $Mg^{2+,}$, Al^{3+} and Fe^{3+} [1] and the monoclinic polymorph, usually M_1 or M_3 is predominant.

In this study, alite was prepared by mixing calcium carbonate ($CaCO_3$) and silica dioxide (SiO_2) (with a molar ratio of 3:1) with the addition of 1 wt% aluminum oxide (Al_2O_3) and 2 wt% magnesium oxide (MgO) according to the protocol developed by Costoya [2]. The details of the reactants are given in Annex 1. The reactants given in Table 2-1 were mixed with demineralized water (1L) by ball milling for 24 hours in a 5L jar mill.

Table 2-1: Mass of reactants used for alite synthesis (in a 5L jar mill). These values include the ignition loss of the raw materials.

$CaCO_3$	635.8 g
SiO_2	130 g
Al_2O_3	5.1 g
MgO	10.3 g

Then the blend was dried (24h at 100°C) and ground (hand grinding using a mortar) to obtain a powder. The powder was pressed into pellets of 5 cm diameter and 1 cm high with a pressure 100kP/cm². The pellets were then burned in an electrical furnace (tubular furnace *Nabertherm RHTH 120-600 /17*) according to the firing process described in Figure 2-1.
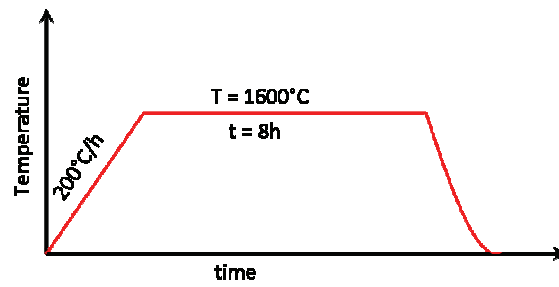
Figure 2-1: Firing cycle used for alite synthesis

At the end of the firing process the pellets were cooled rapidly by air quenching. Finally the pellets were ground (with a ring grinder from *Siebtechnik* 22cm of diameter and 5 cm height) and sieved. Only the particles finer that 100μm were kept for the study of the hydration reaction.

With these Al and Mg proportions the polymorph M_3 is obtained. Al and Mg ions influence the grain growth of C_3S. Magnesium ions increase the quantity of the liquid phase during the firing process and decrease the viscosity of the mix allowing a better diffusion of the chemical species and favoring the growth of larger grains compared to pure C_3S. In alite phase, Mg^{2+} substitutes Ca^{2+} and Al^{3+} substitute preferentially silicon sites stabilizing the T_1, T_2 and M_3 polymorphs at room temperature [2].

The purity of the phases synthesized was checked by x-ray diffraction (XRD) (Figure 2-2) and scanning electron microscopy (SEM) (Figure 2-3). Rietveld refinement was used to quantify the %wt of C_3S and impurities such as CaO. Less than 1% of free lime was detected in the synthesized alite, which was our target. The particle size distribution (PSD) of the final product was measured by laser diffraction (*Mastersizer 2000*, *Malvern Instruments Inc*) using isopropanol as dispersant. A similar particle size distribution to ordinary Portland cement was obtained with this protocol (Figure 2-4).
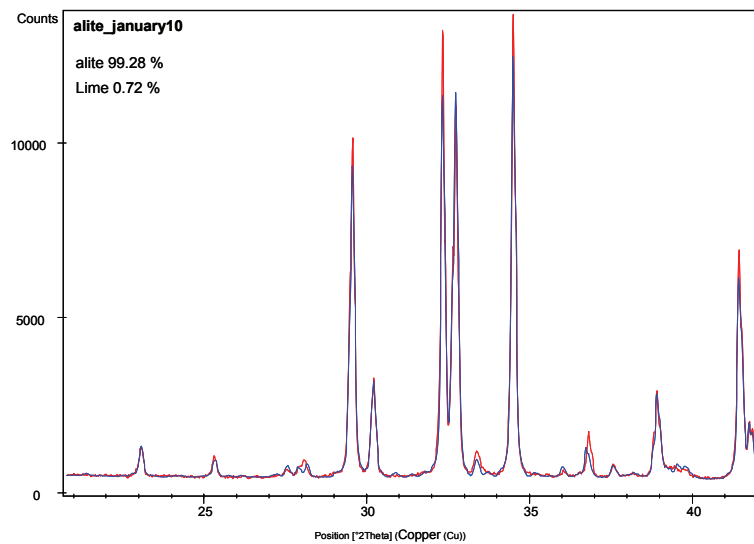
Figure 2-2: Rietveld refinement for alite. 0.72% of free lime was detected.
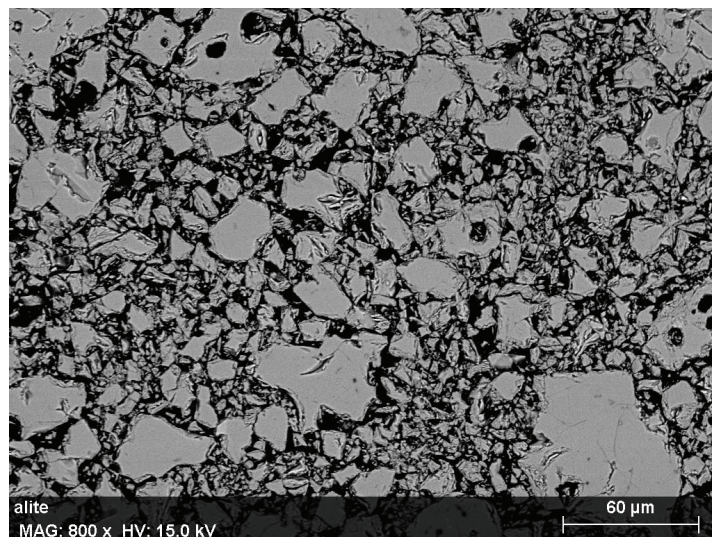

Figure 2-3: SEM – BSE image of anhydrous alite. Only traces of free lime were observed as foreign phases.
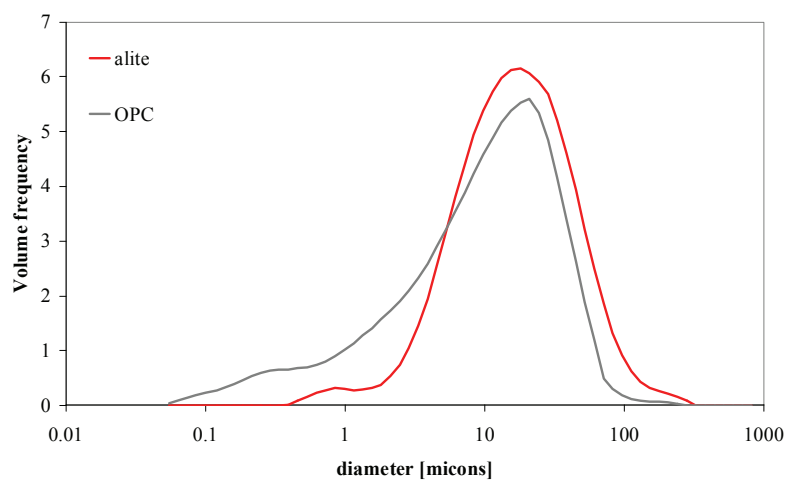

Figure 2-4: Comparison of PSD of the synthesized alite powders and OPC (Italcementi). Similar PSD's were obtained for alite and OPC.

2.2 Tricalcium aluminate (C_3A) synthesis

Tricalcium aluminate is generally cubic when it is pure. In commercial clinker, Fe^{3+}, Mg^{2+}, Na^+, K^+ and Si^{4+} are found in solid solution and the alkalis may change the symmetry of the structure from cubic to orthorhombic and monoclinic [1]. In this study only cubic C_3A was used. The protocol developed to synthesize C_3A was base on the protocol for alite synthesis of Costoya [2] and the protocols for pure phase synthesis of Di Murro [3].

The synthesis of pure C_3A was not straightforward and several unsuccessful attempts lead to the following protocol: C_3A was synthesized first of all by mixing stoichiometric amounts of CaO (from $CaCO_3$) and Al_2O_3. However, in some batches some mayenite ($C_{12}A_7$) was identified by a XRD peak around 18°. This phase is a transitional phase that appears during C_3A synthesis as presented in Figure 2-5 [4]. The presence of mayenite is not acceptable as it was found that this phase completely change the kinetics of the C_3A-gypsum reaction leading to a flash set.
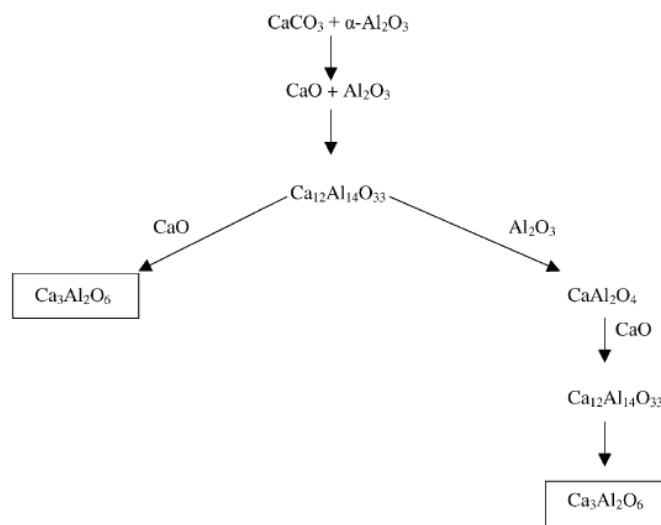

Figure 2-5: Reaction scheme for the formation of C_3A at high temperature from $CaCO_3$ and Al_2O_3. The phase $C_{12}A_7$ (Mayenite) is an intermediate phase that form during the synthesis process. Reproduced from [4].

As XRD patterns of the final product did not show any residual CaO, which would have been the case if the reaction was not complete, some additional CaO (as $CaCO_3$) was added in the initial mix and the total amount of initial material was increased in a second time to avoid material loss during the synthesis process as shown in Table 2-2.

Table 2-2: Correction of mass of reactants for C₃A synthesis used to overcome the problem of the presence of mayenite. Both mass were increased and additional CaCO₃ was added. (Mass of reactant used for a 5L jar mill)

$CaCO_3$	300 g → 460.9 g
Al_2O_3	102 g → 153 g

With this addition of $CaCO_3$ in the initial mix, no traces of mayenite were detected by XRD. However, small amounts of CaO were observed (1 to 2.5 %).

As for alite synthesis, the raw materials were mixed with water by ball milling. Then the blend was dried and ground to obtain a powder. The powder was pressed into pellets of 5 cm diameter and 1 cm high and burned following the firing process described in Figure 2-6.
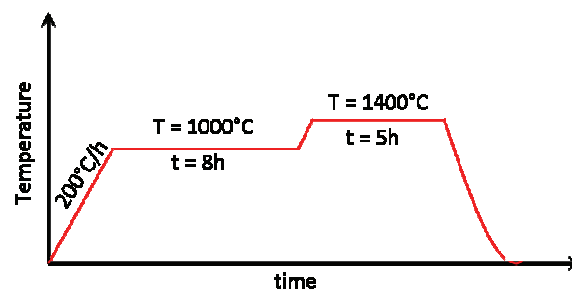

Figure 2-6: Firing cycle used for C₃A synthesis. A plateau at 1000°C was done to ensure complete decarbonation.

Contrary to alite production, a plateau at 1000°C is necessary to ensure complete decarbonation of the $CaCO_3$. A second firing with an intermediate grinding is also required to obtain C₃A. For the second firing the plateau at 1000°C is not necessary. Without this second firing process some Al-rich phase can remain between the grains as shown in Figure 2-7. As this Al-rich phase (that have a composition closer to CA than C₃A from EDS analysis) is amorphous and cannot be detected by XRD. SEM imaging was therefore necessary.
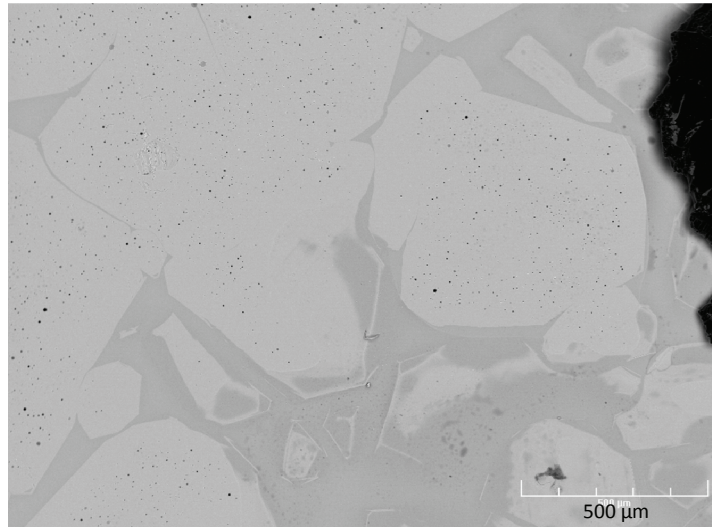
9

Figure 2-7: SEM – BSE image of a C₃A pellets (not ground) after one firing cycle. Amorphous Al-rich phase can be observed between the C₃A grains.

With two firings process pure cubic C_3A was finally obtained. No traces of other phases (except free lime) were observed by XRD (Figure 2-10 to Figure 2-12) and SEM (Figure 2-8).
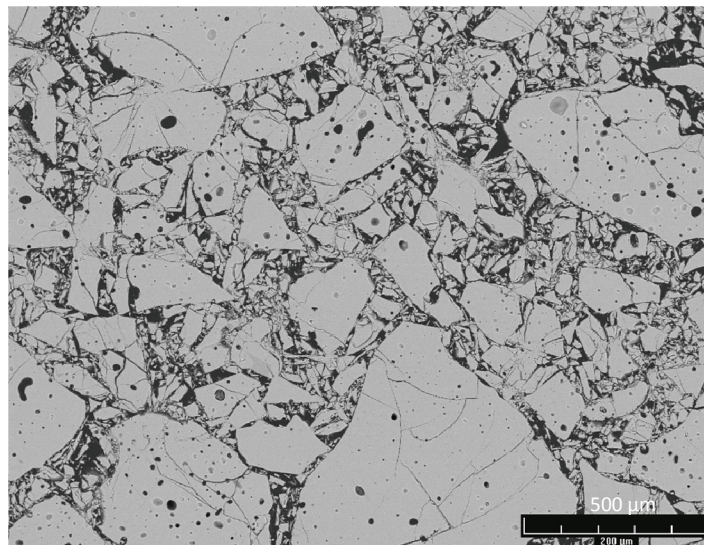

Figure 2-8: SEM – BSE image of a C₃A powder after two firing cycles. The grains are composed of pure C₃A with some traces of free lime.

The final C_3A was sieved and only the particles passing a 80µm sieve were kept and PSD was measured.
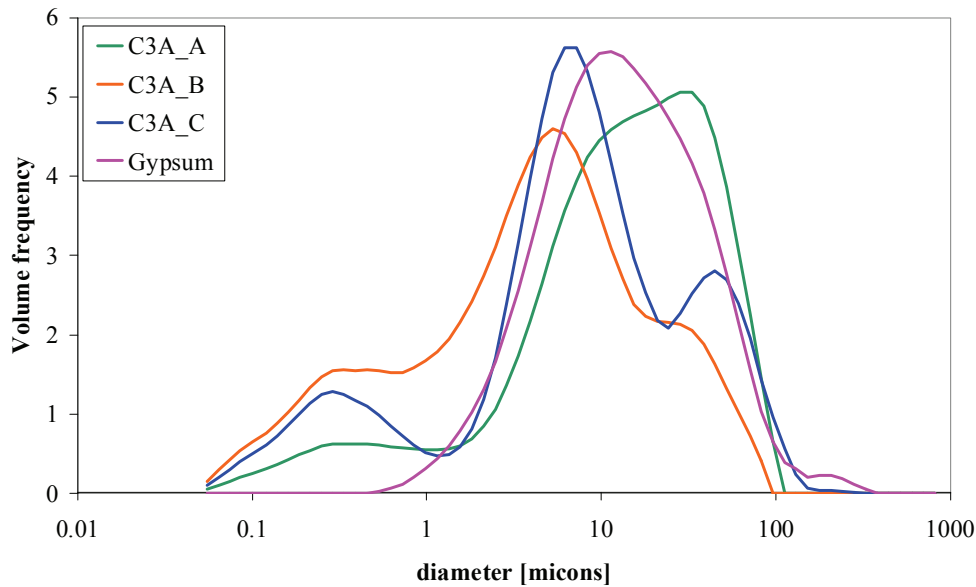
Figure 2-9: PSD of the synthesized C₃A powders and Gypsum. Although the same protocol was used for the synthesis of all the C₃A batches, differences in the PSD's were observed between the different batches.

It was difficult to obtain reproducible PSDs between the different batches as can be seen in Figure 2-9. As the PSD has a large influence on the C_3A reaction kinetics [5] only the results coming from the same batch of powder are compared in the following chapters.

The gypsum used in this study is calcium sulfate dihydrate from Merck ground 1 min in a ring grinder to obtain a finer powder. The PSD of the gypsum used in this study is also presented in Figure 2-9.

Figure 2-10: Rietveld refinement for C₃A - Batch A. 1.2% of free lime was detected.

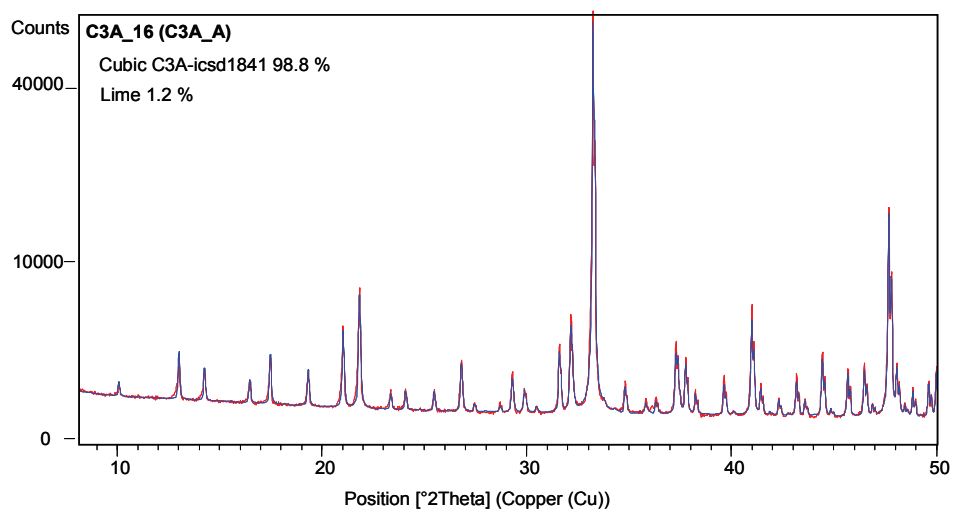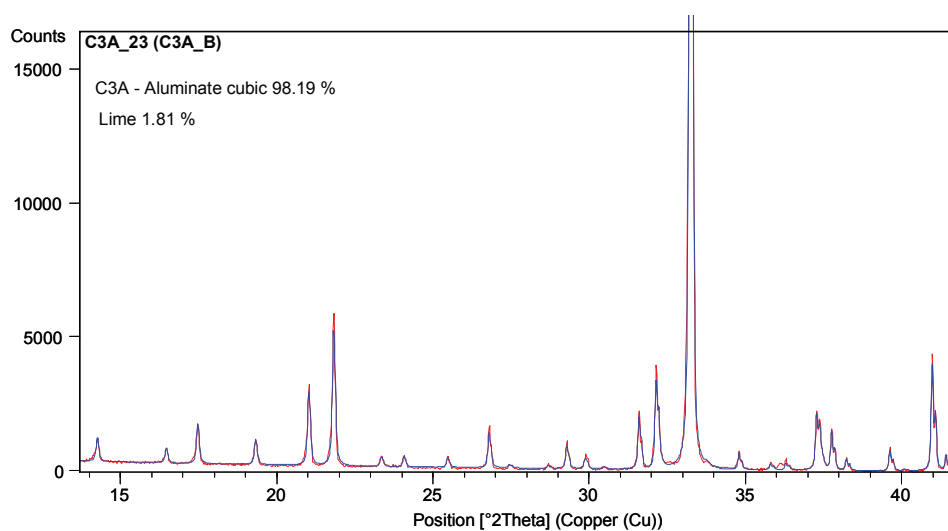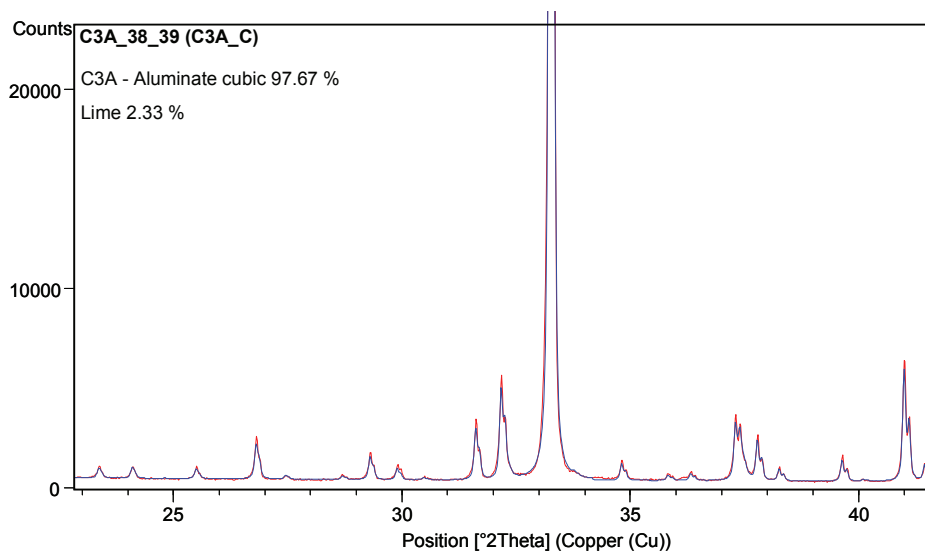**Figure 2-11: Rietveld refinement for C₃A - Batch B. 1.8% of free lime was detected.**

Figure 2-12: Rietveld refinement for C₃A - Batch C. 2.3% of free lime was detected.

12

2.3 Synthesis of polyphase clinkers

In order to study more realistic model cements than mixtures of pure phases, polyphase clinkers made of alite and C_3A were also synthesized. The protocol developed to synthesize these clinkers is based on the protocol for alite synthesis of Costoya [2] and the protocols for polyphase clinker synthesis of Di Murro [3]. To obtain a polyphase clinker with C_3A in the alite grains as represented in Figure 2-13 the reactant for alite and C_3A synthesis were mixed together from the beginning of the process following the proportions given in Table 2-3.
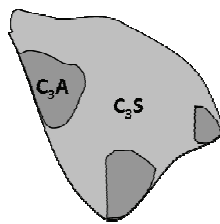
Figure 2-13: Schema of a polyphase clinker made of alite and C_3A

Table 2-3: Mass of reactants used for clinker synthesis (in a 5L jar mill). These values include the ignition loss of the raw materials.

	Clinker 92/8 (92% alite/8% C_3A)	Clinker 90/10 (90% alite/10% C_3A)	Clinker 94/6 (94% alite/6% C_3A)
$CaCO_3$	377.6 g	376.7 g	378.6 g
SiO_2	71.8 g	70.2 g	73.3 g
Al_2O_3	11.9 g	14.1 g	9.7 g
MgO	5.7 g	5.6 g	5.8 g

As in the case of alite and C_3A syntheses the blend was ball milled with water for 24h, dried, ground and pressed into pellets. The pellets were fired following the firing cycle given Figure 2-14 with a rapid cooling by air quenching at the end of the process. The pellets were finally ground and sieved. Only the particles smaller than 100µm were kept.
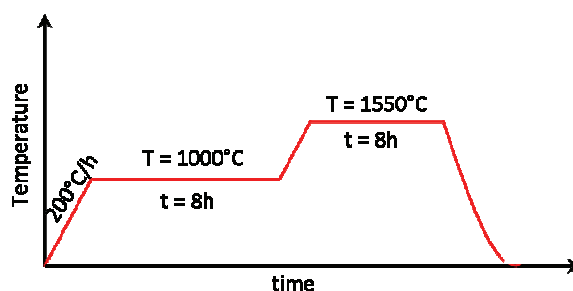
Figure 2-14: Firing cycle used for alite-C$_3$A clinker synthesis. A plateau at 1000°C was done to ensure complete decarbonation.

The purity of the final product as well as the exact composition was checked by XRD and Rietveld refinement as shown in Figure 2-17, Figure 2-18 and Figure 2-19. Alite/ C$_3$A ratios obtained from Rietveld refinement were not exactly the targeted ones as some free lime was always present in the sample. Even thought the targeted composition was not exactly achieved, experiments were carried out with this polyphase powder as three polyphase grains with different C$_3$A content were obtained. The name of the samples refers however to the targeted composition.

SEM imaging was also used to check the polyphase nature of the grains (Figure 2-15) and finally the particle size distributions of the clinkers were measured (Figure 2-16).
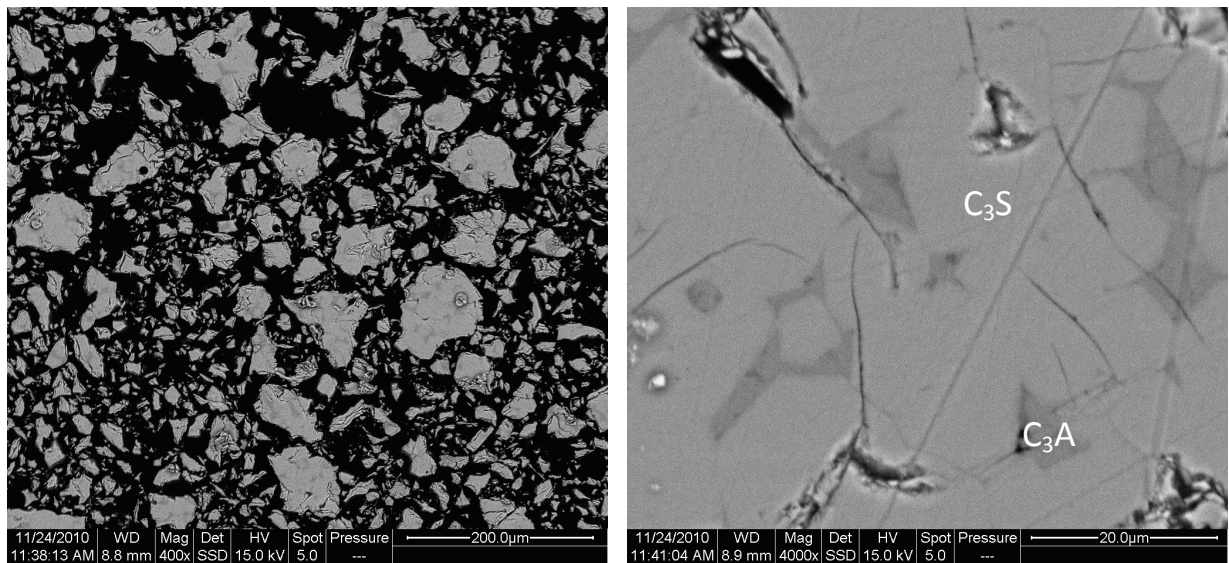
Figure 2-15: SEM-BSE images of an anhydrous polyphase clinker. C₃A can be observed in the alite grains. Traces of free lime can also be observed in the bigger clinker grains.
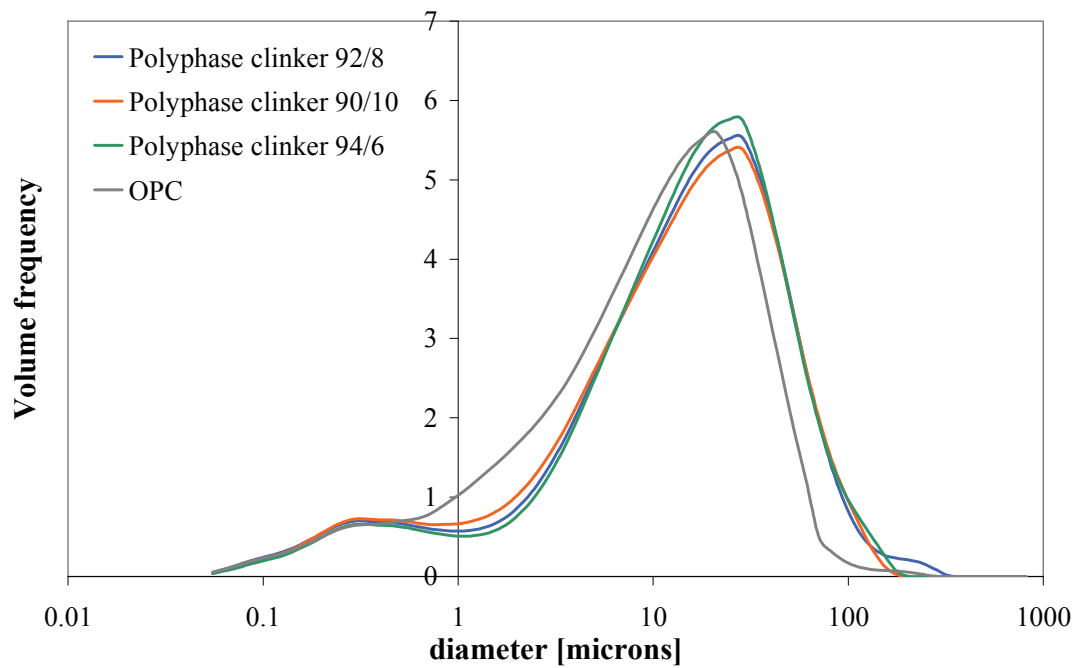
Figure 2-16: PSD of the synthesized polyphase clinkers. Reproducible (and similar to OPC) PSD's were obtained for all the clinkers synthesized with this protocol.
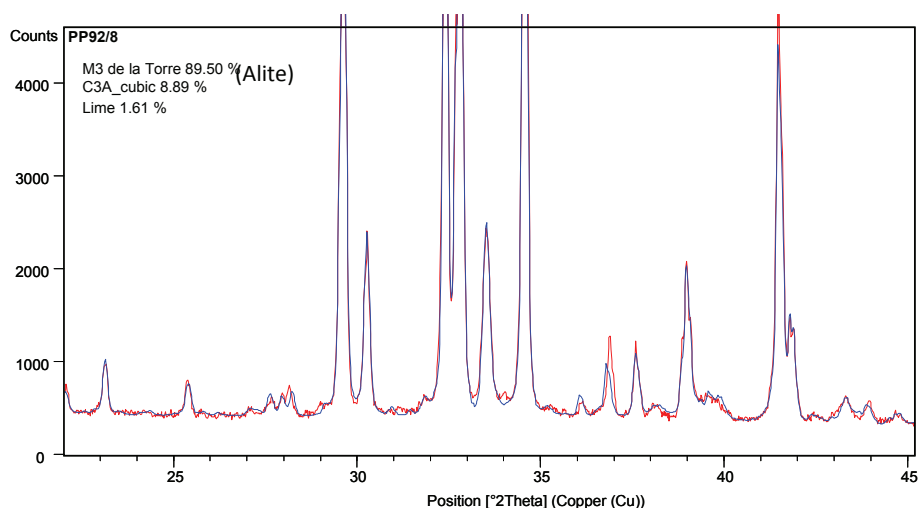
Figure 2-17: Rietveld refinement for Clinker 92/8. An alite to C₃A ratio of 89.5/8.9 was obtained and 1.6% of free lime was detected.
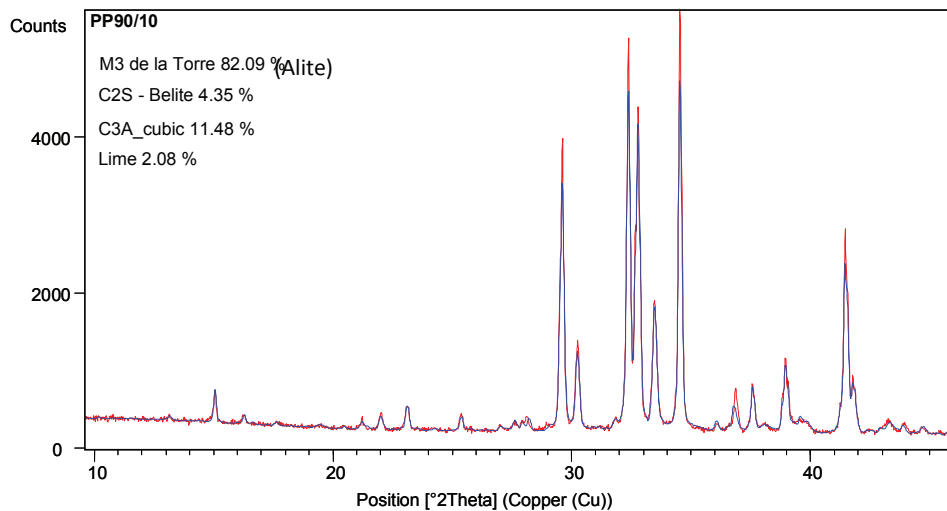
Figure 2-18: Rietveld refinement for Clinker 90/10. An alite to C₃A ratio of 82.1/11.5 was obtained and 4.3 and 2.1% of free lime were detected.
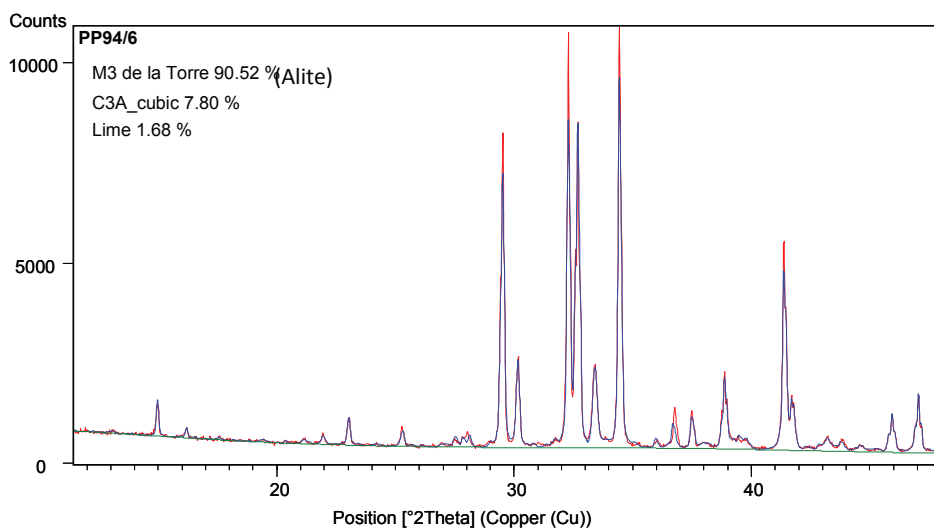
Figure 2-19: Rietveld refinement for Clinker 94/6. An alite to C₃A ratio of 90.5/7.8 was obtained and 1.7% of free lime was detected.

16

2.4 Summary for synthesis of pure phases

- Mix the reactants with water by ball milling for 24h in a 5L jar. The mass of reactant are summarized in Table 2-4.

Table 2-4: Mass of reactant and water used for the synthesis of pure phases in a 5L jar mill.

	CaCO3 [g]	SiO2 [g]	Al2O3 [g]	MgO [g]	Water [g]
Alite	638.5	130	5.1	10.3	1000
C_3A	460.9	-	153	-	750
Clinker 94/6	378.6	73.3	9.7	5.8	750
Clinker 92/8	377.6	71.8	11.9	5.7	750
Clinker 90/10	376.7	70.2	14.1	5.6	750

- Dry the blend in a oven at 100°C for 24 hours.

- Grind the mass by hand using a mortar to obtain a homogenous powder.

- Press the powder into pellets (5 cm diameter, 1 cm thick).

- Firing cycle:
  - For alite: 200°C/h up to 1600°C – 1600°C for 8 hours
  - For C_3A: 200°C/h up to 1000°C – 1000°C for 8h - 200°C/h up to 1400°C – 1400°C for 5h – intermediate grinding - 200°C/h up to 1400°C – 1400°C for 5h
  - For clinker: 200°C/h up to 1000°C – 1000°C for 8h - 200°C/h up to 1550°C – 1550°C for 8h

- Grind the pellets.

- Sieve the powder. In this study a 100μm sieve was used for the alite and clinker powders and a 80 μm sieve was used for C_3A powders.

All the powders used in this study are summarized in Table 2-5. The specific surface area was calculated from the particle size distribution measured by laser diffraction assuming spherical particles and bulk densities (alite: 3150 kg/m^2; C3A= 3030 kg/m^2; gypsum= 2330 kg/m^2). It has to be noted that specific surface areas indicated in Table 2-5 are not precise due to too many assumptions in the calculation and can be used only as comparative values.

Table 2-5: Summary of the powders used in this study and their calculated specific surface area (from the PSD assuming spherical particles and bulk densities)

	Composition (Rietveld refinement)	Specific surface area
Alite	C_3S 99,28% CaO 0.78%	674 cm^2/g
C_3A_A	C_3A 98.80% CaO 1.20%	2760 cm^2/g
C_3A_B	C_3A 98.19% CaO 1.81%	4360 cm^2/g
C_3A_C	C_3A 97.67% CaO 2.33%	4600 cm^2/g
PP92/8	C_3S 89.5% C_3A 8.89% CaO 1.61%	2789 cm^2/g
PP90/10	C_3S 82.90% C_3A 11.48% C_2S 4.35% CaO 2.08%	2800 cm^2/g
PP94/6	C_3S 90.52% C_3A 7.80% CaO 1.68%	2500 cm^2/g
Gypsum	Precipitated for analysis from Merck	795 cm2/g

2.5   Sample preparation and techniques used to investigate the hydration reaction

2.5.1   Preparation of pastes

Model systems containing different phases were prepared by dry mixing in a *Turbula* shaker-mixer (250 ml) for 8 hours and then gently co-ground for 5 min by hand in a mortar. This last operation may probably change the PSD of the powder. However, all the powders follow the same preparation procedure. Even pure alite follow this procedure in order to be compared to other systems.

Pastes were prepared at room temperature with a vertical mixer *IKA Labortechnik RW20.n*. Deionized water corresponding to a w/c ratio of 1 for C_3A-gypsum pastes and 0.4 for the other systems was added to 10 to 25g of powder and mixed for 2 min at 500 rpm.

2.5.2   Hydration kinetics: Isothermal calorimetry

As the overall heat balance of cement hydration is sufficiently exothermic, its reaction can be continuously followed by isothermal calorimetry. Isothermal calorimetry is a non invasive and easy method to investigate hydration kinetics. It is however important to note that the heat evolution curve corresponds to the contribution of all the on going reactions and the peaks may be due to more than one reaction. Calorimetric measurements were carried out in an isothermal calorimeter *TAM Air* from *Thermometric*. This machine consists of 8 parallel twin measurement channels. One cell is dedicated to the sample, the other to a reference vessel. The reference is used to improve the signal to noise ratio and to correct measurement and temperature artifacts. The difference of heat flow measured between the hydrating cement and the reference is proportional to the rate of heat evolution of the cement paste. In this work 20ml glass ampoules were used for both the sample and the reference container. Water with the same thermal mass as the sample was used as reference.

Pastes were mixed outside with the procedure previously described and the samples were introduced into the calorimeter as soon as possible after the mixing. Due to the difficulty to produce large amount of pure phases, the amount of paste used for the isothermal calorimetry experiments was reduces to a minimum quantity: 3 to 5g of paste.

2.5.3 Phase assemblage: x-ray diffraction

X-ray diffraction (XRD) patterns were collected using a *PANalytical X'Pert Pro MPD* diffractometer (*X'Celerator* detector) in a θ-θ configuration with a CuKα radiation (λ=1.54 Å), a fixed divergence slit size 0.5° and a rotating sample stage.

To follow the evolution of the phase assemblage at early ages, in-situ XRD measurements were carried out. The same sample of fresh paste was measured continuously during the first 2 to 3 days of hydration. To avoid water loss and contact with CO_2 during hydration, a protective film *(kapton film HN50 form Maagtechnic)* was used to cover the cement paste. In order to follow the reaction with a representative sampling rate, the range of angles scanned was reduced to the minimum necessary for phase identification: 7 to 36°, leading to a sampling rate of 14 minutes with a step size of 0.017° acquired for 57 s at a scan speed of 0.04°.s-1.

This technique presents several advantages for the hydration study. Patterns of a good resolution can be obtained with realistic samplings rate. The use of wet samples instead of dry slices is particularly useful in the case of study of the aluminate hydrates such as ettringite and AFm as these hydrates deteriorate using usual drying techniques (e.g. [6]). Moreover the C_3A-gypsum samples, that are very sensitive to carbonation, seem to be quite well protected from reaction with CO_2 with the use of the kapton film.

All the collected scans were plotted in a tridimensional plot (x= time, y= angles, z=counts). The background was calculated and removed. A peak representative of a phase was then isolated and the evolution of this phase was calculated from the peak area (see Figure 2-20). The evolution of each phase was normalized to its maximum measurement.
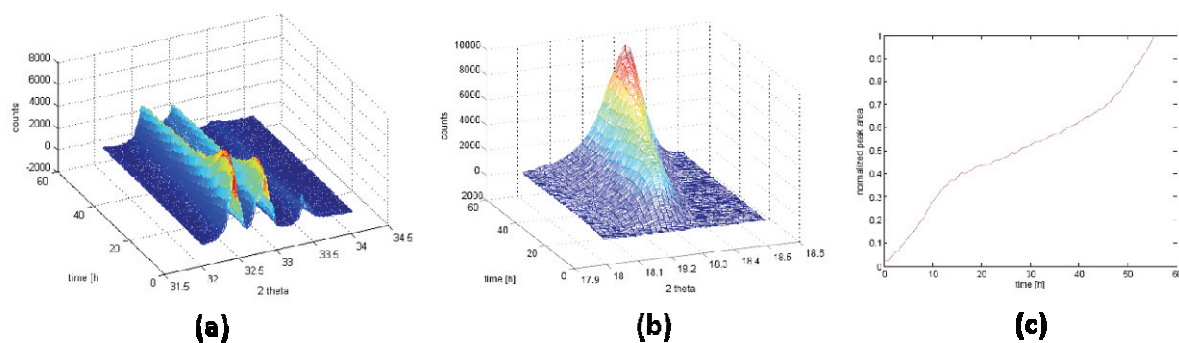

Figure 2-20: In-situ XRD data processing: (a) XRD pattern were collected during the first days of hydration with a sampling rate of 14min. (b) For each phase one representative peak was selected. (c) The evolution of the phase over time calculated from the peak area and normalized to its maximum.

One observed possible sources of error is the absorption of the signal by the water film that forms between the sample and the kapton foil during the first 2 to 5 hours of hydration. Due to this absorption it can sometimes seems that a phase is forming (peak increases) while it should be dissolving. This is a measurement artifact that cannot be avoided at realistic w/c ratios. Moreover, possible preferential precipitation of hydrates at the surface may occur.

With this technique it was possible to follow the phase assemblage during the first hours of hydration and compare it to the calorimetric heat evolution profile. To ensure the comparability of the results the same original paste was separated in two parts after mixing: one part for the XRD measurements and the other for the calorimetry. The temperature in the XRD chamber was quite high but stable around 26- 26.5 °C when XRD measurements were running. The calorimetric measurements were therefore carried out at the same temperature (26°C) to ensure the comparability of the results.

For the study of the phase assemblage at later ages, pastes were prepared and hydrated in sealed containers. At defined times, the cylinder of cement paste was cut into slices for XRD measurements. With this technique, XRD patterns of good quality can be obtained as there is no absorption of the signal by kapton or water film. However, this technique can be used only for set samples. Even if great care was taken to refill the sample container with N_2 after opening; some carbonation of the very sensitive samples could not be avoided.

2.5.4 Microstructure: Scanning Electron Microscopy

Scanning electron microscopy is one of the most used techniques for investigating the microstructure of cementitious materials during hydration reaction. In this study a *FEI quanta 200* SEM microscope with an accelerating voltage of 15kV and a *Bruker AXS XFlash Detector* for energy dispersive X-ray analyses were used.

Cements pastes for microscopy study were cast into small plastic containers and stored for hydration at controlled temperature. The hydration was stopped by freeze drying. The sample (with its container) was immersed in liquid nitrogen (-196°C) for about 15 min. Due to the small size of the sample the pore water is almost instantly frozen and excessive microcraking is reduced. The frozen water was then removed by sublimation in a *Telstar Cryodos* freeze-dryer. Once dried, the samples were prepared for BSE-SEM observation by epoxy-impregnation (EPOTEK-301) and polished with a diamond powder down to 1µm.

References

1. Bye, G.C., *Portland Cement second edition*. Thomas Telford ed.

2. Costoya, M., *Synthesis and Hydration Mechanism Study of Tricalcium Silicate* Thèse de Doctorat, Ecole Polytechnique Fédérale de Lausanne, 2008.

3. Di Murro, H., *Mécanismes d'élaboration de la microstructure des bétons.* Thèse de Doctorat, Université de Bourgogne, 2007.

4. Mohamed, B.M. and J.H. Sharp, *Kinetics and mechanism of formation of tricalcium aluminate, Ca3Al2O6.* Thermochimica Acta, 2002. 388(1-2): p. 105-114.

5. Minard, H., et al., *Mechanisms and parameters controlling the tricalcium aluminate reactivity in presence of gypsum.* Cement and Concrete Research, 2007.

6. Le Saoût, G., et al. *Quantitative study of cementitious materials by X-ray diffraction / Rietveld analysis using external standard*. in *Proceedings of the 12th Iternational Congress of the Chemistry of Cement*. 2007. Montreal, Canada.

# CHAPTER 3　　　TRICALCIUM ALUMINATE- GYPSUM SYSTEMS

3.1　State of the art

3.1.1　Overview

When hydration of C_3A occurs alone, C_3A reacts quickly with water to form platelets of calcium aluminate hydrates:

$$2C_3A + 21H \rightarrow C_4AH_{13} + C_2AH_8$$
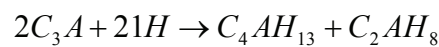
Depending on the water activity the AFm phase C_4AH_{13} may contain more water in the interlayer and exists as C_4AH_{19}. All these hydrates are metastable with respect to cubic hydrogarnet (C_3AH_6) to which they finally convert [1]. The formation of C_4AH_{13} or C_2AH_8 during hydration depends on the concentration of calcium hydroxide in solution. It is expected that solutions with low Ca^{2+} content will lead to the preferential precipitation of C_2AH_8 and solutions rich in Ca^{2+} like in Portland cement will lead to the formation of C_4AH_{13} [2]. As the x-ray diffraction patterns of these two hydrates are very close, the distinction between the two products has to be done considering the intensities of the peaks. For example, in C_3A-water solutions Jupe [3] identified C_2AH_8 as an intermediate hydrate and Christensen [4] observed C_4AH_{19} before the formation of C_3AH_6 in C_3A-water systems containing low amount of gypsum (less than 10 wt%). In her conductimetry experiments of C_3A hydration in water and in solution saturated with respect to CH Minard [2] observed that the hydrates forming during hydration in both systems did not have the exact stoichiometry of one of these hydrates but always had a C/A ratio between the two compositions. She concluded that there exist solid solutions between these two products during C_3A hydration with, in any case, the final conversion into hydrogarnet.

The reaction of C_3A with water is a rapid and highly exothermic reaction. Even though cements contain only about 10wt% of C_3A, the high reactivity of this phase can lead to rapid setting of the cement paste called flash set. Calcium sulfates such as gypsum, anhydrite and hemihydrate are generally added to cement to control C_3A hydration. In the presence of calcium sulfate a calcium sulfoaluminate compound, named ettringite or AFt, is formed:

$$C_3A + 3C\$H_2 + 26H \rightarrow C_6A\$_3H_{32}$$
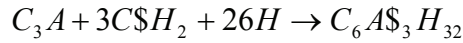
If, as it is always the case in cement pastes, unreacted C$_3$A remains when the supply of sulfate ions runs out, there is a surge in its hydration and the remaining C$_3$A reacts with ettringite and water to form monosulfoaluminate (AFm):

$$2C_3A + C_6A\$_3H_{32} + 4H \rightarrow 3C_4A\$H_{12}$$
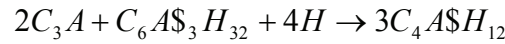
The different calcium (sulfo)- aluminate hydrates have characteristic morphologies. AFm phases form hexagonal platelet crystals [1] and ettringite crystallizes as long needle-like crystals under condition of low supersaturation and as short prisms with hexagonal cross section under high supersaturated conditions [5, 6].

Different evolutions of the microstructure are reported in the literature depending on the gypsum content.

- At low gypsum contents, the formation of a foil-like amorphous coating on C$_3$A grains was observed by Meredith et al. [7] within the first minutes of hydration. As hydration proceeds the formation of irregular plates of calcium aluminate hydrates is reported.

- For pastes with intermediate gypsum content, the formation of AFm phase on C$_3$A grains at the very beginning of the reaction has been reported [6, 8, 9], followed by crystallization of ettringite rods and the development of hexagonal platelets near the C$_3$A grains [7]. Ettringite dissolves when the sulfate content of the solution is low, transferring ions through solution to the hexagonal platelet phase forming a solid solution of hydroxy-AFm and monosulfoaluminate [8]. The solid solution series between hydroxy-AFm and monosulfoaluminate was investigated by Matschei et al. [10]. They show that up to a substitution of 50 mol% SO$_4$ by OH$^-$ a single solid solution with XRD peaks close to monosulfoaluminate exists (Figure 3-1). A limited incorporation of sulfate in the hydroxy-AFm end member was also observed. The existence of a miscibility gap between both end members was confirmed by this study.
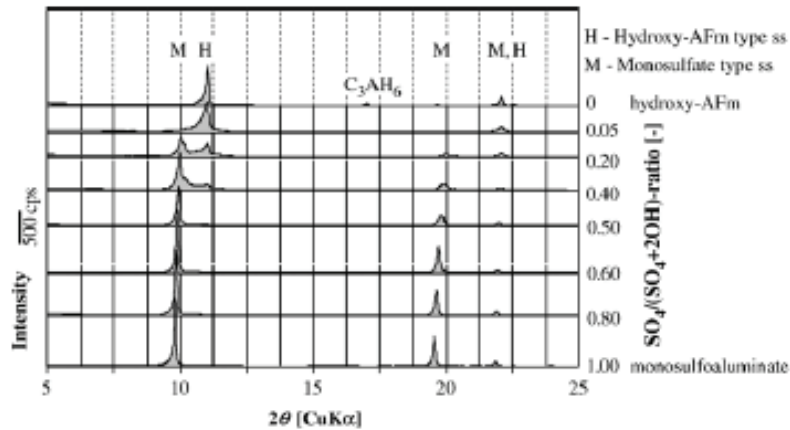
Figure 3-1: XRD patterns of solid solutions between monosulfoaluminate and hydroxy-AFm. Up to a substitution of 50 mol% SO$_4$ by OH$^-$ a single solid solution with XRD peaks close to monosulfoaluminate exists. Reproduced from [10].

- For higher gypsum content pastes, only the formation of ettringite needle-like crystals is reported in the literature [8].

The studies of Minard et al. [9] and Pourchet et al. [11] show that in the presence of gypsum, AFm phase is always formed at the very beginning of the reaction independently of the gypsum content in the C$_3$A-gypsum paste. Pourchet et al. also showed that this initial precipitation of AFm that occurs in the presence of gypsum is avoided when hemihydrate is present. This was attributed to the fact that the concentration of sulfate in solution increases in the presence of hemihydrate.

As already shown by Mehta in 1969 [5], the saturation of the solution with respect to CH may influence the morphology of the hydrates. Hampson and Bailey [8, 12, 13] carried out many experiments in the early 80's on the influence of the pH of the solution on the microstructural development on C$_3$A-gypsum pastes at early ages. They observed at low pH (11.8), a rapid dissolution of C$_3$A grains resulting in a microstructure of only long ettringite needles, or ettringite needles and platelets of AFm depending on the gypsum content after only 30minutes of hydration. At high pH (12.5), substantial amounts of unreacted C$_3$A with short ettringite crystals were observed by the authors even after several hours of hydration [8]. Another important feature of their research is the effect of the pH on the location of the precipitated hydrates in the microstructure. At low pH they observe the rapid precipitation of fibrous calcium alumino-sulfate hydrates at distance from the dissolving phases while when pH was raised to 12.5 the hydrates precipitated only in the region adjacent to the C$_3$A surface [8].This phenomenon was related by the authors to the gradient in

25

concentration and the degree of super saturation of the solution with respect to the dissolving phase.

3.1.2 Effect of calcium sulfate on C_3A hydration

The mechanisms by which the calcium sulfate acts with C_3A to slow down the hydration process have been intensively discussed in the last 30 years and two main hypotheses exist.

On the one hand, some authors state that in the presence of sulfate ions the C_3A hydration is controlled by diffusion though a hydrate layer. However a variety of opinions exist on the nature of this layer:

- For several authors the hydration of C_3A it is slowed down by the formation of a coating of ettringite crystals on C_3A grains. Due to increment of volume resulting from the ettringite crystallization, the pressure increase and the layer breaks leading to an acceleration of C_3A hydration [14, 15].
- Corstanje [16-18] evokes an aluminate gel barrier on the C_3A grains with incorporated calcium and sulfate.
- For others, the reaction is slowed down by the precipitation of AFm platelets on the grains together with ettringite [19, 20].
- Scrivener reported a complex layer composed of AH_3 and ettringite that may also contain C_4AH_{19} and monosulfoaluminate and/or their solid solutions. [6, 21].

On the other hand, the adsorption of sulfate ions on C_3A grains is proposed to be at the origin of the slow down of the C_3A hydration in the presence of calcium sulfate.

- Feldman and Ramachadran [22] consider that it is the adsorption of the sulfates on C_3A grains that decreases the dissolution rate of C_3A blocking active sites. However Collepardi et al. [14] showed that the presence of other sulfate compounds such as Na_2SO_4 does not influence the C_3A hydration.
- In their paper Skalny and Tadros [23] state that both calcium and sulfate ions of the gypsum are responsible of the slow down of the C_3A hydration. The Ca ions are chemisorbed on the C_3A grains leading to a positively charged surface where the sulfate ions can be adsorbed. The slow down of the reaction is then due to the adsorption of sulfate on active dissolution sites. Just positively charging the C_3A surface (with $CaCl_2$ or NaCl in solution) does not affect the kinetics of the C_3A dissolution.

The recent work of Minard et al. [9] suggest that the slow down of the rate of reaction of C_3A in the presence of gypsum is certainly due to the adsorption of calcium and/or sulfate ions on C_3A grains, and not to the presence of a protective membrane. Indeed they observed a constant reaction rate of C_3A (for monosized particles) during the first part of the reaction. This means that the reaction rate is controlled by surface mechanisms. If a protective membrane (composed of ettringite or AFm) was controlling the reaction rate, the rate would have change with the thickening of the hydrate layer. In addition, Scrivener and Pratt [6] pointed out that the morphology of ettringite is unlikely to provide a substantial barrier to ion transport. Moreover, Minard et al. clearly showed that calcium aluminate phase observed by several authors on C_3A surface is an AFm hydrate. This hydrate cannot be at the origin of the slow down of the reaction as this phase forms also in pure C_3A where the reaction is not slowed down and does not form in the presence of hemihydrate whereas the reaction rate is similar to that in the presence of gypsum.

3.1.3   Kinetics

The kinetics of the C_3A-gypsum systems have been studied is pastes by Tenoutasse [24] and Collepardi et al. [14] and in diluted solutions by Minard et al. [9]. They all observed that this reaction occurs in two stages as presented in Figure 3-2. A dissolution peak, followed by a period of low heat development is generally observed first. This period of the reaction is called "the first stage" and continues until the sulfate ions present in solution have been entirely consumed. A small exothermic peak was observed during this period (Figure 3-2 left) by Minard et al. and was considered by the authors to be the acceleration of ettringite formation which follows a classical process of nucleation and growth. This peak was only observed in diluted solutions. Several authors report that ettringite is not the only hydrate that is precipitated in this first period of hydration, a hydroxy-AFm phase containing sulfate ions is also precipitated during the first minutes of hydration [8, 9, 11].

After the consumption of gypsum, a second strong exothermic peak occurs and finally the heat flow decreases slowly to zero. This is the second stage of the reaction.

Calorimetric curve of a C₃A-gypsum systems in diluted suspension (W/S = 25): **Calorimetric curve of a C₃A-gypsum systems in paste (W/S = 0.4):**
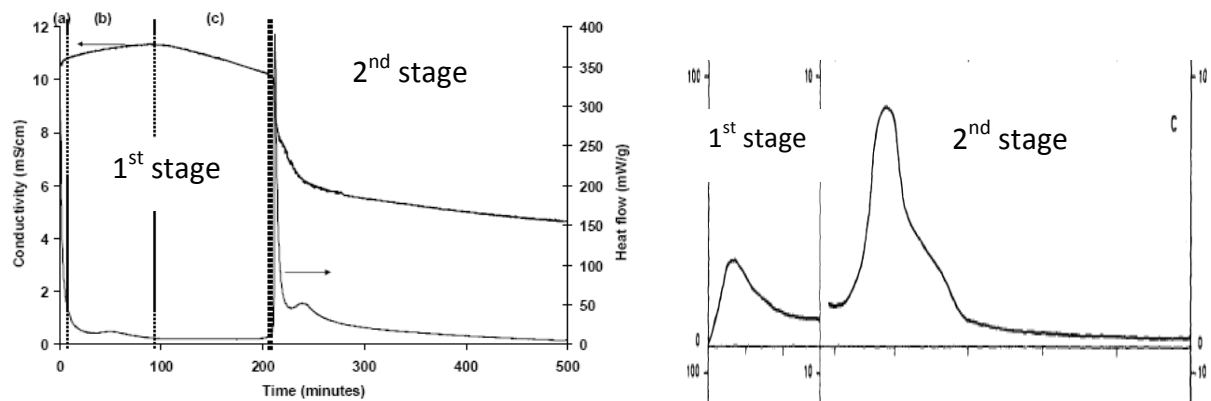

Figure 3-2: *Left:* Heat flow and conductivity evolutions during hydration of C₃A – Gypsum a solution saturated with respect to CH (W/S=25). Adapted form [9]. *Right:* Calorimetric curve of C₃A+Gypsum+inert quartz paste (W/S=0.4). Adapted from [14]. 1st stage of the reaction: hydration in the presence of gypsum. 2nd stage: hydration after the depletion of gypsum.

Three possible processes could control the reaction rate during the first stage of the reaction:

- The formation of ettringite
- The dissolution of gypsum
- The dissolution of C₃A

The measurements of the ionic concentration in solution done by Minard et al. [9] show that during this period of hydration, the concentration of sulfate ions remains constant in solution, meaning that all the sulfate consumed by the formation of ettringite are replaced by dissolution of gypsum. The dissolution of gypsum is therefore not the process that limits the reaction rate.

The effect of the gypsum amount on C₃A hydration was investigated in diluted suspension by Minard et al. [9] and in pastes by Tenoutasse [24]. They both observed that the time of occurrence of the second exothermic peak, i.e. the time necessary for gypsum consumption, increased with the gypsum quantity as shown in Figure 3-3. However, it can be observed on the calorimetric curves presented in Figure 3-3 that all the samples have the same heat evolution curves before the occurrence of the exothermic peak whatever the gypsum content is. Therefore, it seems that the reaction rate during this period doesn't depend of the gypsum content.

In addition, the aluminum concentration is below detection limit. This last observation indicates that the limiting factor cannot be the formation of ettringite as all the Al ions provided by the dissolution of C_3A are immediately "used" to form ettringite.
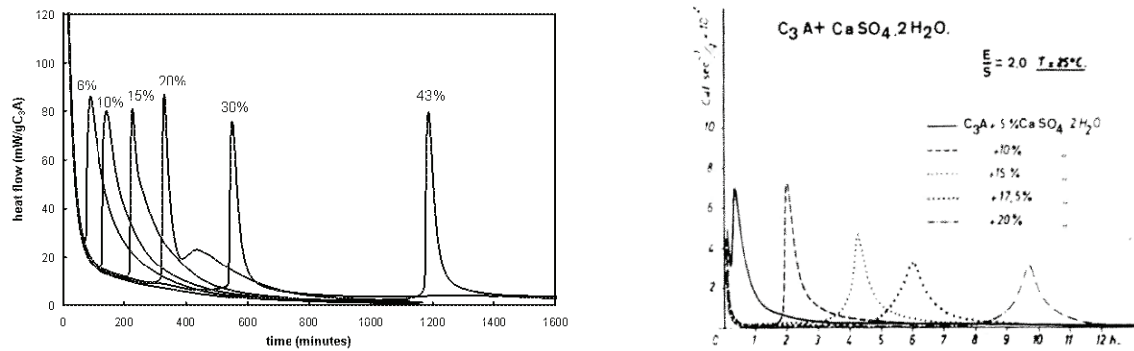

Figure 3-3: Influence of the gypsum amount on the kinetics of the reaction in diluted suspension - W/S=25- (*left* reproduced from [9]) and in pastes - W/S = 2- (*right* reproduced from [24]). The time of occurrence of the exothermic peak is delayed with increasing gypsum content. A peak broadening with increasing gypsum content can be observed in pastes.

The overall reaction rate seems therefore to be controlled by the rate of dissolution of C_3A whatever the gypsum content of the systems is. The gypsum content influences only the time of occurrence of the exothermic peak. Moreover Minard shows that, with monosized particles of C_3A, the rate of consumption of C_3A is linear during the first stage of the reaction (Figure 3-4) and depends on the specific surface of C_3A particles.
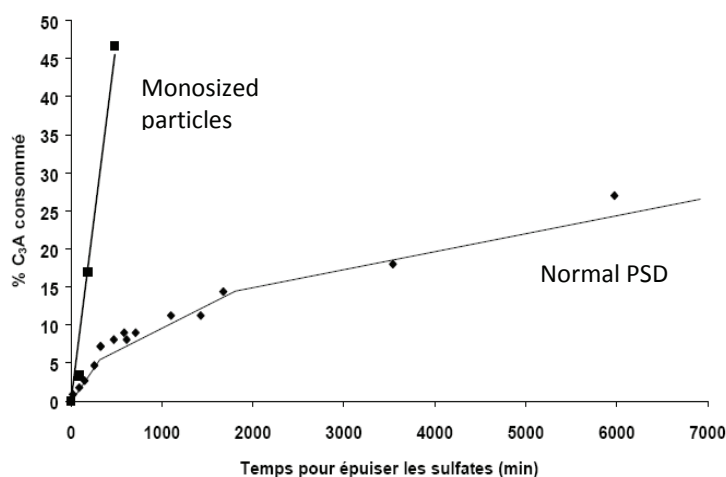

Figure 3-4: % of reacted C_3A vs. time necessary to consume the gypsum. In the case of monosize particles the rate of reaction is constant during the first stage of the reaction. Adapted from [2].

The second stage of reaction begins when all the sulfates ions have been consumed. The mechanism that is controlling the reaction rate during the exothermic peak that occurs at the beginning of this second period is still not clear.

Tenoutasse [24] observed a broadening of the calorimetric peaks with increasing gypsum content, leading to the conclusion that the gypsum content influences the hydration rate during the second stage of the reaction. However this point was not further developed. It is interesting to note that this phenomenon cannot be clearly observed in dilute suspension. This indicates that the space available for the reaction may affect the reaction as discussed later in this chapter.

The kinetics of the evolution of the phase assemblage during this period is also unclear. For Collepardi et al. [14] the reaction of C_3A and ettringite to form monosulfoaluminate is a rapid reaction while for Minard et al. [9], the formation of monosulfoaluminate is thought to be a slow process.

3.2 Objectives of the study and experimental plan

The phase assemblage generated upon hydration of C_3A in the presence of gypsum depends on the gypsum content. The reaction can be divided qualitatively in two stages: the formation of ettringite, the duration of which depends on the gypsum content, and then the formation of monosulfoaluminate and/or hydroxy-AFm phases. The phase assemblage after gypsum depletion depends on the amount of sulfate in the anhydrous mix as summarized in Figure 3-5. In order to simplify the comparison between different studies and systems the expressions low, intermediate, high and very high gypsum content will be used to describe the C_3A-gypsum systems in this study according to the amount of gypsum as presented in Figure 3-5. In Portland cement (PC) the gypsum/C_3A ratio is usually high or very high (> 35%) following this classification.
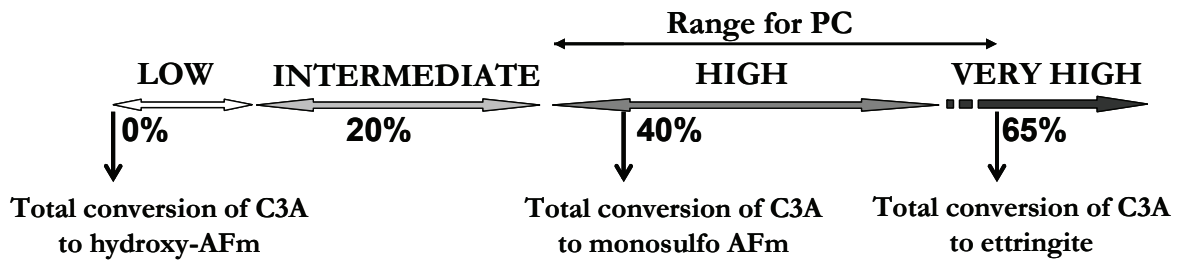

Figure 3-5: Phase assemblage that is expected for the stoichiometry depending on the initial gypsum content (wt%) after the depletion of gypsum.

As describe in the literature review, the mechanism that controls the reaction rate during the first stage of C_3A reaction in the presence of gypsum was identified by Minard et al. [9] as the dissolution of C_3A controlled by adsorption of sulfate ions.

The second stage as well as the later ages have been less extensively studied and many points are still unclear, starting from the evolution of the phases after the gypsum consumption as highlighted in the literature review. The new contribution of this study is therefore mainly in the second stage. The phase assemblage depending on the gypsum content was monitored by in-situ XRD during the first days of reaction to elucidate the evolution of the phases after gypsum depletion. The microstructural development was also investigated. The influence of the gypsum content on the microstructure of C_3A-gypsum paste was of particular interest.

Finally, the hydration kinetics of different systems was studied by calorimetry in order to understand the mechanisms that control the hydration rate during the second stage of the reaction. The effect of the temperature on the hydration kinetics was also investigated.

Different batches of C_3A were synthesized for this study. We consider as "a batch" powders produced in the same conditions and homogenized before the sieving process. Even though great care was taken to synthesize all the C_3A batches in the same way, different particles size distributions and therefore different reaction rates were obtained. Therefore the results between the different batches of C_3A- gypsum cannot be directly compared and are presented separately. However some trends characteristic of the general C_3A-gypsum system can be observed. Gypsum additions between 7 % C_3A replacement to 40% were studied. The compositions of all the C_3A-gypsum samples presented in this study are given in Table 3-1.

Table 3-1: Names and compositions of the C_3A-gypsum samples

BATCH A	wt% C_3A (batch 16)	wt% gypsum (Merck)	mol% gypsum	Molar ratio $C\$H_2/C_3A$
C3A_7%G	93	7	10.57	0.12
C3A_12%G	88	12	17.63	0.21
C3A_20%G	80	20	28.18	0.39
C3A_27%G	73	27	36.73	0.58

BATCH B	wt% C_3A (batch 23)	wt% gypsum (Merck)	mol% gypsum	Molar ratio $C\$H_2/C_3A$
C3A_10%G	90	10	14.85	0.17
C3A_20%G	80	20	28.18	0.39
C3A_35%G	65	35	45.81	0.85

BATCH C	wt% C_3A (batch 38)	wt% gypsum (Merck)	mol% gypsum	Molar ratio $C\$H_2/C_3A$
C3A_10%G	90	10	14.85	0.17
C3A_30%G	70	30	40.22	0.67
C3A_40%G	63	40	51.14	1.05

The x-ray diffraction patterns, the SEM images, particles size distributions and calculated specific surface areas of the powders are reported in CHAPTER 2.

The experiments carried out on these samples are summarized in Table 3-2.

Table 3-2: Summary of the C$_3$A-gypsum samples and experiments carried out

Samples\ experiments	Phase assemblage (XRD)	Microstructure (SEM)	Kinetics (calorimetry)
C3A_7%G (Batch A)			@20°C
C3A_12%G (Batch A)			@20°C
C3A_20%G (Batch A)			@20°C
C3A_27%G (Batch A)			@20°C
C3A_10%G (Batch B)	In-situ at early ages @26°C + slices at later ages	1d, 3d, 7d, 28d	@20, 26, 30 °C
C3A_20%G (Batch B)	In-situ at early ages @26°C + slices at later ages	3d, 7d, 28d	@20, 26, 30 °C
C3A_35%G (Batch B)	In-situ at early ages @26°C + slices at later ages	3d, 7d, 28d	@20, 26, 30 °C
C3A_10%G (Batch C)			@20°C
C3A_30%G (Batch C)			@20°C
C3A_40%G (Batch C)			@20°C
C3A_20%G (Batch D)		Evolution up to 35h	

3.3   Phase assemblage of C$_3$A-gypsum systems

In-situ XRD was used to follow the phase evolution during the first hours of hydration and the results obtained were compared to the calorimetric curves. The evolution of the phase assemblage at early ages was monitored for the three samples of Batch B: C3A_10G, C3A_20G and C3A_35G, respectively low, intermediate and high gypsum content samples by in-situ XRD with the kapton method that consists of collecting XRD patterns every 15 min of a hydrating sample. To avoid contact with CO$_2$ and extensive drying, the sample is covered by a kapton foil as described in Chapter 2. The evolutions of the phase assemblage during the first hours of hydration for the three samples are presented in Figure 3-6. It has to be noted that the experiments were carried out at a temperature of 26°C due to constrain of the experimental device. Moreover, even if great care was taken in order to carry out in-situ XRD and calorimetric measurements at the same temperature, a delay of the exothermic peak compared to the reactions measured by XRD can be observed. This delay was observed for the three studied samples. It is thought that this acceleration of the reaction measured by XRD may be due to an increase of the temperature in the vicinity of the sample in the XRD chamber probably caused by the heat developed by the sample during hydration. Therefore, both effectively measured in the calorimeter (plain curve) and presumed calorimetric curve of the XRD samples (dot curve) were represented in Figure 3-6.

The evolution of the phase assemblage at later ages was investigated by preparing a cylinder of C$_3$A-gypsum paste and cutting slices at certain time for X-ray diffraction. Generally samples aged 1, 3 and 7 days were investigated. The XRD patterns of the samples C3A_35G, C3A_20G and C3A_10G are reported in Figure 3-7. Even if great care was taken to refill the sample containers with nitrogen after each measurement, all the samples showed some carbonation with hemicarboaluminate present in the systems.

In the figures presented in this chapter the following abbreviations are used to label the phases:

C3A = tricalcium aluminate = C$_3$A   *Gypsum* = C\$H$_2$

Ettringite = C$_6$A\$$_3H_{32}$ *AFm 14* = monosulfo-AFm type 14 = C$_4$A\$H$_{14}$

AFm 12 = monosulfo-AFm type 12 = C$_4$A\$H$_{12}$ *H-AFm* = hydroxy-AFm = C$_4$AH$_{19}$/C$_2$AH$_8$

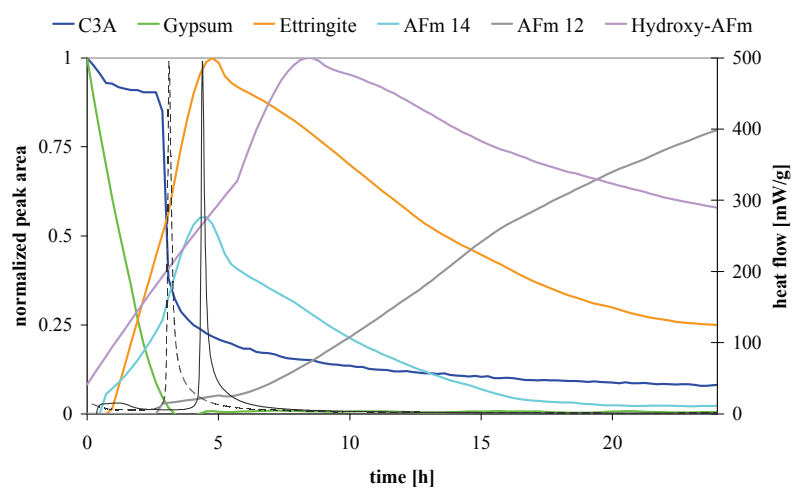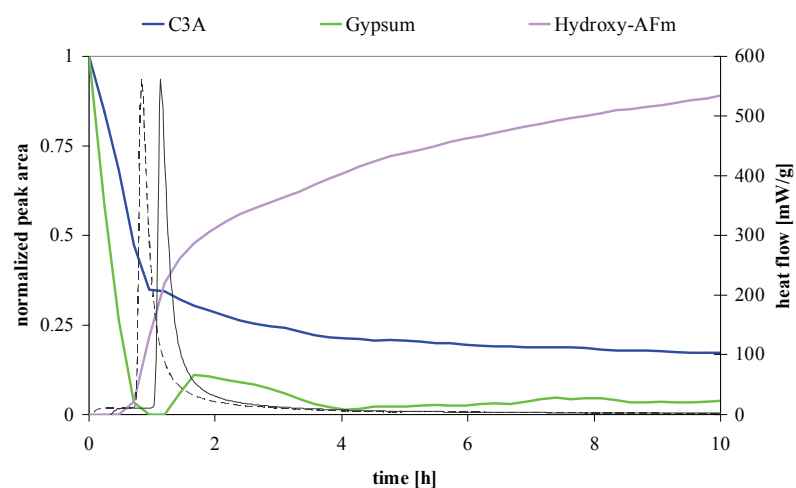*C$_3$AH$_6$* = hydrogarnet   *H-carbo* = hemicarboaluminate
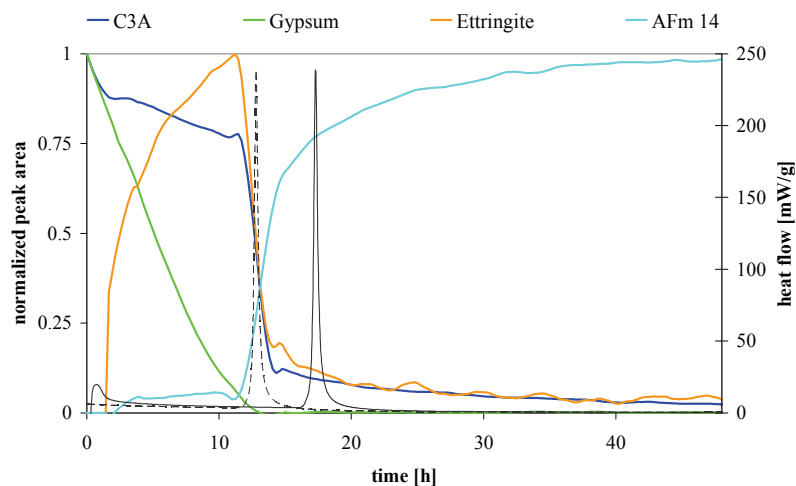
Figure 3-6: Evolution of the phase assemblage during the first hours of hydration measured by in-situ XRD for three gypsum additions. The evolution of the phase assemblage depends on the initial gypsum content. The calorimetric curves of these systems are also represented on the plots. The measured (plain line) curve and presumed curve (dot line) due to a possible modification of the temperature in the XRD chamber are plotted.
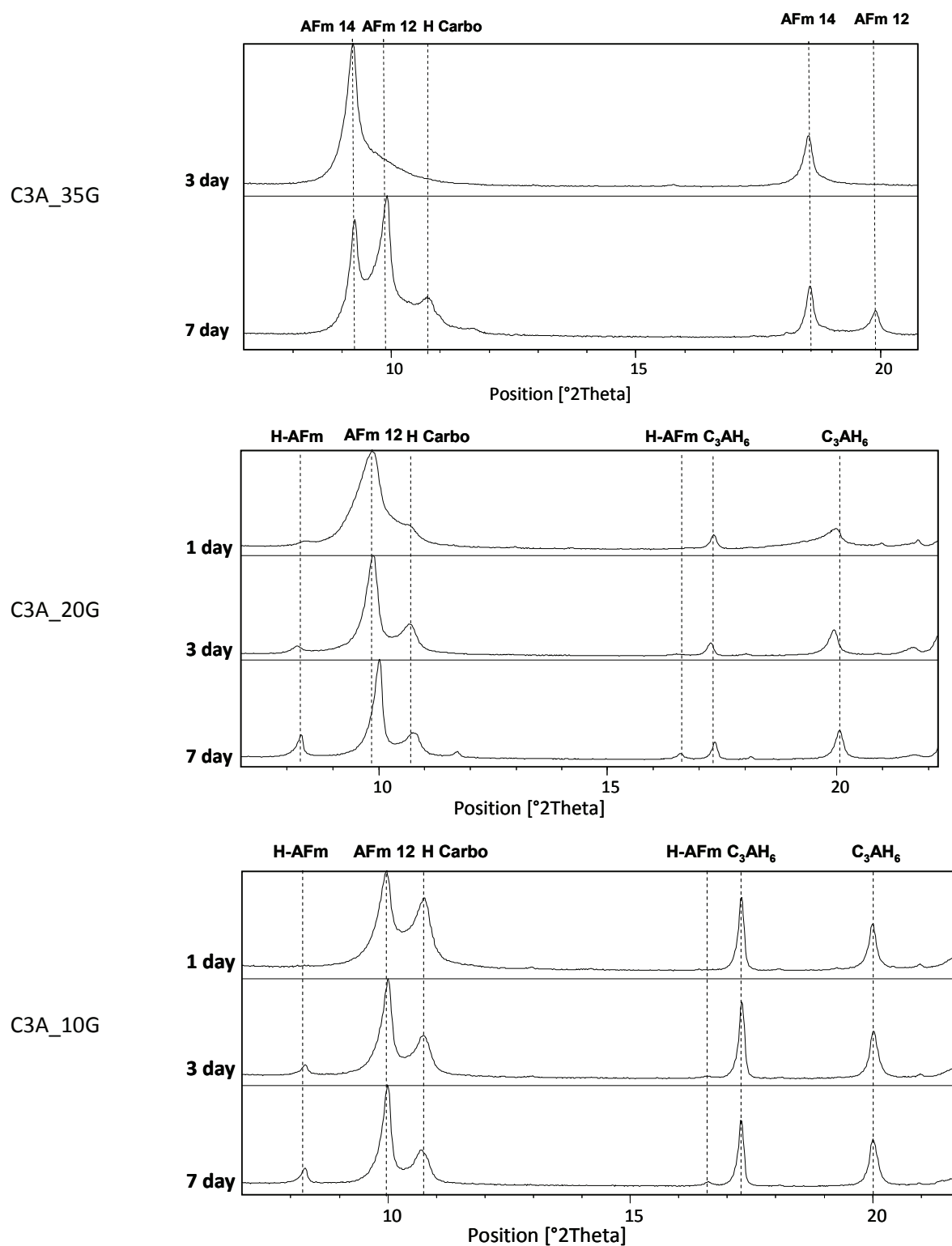
Figure 3-7: Evolution of the phase assemblage at later ages measured on sliced set samples. Hydrogarnet was observed at later ages in the samples that contain the metastable hydroxy-AFm phases at early ages. Some carbonation was observed even if great care was taken to fill the sample containers with nitrogen.

As expected, different phase assemblages were observed depending on the initial gypsum content of the sample. For the samples with high gypsum content (C3A_35G), ettringite is the only hydrate formed during the first period of hydration (Figure 3-6). Some authors reported the formation of AFm phase at early ages [8, 9, 11, 21] . These phases were not observed here, probably due to their poor crystallinity and the small amount that is formed. After gypsum depletion, ettringite and C_3A dissolve to form monosulfo AFm ($C_4A\$H_{14}$). At later ages (Figure 3-7), when less water is present in the systems, monosulfoaluminate type 12 ($C_4A\$H_{12}$) was observed instead of monosulfo AFm type 14 ($C_4A\$H_{14}$). For this sample with high gypsum content no AFm hydrates other than monosulfo were observed at later ages (except hemicarboaluminate due to carbonation as previously described).

For the sample C3A_10G, only hydroxy-AFm (C_4AH_{19} and /or C_2AH_8) were observed after gypsum consumption due to the lower gypsum content. A very small peak of ettringite (too small to be reported in Figure 3-6) was observed before gypsum depletion. After gypsum depletion, the sulfate ions present in the systems are incorporated in solid solution in the hydroxy-AFm phase. Indeed, many studies, the most recent being the work of Matschei et al. [10], have reported the possible formation of solid solutions between hydroxy-AFm and monosulfo-AFm phases. Hydrogarnet peaks were present in the XRD pattern at later ages (Figure 3-7). The hydrogarnet phase is formed from the evolution of the metastable hydroxy-AFm phases C_4AH_{19} and C_2AH_8. Some monosulfo-AFm 12 was also observed at later ages. This later formation of monosulfoaluminate can come from the fact that the hydroxy-AFm phases (C_4AH_{19} and/or C_2AH_8) that contain sulfate ions have evolved into hydrogarnet. As this last phase is not able to incorporate sulfate ions like hydroxy-Afm phases, the sulfate ions become available to form monosulfo-AFm.

The samples C3A_20G show an intermediate phase assemblage between the C3A_35G and the C3A_10G sample. As expected, ettringite is the only hydrate detected during the first period of hydration (Figure 3-6). After gypsum consumption C_3A and ettringite dissolve and both monosulfo-AFm and hydroxy- AFm (C_4AH_{19} and /or C_2AH_8) are formed. But only very small peaks due to the reflexion of hydroxy-AFm were observed in the original XRD patterns. As a miscibility gap exists in the solid solution series between monosulfoaluminate and hydroxy-AFm, both phases can co-exist [10]. The plots of the evolution of the phase assemblage reported in the present work do not show quantification of the phases with respect to the overall composition only their relative own evolution is presented. However, when a particular phase was present in the system in small quantities, very noisy evolution curves were obtained, as it is the case for ettringite in Figure 3-6 for the sample C3A_35G. The hydroxy-AFm formed in the sample C3A_20G after gypsum depletion seems to not be

stable and dissolves slowly as the hydration proceeds. This phase is probably formed in areas where the concentration of sulfate ions is low due to the rapid dissolution of C_3A compare to ettringite. Then, when the sulfate content increases, due to ettringite dissolution, hydroxy-AFm becomes unstable with respect to monosulfo AFm and dissolves. A solid solution of hydroxy-AFm with monosulfo AFm is then probably present. The resolution of the obtained XRD pattern and the peak shift that is induced by the shrinkage of the paste during hydration did not allow us to observe the small shift of monosulfo AFm peaks due to the solid solution. At later ages (Figure 3-7) hydrogarnet was also observed in the sample. For this sample, monosulfoaluminate type 12 appears already at early ages.

For the sample C3A_20G, ettringite starts to dissolve after gypsum consumption but at a slower rate than in the case of the C3A_35G sample. As some drying of the sample (that lead to a slow down of the reaction) may occur, the experiment was repeated with a similar sample (C3A_20%G (Batch C)). The same phase assemblage was observed: formation of monosulfoaluminate type 14 and 12 as well as hydroxy-AFm after gypsum consumption. However, in this case ettringite dissolves rapidly after gypsum consumption together with C_3A (Figure 3-8) as observed for the sample C3A_35G in the first experiment.
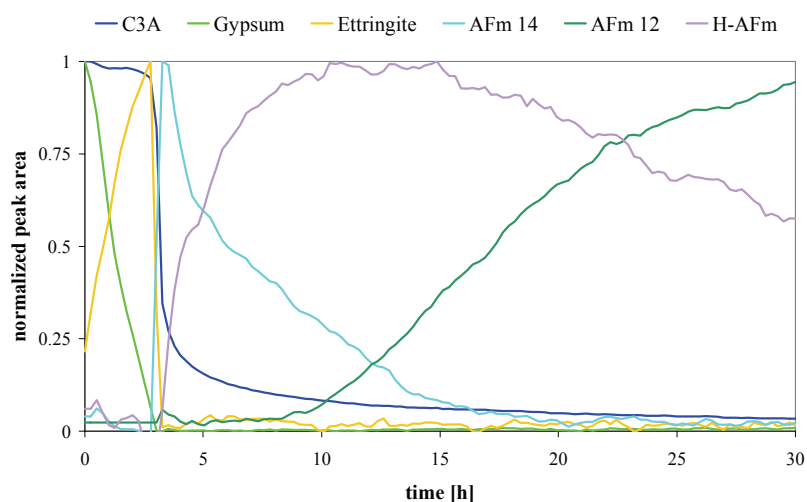

Figure 3-8: Evolution of the phase assemblage for a C3A_20%G sample measured by in-situ XRD (Second experiment). In this case ettringite dissolves rapidly after gypsum consumption.

In this work it was observed the C_3A and ettringite dissolve rapidly and simultaneously right after gypsum depletion. Meaning that ettringite is unstable rapidly after the depletion of gypsum in the system. Contrary to the work of Minard et al. [9] that reported that the dissolution of ettringite does not occur directly after gypsum depletion and that the formation of monosulfoaluminate is a slow process, in this study it can be clearly seen that this reaction occurs rapidly.

3.4 Microstructural development

This chapter presents the development of the microstructure after gypsum consumption, with special interest on the localization of the hydrates in the microstructure and their chemical composition depending on the gypsum content.

In the first part of this section, the development of the C_3A-gypsum paste with intermediate gypsum content is presented. Then, in a second part, the influence of the gypsum content on the microstructure is discussed. The microstructural study of these pastes was carried out by scanning electron microscopy (SEM) on polished sections.

3.4.1 Microstructural development of a C_3A-gypsum paste

The microstructural development of a C3A_20G sample was studied at different ages over the first days of hydration. The composition of the hydrates was investigated by EDS microanalyses. The results were statistically analyzed and plotted on Al/Ca vs. S/Ca ratio graphs. This representation leads to identification of phases or mixture of phases: when the points lie on the line joining the composition of two phases, we assume that we have a mixture of these phases. The heat evolution of this system was measured by isothermal calorimetry (Figure 3-9) at the same temperature of the room where the samples for microscopy where stored (22°C – controlled temperature). In these conditions the exothermic peak induced by C_3A reaction after gypsum depletion to form monosulfoaluminate and/or hydroxy-AFm occurs at 10-11 hours of hydration.
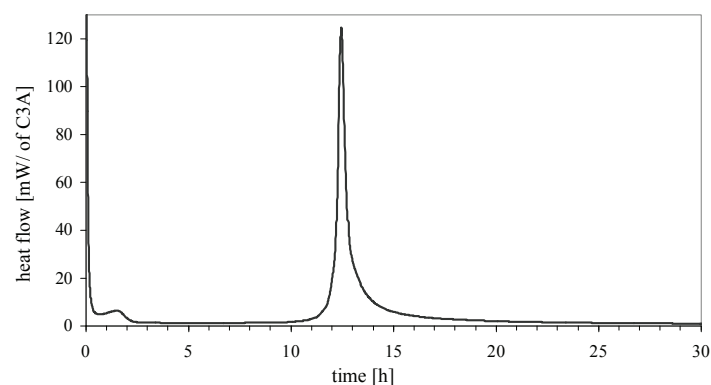

Figure 3-9: Heat evolution curve at 22°C of the C3A_20G system used for the microstructural study. The exothermic peak characteristic of the second stage occurs at 10-11h of hydration.

During the first period of hydration, in the presence of gypsum, little hydration product was present close to the C_3A grains as shown in the microstructure in Figure 3-10. Just before gypsum depletion, mainly ettringite was detected in the matrix by EDS analysis (Figure 3-10). Some monosulfo AFm was already present at 9 hours of hydration, probably in areas where the sulfate content was locally low.

Between 9 and 12h of hydration a significant densification of the matrix was observed (Figure 3-11). This densification occurs after gypsum depletion when there is a surge in the hydration of the remaining C_3A. At 12 hours of hydration no more ettringite was detected by EDS analyses, only hydrates with a composition dispersed between the compositions of monosulfo AFm and the hydroxy-AFm C_4AH_{19} and C_2AH_8 were present in the matrix (Figure 3-11). The XRD analysis of a similar sample (described in Figure 3-6) showed the presence of both hydroxy-AFm and monosulfo-AFm in the samples. Therefore the microstructure may be composed of finely intermixed hydroxy-AFm and monosulfoaluminate or, as previously described, solid solutions can form.
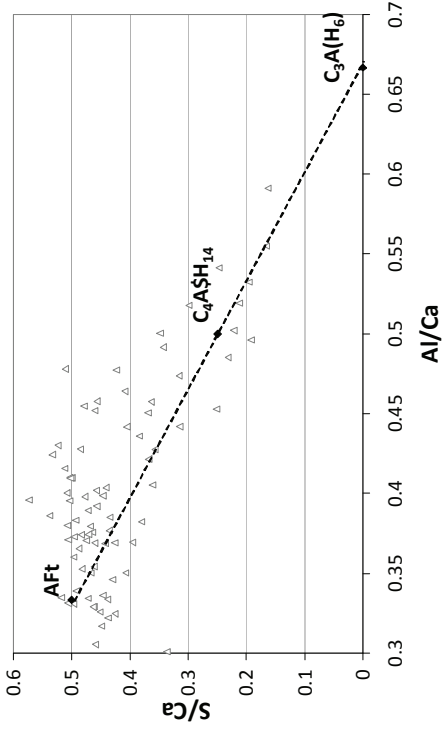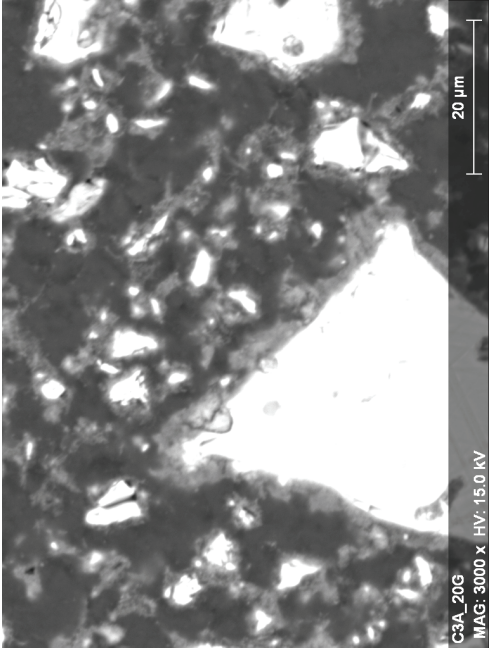
Figure 3-10: SEM image and EDS analysis at 9h of hydration (Sample C3A_20G). Mainly ettringite was detected by EDS analysis at 9h of hydration (before the exothermic peak)
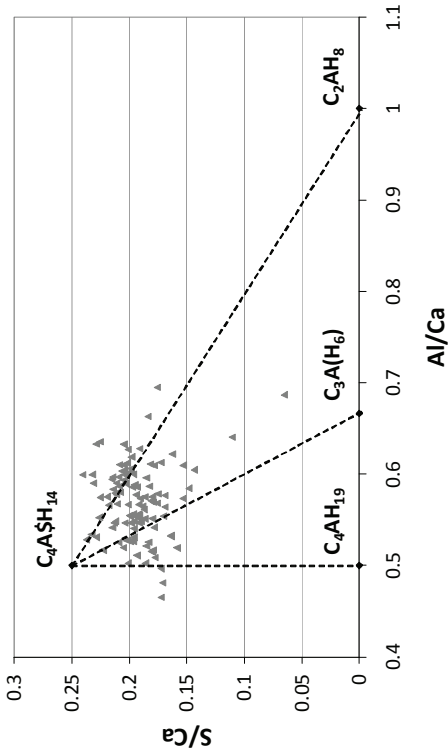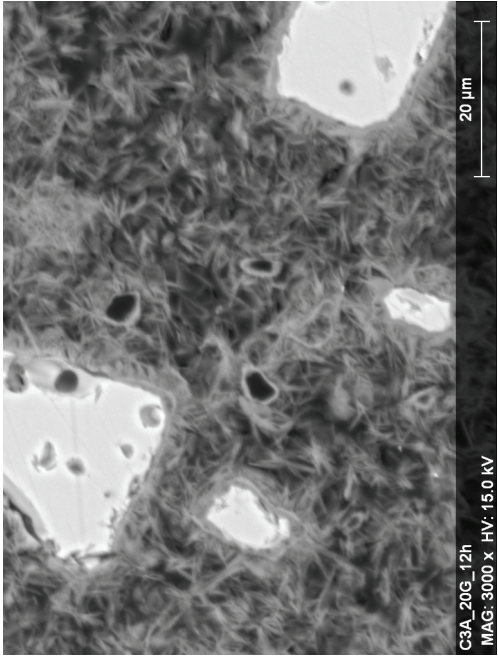

Figure 3-11: SEM image and EDS analysis at 12h of hydration (Sample C3A_20G). A solid solution (or a mixture) of monosulfo and hydroxy-AFm phases was detected by EDS analysis at 12h of hydration (after the exothermic peak). A significant densification of the matrix can be observed in the SEM images.

Close to the dissolving grains, hydrates that are packed more densely than the hydrate formed in the space between the grains were observed. These dense regions seem to develop within the original grain boundaries as the hydration proceeds (Figure 3-12 at 21h of hydration). EDS microanalysis of this "dense inner hydrate" at 21 hours of hydration showed that its chemical composition is very close to the one of the matrix hydrate but with a slightly lower sulfate content (Figure 3-13). The difference in the composition is probably due to the close presence of the C_3A grain. The C_3A grain may have affected the EDS analyses, but it is also that areas close to C_3A grains may have a lower sulfate content compare to the matrix hydrates. Solid solutions with a lower amount of sulfate are then possible in the vicinity of dissolving C_3A.
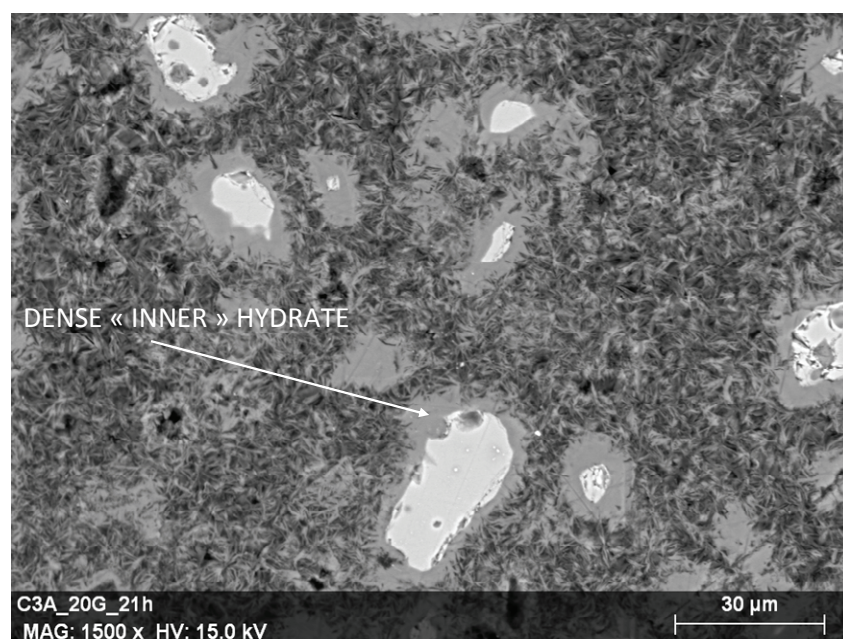
Figure 3-12: SEM image at 21h of hydration (Sample C3A_20G). The formation of a denser product within the C_3A grain boundaries can be observed.
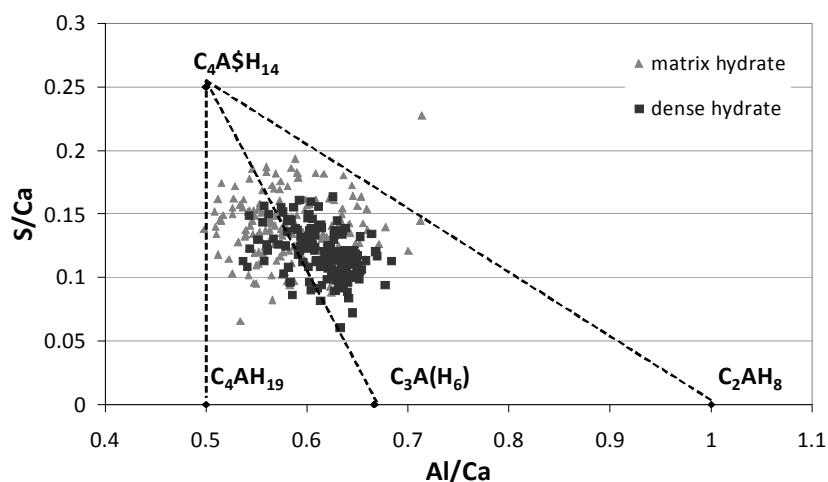

Figure 3-13: EDS analysis at 21h of hydration (Sample C3A_20G). Similar chemical compositions of the matrix and dense product were measured.

From 24 hours of hydration, another product forming a thin rim around the dense hydrate was observed in the microstructure (Figure 3-14). At 35h of hydration this layer was even thicker (Figure 3-15).
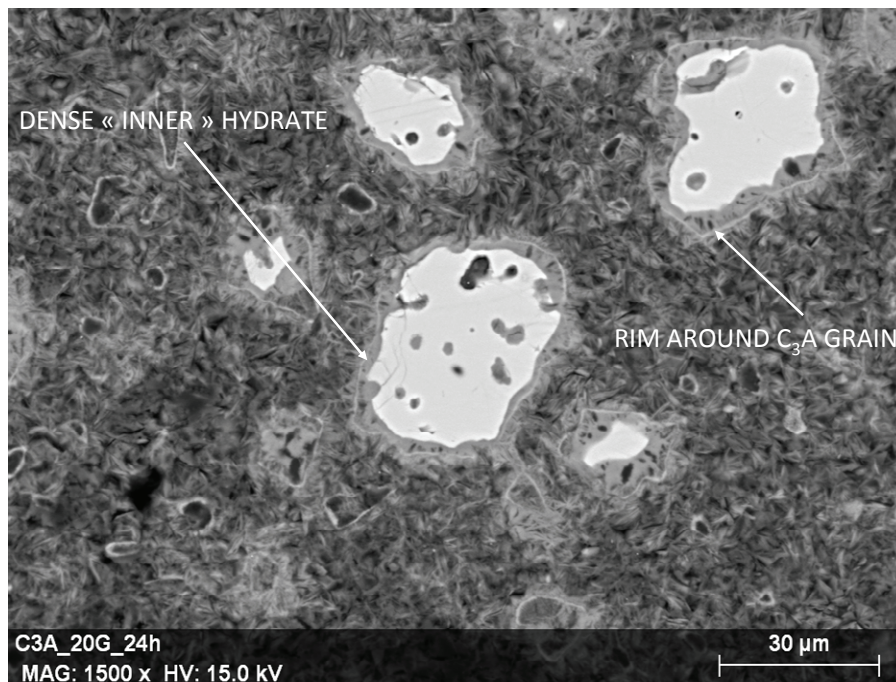

Figure 3-14: SEM image at 24h of hydration (Sample C3A_20G). Hydrogarnet precipitate as a rim around C$_3$A grains.
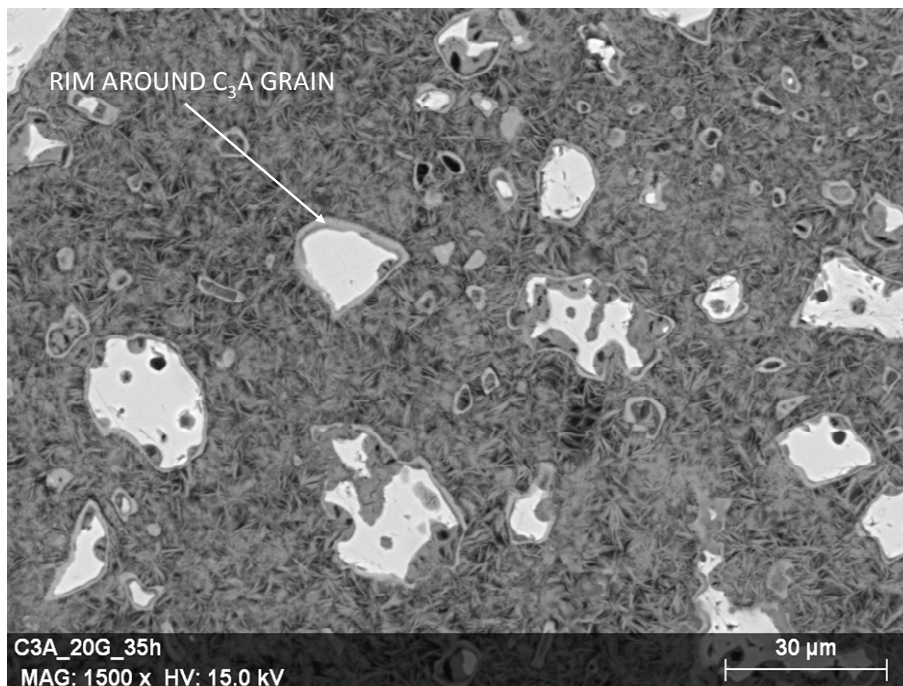

Figure 3-15: SEM image at 35h of hydration (Sample C3A_20G). At 35h of hydration the hydrogarnet rim around C$_3$A grains is thicker.

This hydrate was identified by EDS analysis as C_3AH_6 (Figure 3-16). It is hypothesized that the hydrogarnet layer is located at the original C_3A grain boundaries. Indeed, at the very beginning of the reaction several authors observed the formation of hydroxy-AFm phases on the C_3A surface [8, 9, 11]. As these AFm phases are metastable, they may have converted at later ages to hydrogarnet remaining where they originally formed. EDS analyses of the hydrogarnet layer show the presence of sulfur in the hydrogarnet rim, but it has to be kept into mind that this layer of hydrate is very thin and the products present around the analyzed point may have influenced the EDS results.
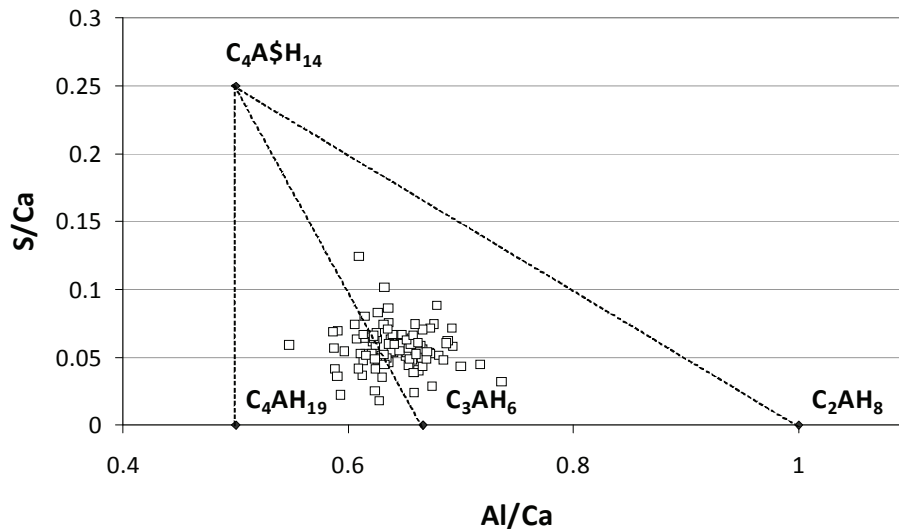

Figure 3-16: The EDS analysis of the rim of hydrate (see Figure 3-15) around the C_3A grains at 35h of hydration indicate a composition very close to hydrogarnet (C_3AH_6) . (Sample C3A_20G)

Comparing EDS analysis carried out on the samples at 21h and 35h of hydration it was observed that the difference in chemical composition of the "matrix" and the "dense" products increases as hydration proceeds. Hydrates richer in sulfate preferentially form at distance from the C_3A grains.
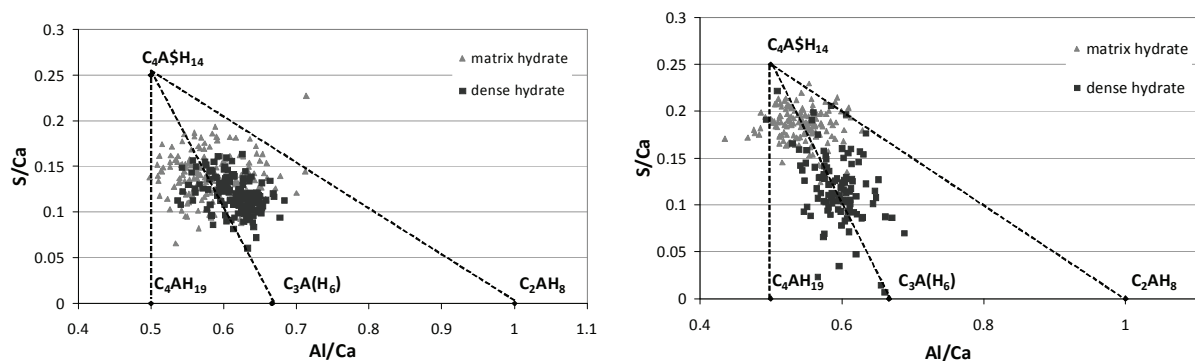

Figure 3-17: Comparison of the chemical composition of the dense and matrix hydrates at 21h and 35h of hydration (Sample C3A_20G). As the hydration proceeds, the difference in the chemical composition between the matrix and dense "inner" product is more pronounced. Solid solutions with higher sulfate content tend to form at distance from the C_3A grains.

3.4.2 Influence of the gypsum content on the microstructural development

In order to study the influence of the gypsum content on the microstructure of C_3A-gypsum pastes samples containing 10, 20 and 35% of gypsum were prepared with C_3A from Batch B.

At 3 days of hydration the microstructure of the sample containing intermediate gypsum content (20%) had a microstructure very similar to the sample described in section 3.4.1. The same matrix and dense hydrates are present in the microstructure with similar chemical compositions (Figure 3-18 (middle)). Both hydrates are probably finely intermixed or present as solid solution of monosulfoaluminate and hydroxy-AFm with lower sulfate content in the dense product as described previously. The hydrogarnet shell is also present at the original grain boundaries. However, this shell seems to be thinner at this point of the hydration than for the systems previously described. This is probably due to the different reactivity of the C_3A coming from different batches.

Quite a similar microstructural development was observed for the sample with high gypsum content except that no hydrogarnet shell was present in the microstructure (Figure 3-18 (right)). Only the dense product or empty grains surrounded by monosulfoaluminate were observed. However, the chemical composition and the morphology of the hydrates vary significantly. The composition of the matrix hydrate is very close to the stoichiometric composition of monosulfoaluminate and the dense product seemed to be a solid solution between monosulfoaluminate and C_4AH_{19} with higher sulfate content with respect to the composition of the same hydrate in the sample with intermediate gypsum content. The morphology of the hydrates is also different. The AFm platelets of the matrix hydrate seems to be shorter than the platelets observed for the samples with intermediate gypsum content (Figure 3-19). This maybe because less space is available in the paste during the second stage of the reaction for samples with higher initial gypsum content due to the fact that more ettringite is formed during the first stage of the reaction.

At low gypsum content the microstructure was drastically different compare to the other two systems (Figure 3-18 (left)). The three hydrates observed for the others gypsum replacements (matrix hydrate, dense product and hydrogarnet shell) are also present but in different amounts. The paste is mainly composed of thick hydrogarnet shells with little matrix product. The AFm platelets of the matrix hydrates are even more elongated than the ones observed for the samples with intermediate gypsum content (Figure 3-19).
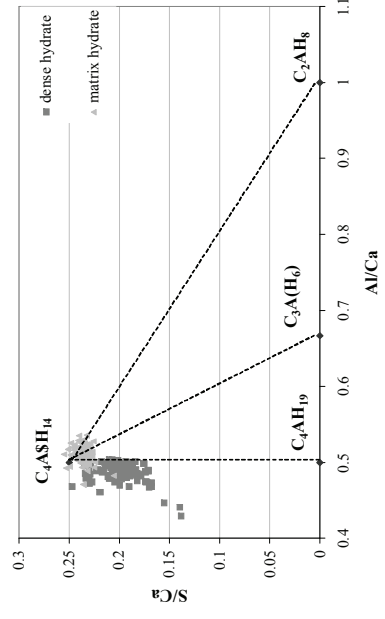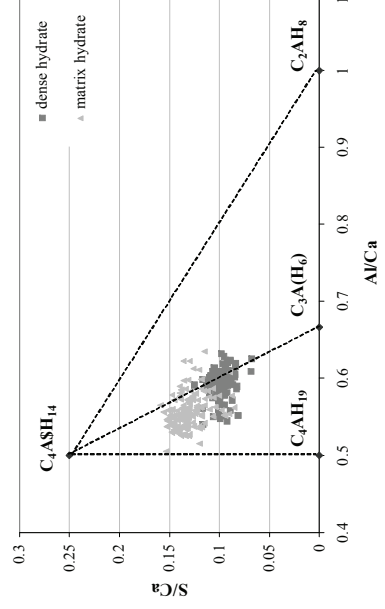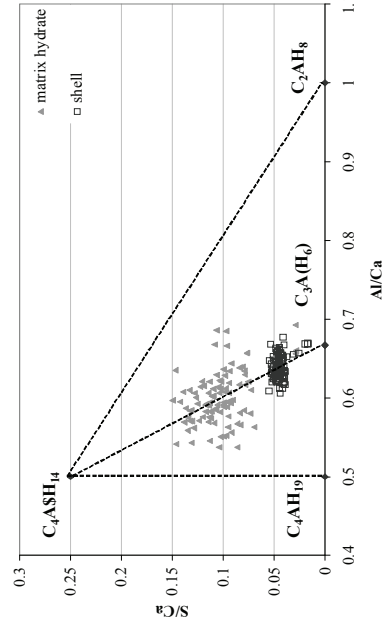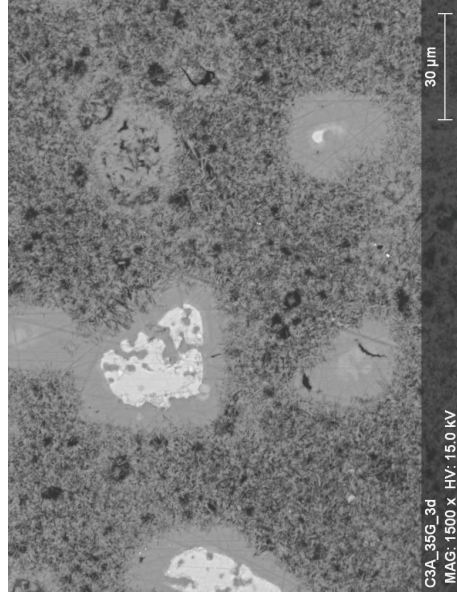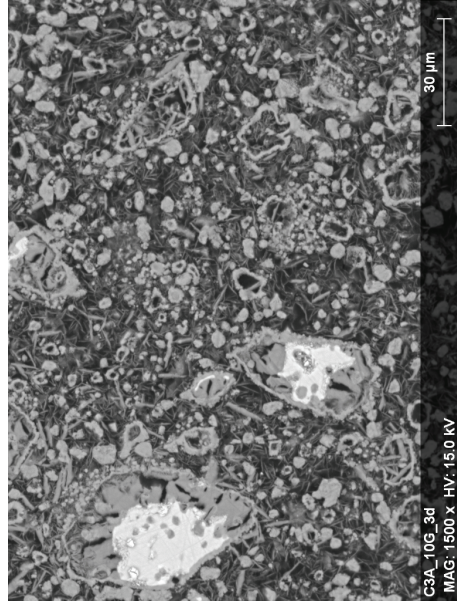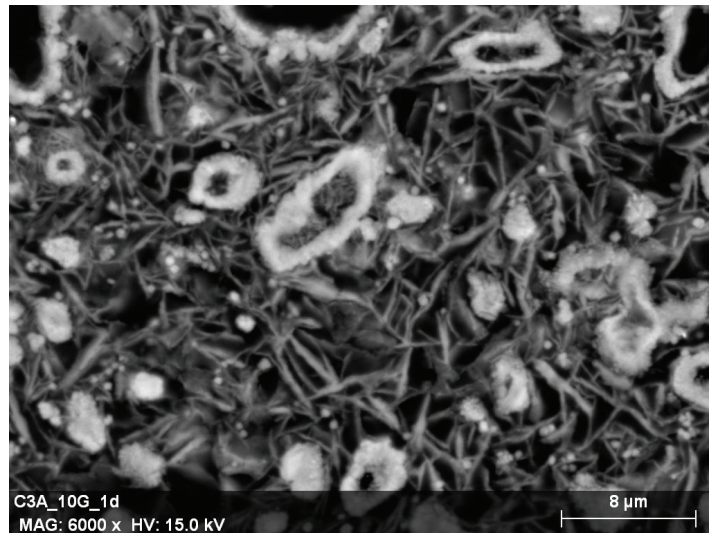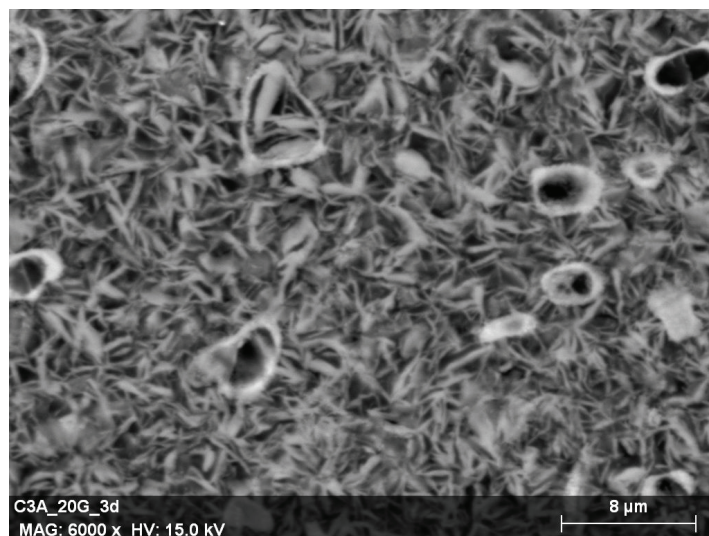
Figure 3-18: SEM images and EDS analysis for the samples C3A_10G (left), C3A_20G (middle) and C3A_35G (right). Different microstructure and different chemical compositions of the hydrates can be observed depending on the initial gypsum content.

46

C3A_10G
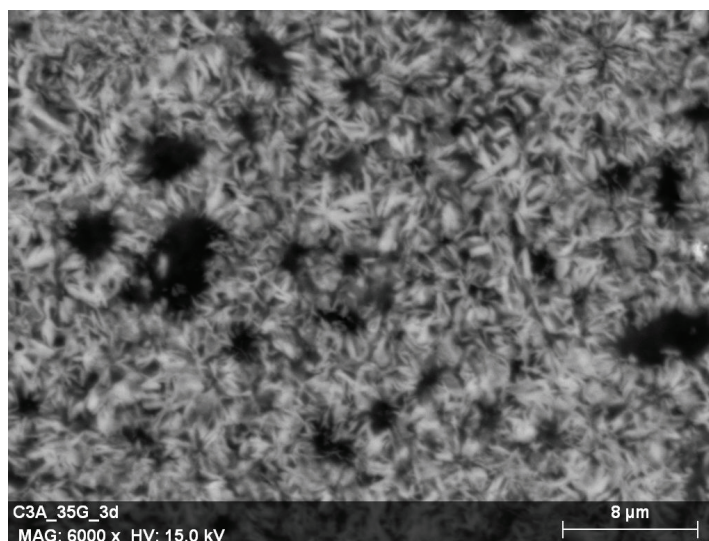
1d

C3A_20G

3d

C3A_35G

3d

Figure 3-19: Different morphologies of the matrix hydrates depending on the gypsum content were observed. Longer AFm platelets form in the systems containing lower gypsum additions.

3.4.3 Evolution of the microstructure at later ages

At later ages the hydration had continued. For the samples with intermediate gypsum content, most of the C_3A grains are fully hydrated and only the dense "inner" product surrounded by hydrogarnet shells remain where the original grains were (Figure 3-21 (middle)). However, the presence of the dense "inner" product is less obvious at 28 days. Only the bigger C_3A grains are still surrounded by this hydrate, while around the smaller grains, only a hollow hydrogarnet shell remains in the microstructure. It seems therefore that this hydrate dissolves and re-crystallizes as hydrogarnet and/or matrix product at later ages. The composition of the matrix hydrate remains unchanged.

For the sample with high gypsum content, the same features are observed. At 28 days of hydration, almost no dense product remains in the microstructure. Only some traces can be observed around the bigger C_3A grains. The microstructure is composed of many empty spaces surrounded by monosulfoaluminate that are the relic of the fully hydrated C_3A grains. The chemical composition of the matrix hydrate is unchanged (Figure 3-21 (right)).

For the low gypsum content sample, also, the dense inner product had almost completely disappeared of the microstructure at 28 days of hydration. Thick hydrogarnet shells and few platelets of AFm phase are present. (Figure 3-21 (left)). The composition of the matrix product, the AFm platelets, had evolves toward monosulfoaluminate composition compare to the hydration product analyzed at 3 days of hydration. As already observed by XRD (Figure 3-7) the sulfate groups present in solid solution with hydroxy-AFm may became available to form monosulfo-AFm when the hydroxy-AFm phases evolve into hydrogarnet.

The modification of the dense "inner" hydrate (that occurs for the three studied compositions) can be better observed in Figure 3-20 for the sample C3A-35G. Less "inner" product can be observed in the microstructure at 28 days of hydration.
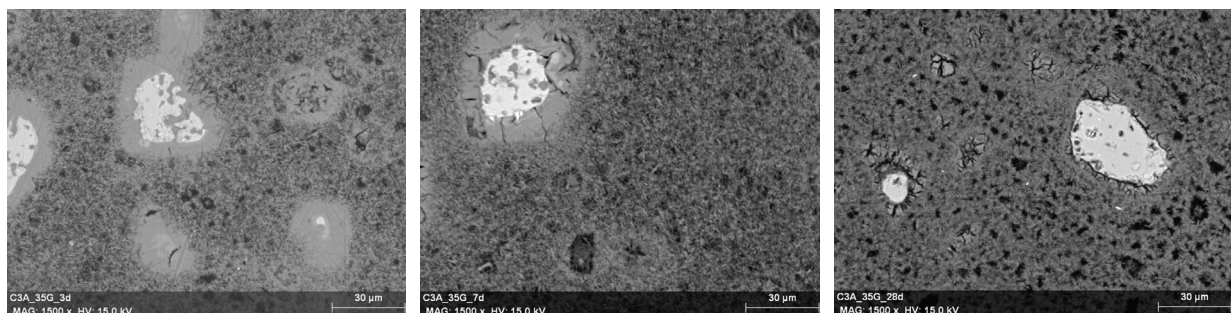

Figure 3-20: Evolution of the dense inner hydrate for the sample C3A-35G at 3, 7 and 28days of hydration. The presence dense product is less obvious at later ages. A re-crystallization as matrix product can be hypothesized.
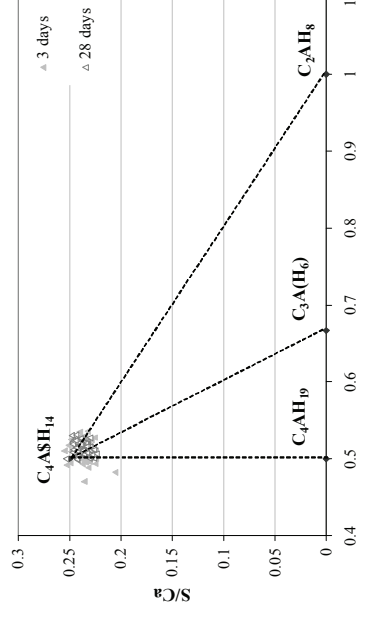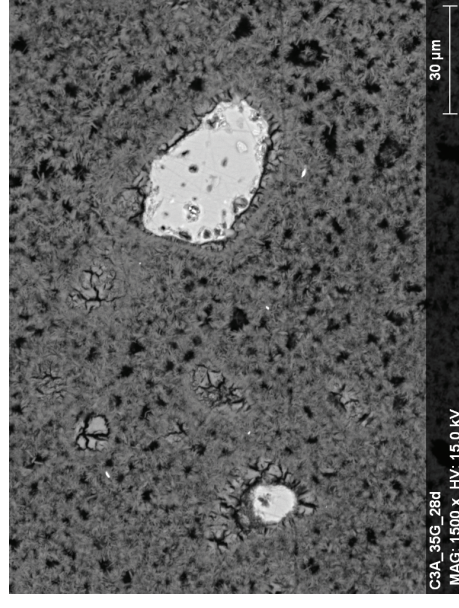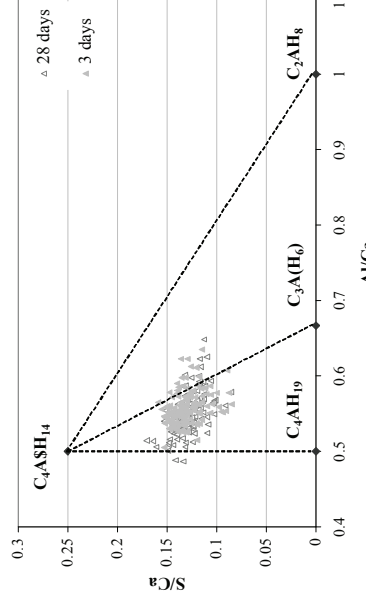
Figure 3-21: SEM images and EDS analysis of the samples at later ages. Samples C3A_10G (left), C3A_20G (middle) and C3A_35G (right). The hydrogarnet shells are thicker and the dense "inner" product is less obvious than at earlier ages. The chemical composition of the matrix product is not modified at later ages except for the sample C3A_10G were solid solution closer to monosulfoaluminate were measured at 28 days of hydration.

3.4.4 Conclusions on influence of the gypsum content on the phase assemblage and microstructural development of C_3A-gypsum pastes
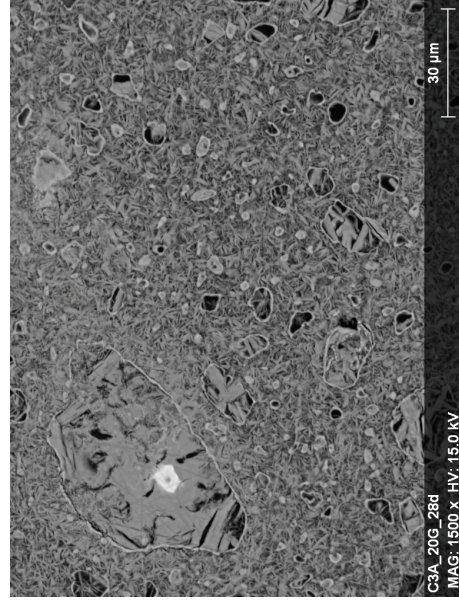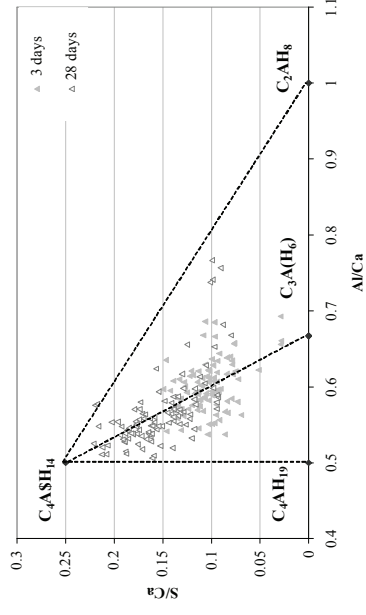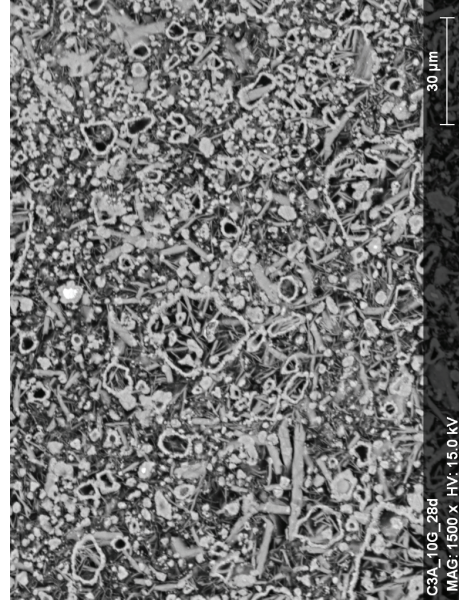
When gypsum is still present in the system, ettringite is the only crystalline hydrate formed in all the studied samples. Some authors reported the formation of AFm phases at the beginning of the reaction [8, 9, 11, 21]. In the present study this phase was not observed by XRD, probably because it is a poorly crystalline phase and its amount is very small. This study shows that the phase assemblage generated after gypsum depletion strongly depends on the gypsum content of the original mix. In pastes with high gypsum contents monosulfo AFm forms, while with low gypsum contents hydroxy-AFm was identified as the main hydrate. In the paste with intermediate gypsum content, both hydroxy- and monosulfo AFm phase were observed. Solid solutions between these hydrates can exist [10] and are probably formed in the studied samples as suggested by the EDS analysis that show that the matrix hydrate has a composition between monosulfoaluminate and hydroxy-AFm phases.

EDS analysis reported also that the chemical composition of the matrix product that fill the space between the C_3A grains varies significantly with the initial gypsum content of the sample (Figure 3-22).
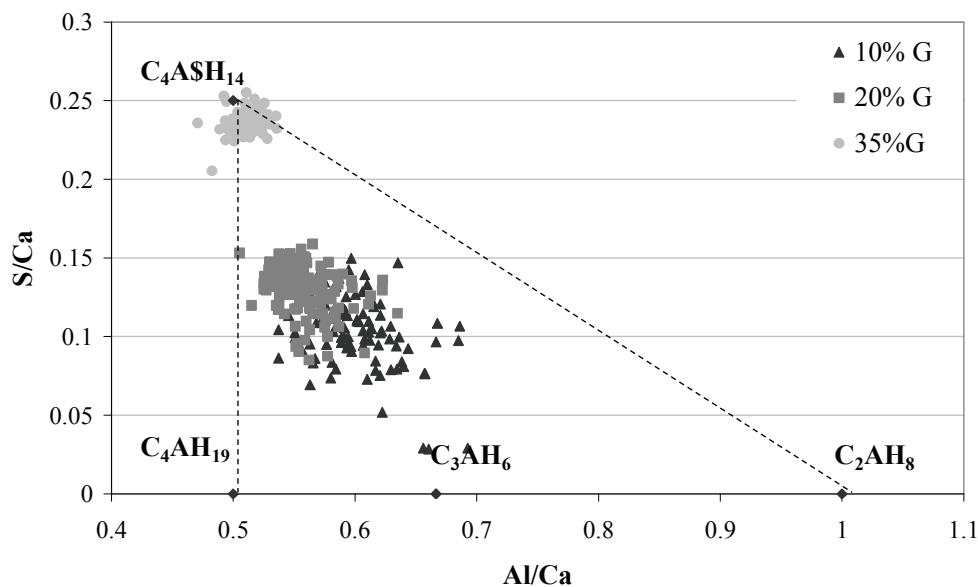

Figure 3-22: Comparison of the composition of the matrix hydrates for the samples containing 10%, 20% and 35% of gypsum. Solid solutions between monosulfo and hydroxy-AFm phases containing more sulfate form in systems with higher initial gypsum content.

50

The microstructural study shows that the AFm phases precipitates as platelets that fill the space between the C_3A grains, but also as a denser hydrate that seems to form within the original grain boundaries. This hydrate has a chemical composition similar to the matrix product, but with slightly lower sulfur content. The microstructural development of C_3A-gypsum pastes show therefore similar features to C_3S and cement hydration with the precipitation of hydrates that fill the space between the grains and the development of a dense product within the original grain boundaries. However, in the case of C_3A-gypsum pastes, the inner product seems to be less present in the microstructure at later ages. It is hypothesized that this hydrate re-crystallizes as matrix hydrate or hydrogarnet. When hydroxy-AFm phases were present, hydrogarnet formed at later ages. This phase was observed to grow at the original grain boundaries as a thin shell around the C_3A grains.

The morphology of the AFm platelet is influenced by the initial gypsum content. With decreasing sulfate amount, the platelets of AFm that form in the space between the grains were observed to be longer. This maybe because more space is available in the paste at this point of the reaction as less ettringite is formed during the first stage of the reaction for samples with lower initial gypsum content.

In terms of kinetics of the reaction, this work clearly shows that the dissolutions of C_3A and ettringite to form monosulfoaluminate and/or hydroxy-AFm occur simultaneously and rapidly after the depletion of gypsum. Ettringite is therefore not stable as soon as the gypsum id depleted.

3.5 Kinetics of the C$_3$A-gypsum reaction

The hydration kinetics of the three batches of C$_3$A with gypsum additions was investigated by isothermal calorimetry. The heat evolution curves as well as the cumulative heat curves are reported in Figure 3-24 to Figure 3-29.

As expected, the time of occurrence of the exothermic peak is delayed as the gypsum content increases. In Figure 3-23 (left) the time necessary for sulfate consumption has been plotted vs. the initial amount of gypsum, it can be observed that Batch B and C follow a same trend while Batch A reacts at a slower rate, more time is necessary to consume the same amount of gypsum. The main difference between Batches B/C and Batch A is the specific surface area of the C$_3$A. C$_3$A from Batches B and C are finer. If the time necessary for the sulfate consumption is normalized by the initial specific surface area, all the Batches follow a more similar trend as presented in Figure 3-23 (right).

The normalization was obtained with the following formula:

$$Normalized\_time = time \cdot \frac{specific\ surface\ area}{mean\ specific\ surface\ area}$$
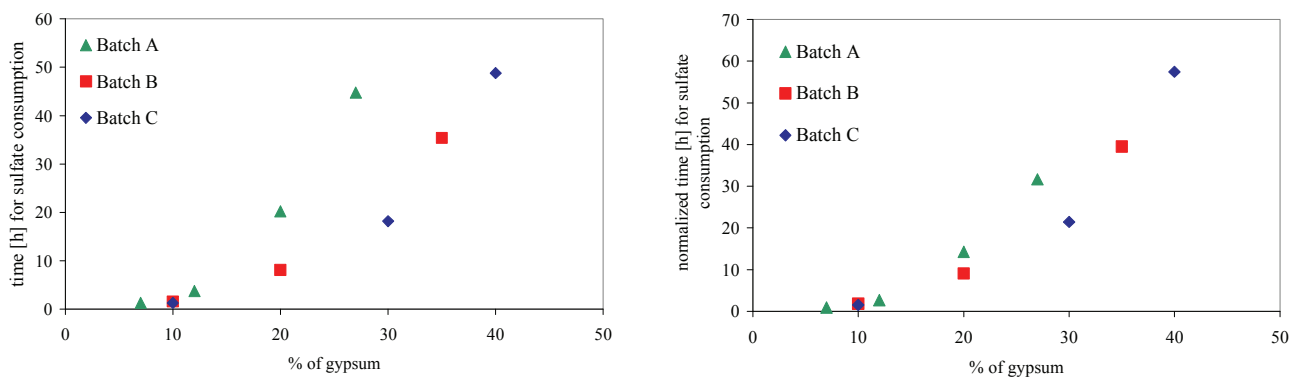
Figure 3-23: Time for sulfate consumption vs. gypsum content without (left) and with (right) normalization with initial specific surface area of the C$_3$A powder. Similar trend of the hydration rate were obtained after normalization for all the batches.

This observation are consistent with the findings of Minard et al. [9] that shows that the hydration rate during the first step of the reaction is controlled by C$_3$A dissolution which depends on its specific surface area.

Figure 3-24: Heat evolution curves of C₃A-gypsum systems (Batch A)

Figure 3-25: Heat evolution curves of C₃A-gypsum systems (Batch B)

Figure 3-26: Heat evolution curves of C₃A-gypsum systems (Batch C)

53

Figure 3-27: Cumulative heat curves (Batch A)

Figure 3-28: Cumulative heat curves (Batch B)

Figure 3-29: Cumulative heat curves (Batch C)
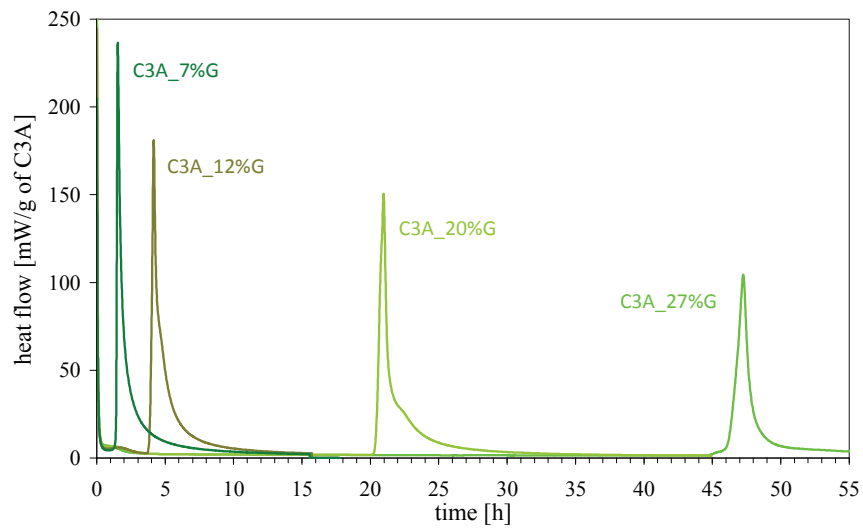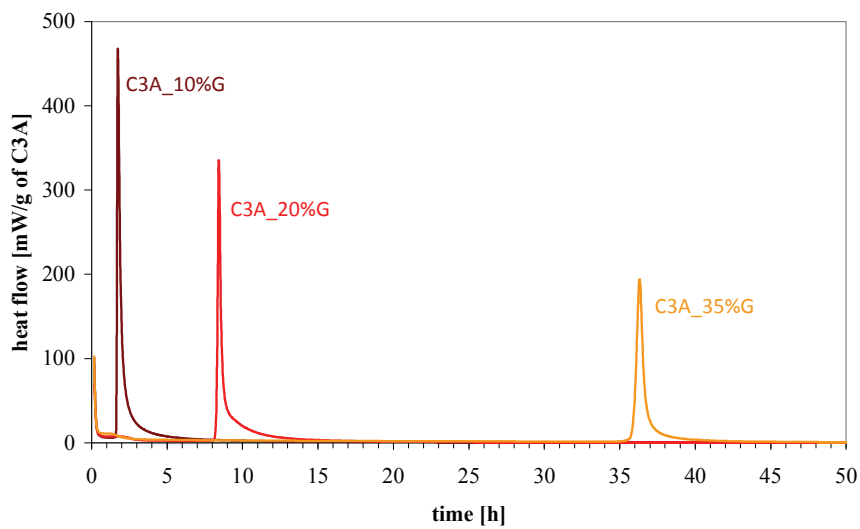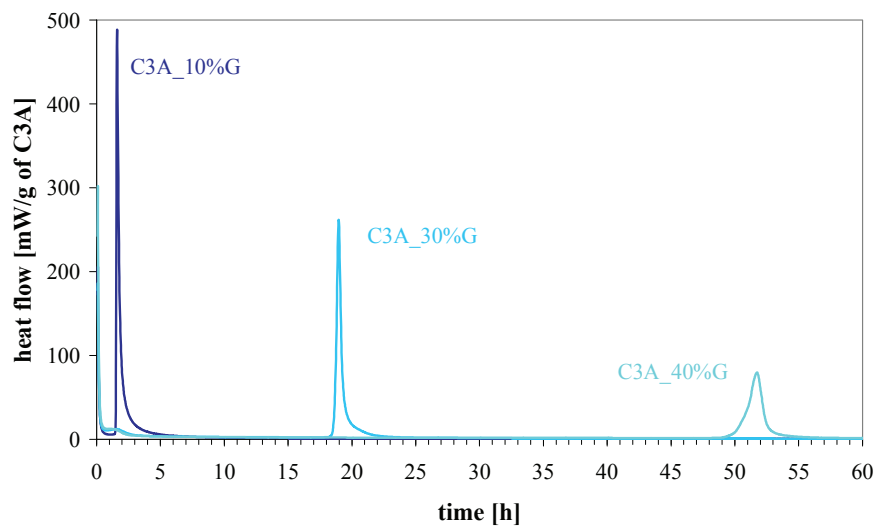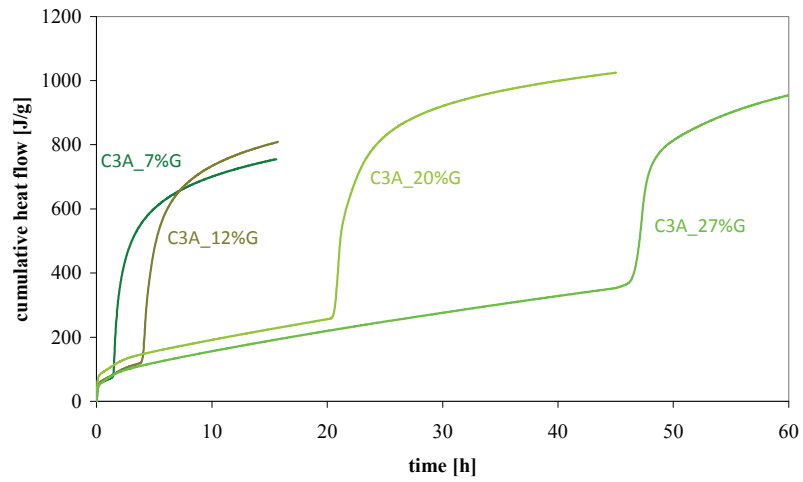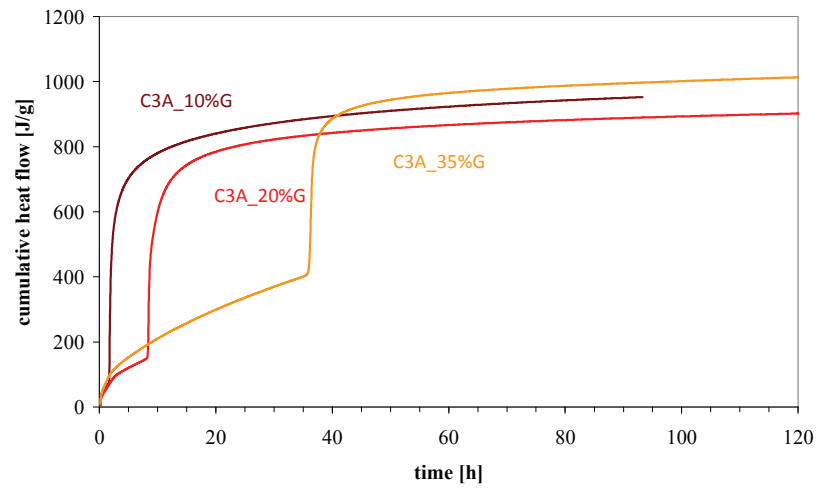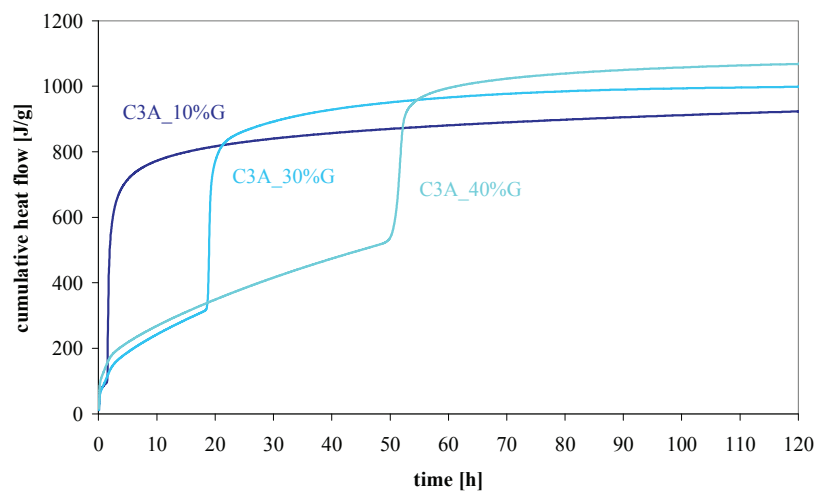
54

3.5.1 Kinetics of hydration after gypsum depletion (second stage)

In the study of the evolution of the phase assemblage previously described it was shown that right after gypsum depletion C_3A and ettringite dissolve rapidly to form AFm phases. However, the mechanisms that control the hydration rate during this second stage of the reaction are still unclear.

3.5.1.1 Total heat released during the second stage of reaction

It can be observed on Figure 3-24, Figure 3-25 and Figure 3-26 that the height of the peak, and therefore the total amount of reaction during the second stage of reaction, changes with the gypsum content. This phenomenon can be better observed on the cumulative curves on Figure 3-27, Figure 3-28 and Figure 3-29. The heat released during the second stage of reaction was calculated from cumulative curves, the results are given in Table 3-3. As the plateau was not reached for Batch A (due to the too short time of measurement), the total heat of reaction was calculated only for Batches B and C. The result show a decrease of the heat release during the second stage of reaction as the gypsum content of the original mix increases.

Table 3-3: The total heat released during the second stage of reaction (calculated from the cumulative curves) decreases with increasing gypsum addition.

	J/g of C_3A			J/g of C3A
10%	879		10%	835
20%	761		30%	684
35%	622		40%	557
	Batch B			**Batch C**

Plotting these heats vs. the theoretical values of remaining C_3A after gypsum consumption a quasi linear trend can be observed (Figure 3-30).
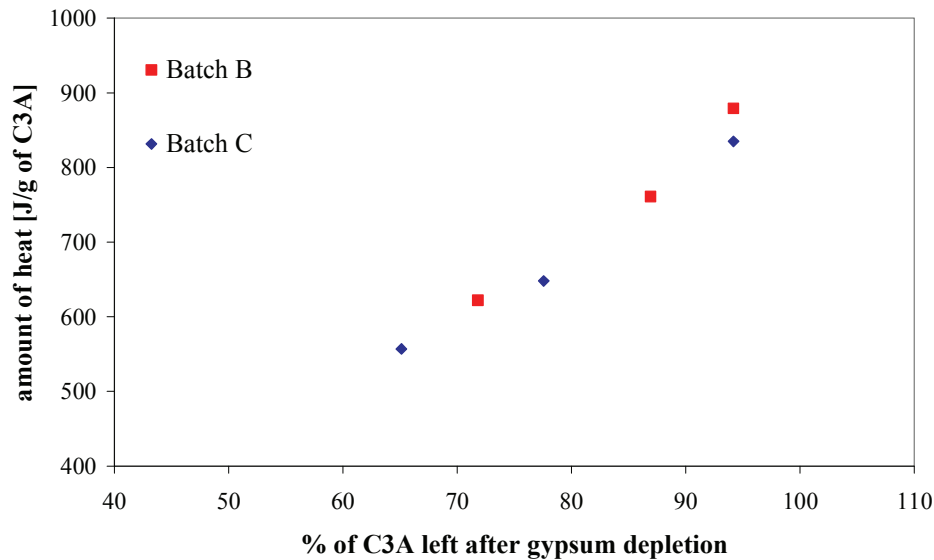
Figure 3-30: Heat released during the second stage of reaction vs. % of C$_3$A left in the sample after gypsum depletion. A linear trend between the heat released and the % of C$_3$A left can be observed. (The % of C$_3$A left was calculated assuming that all the gypsum reacts with C$_3$A to form ettringite during the first period of the reaction)

These results show that the heat released during the second stage of reaction is proportional to the amount of remaining C$_3$A. For systems with low gypsum content, more C$_3$A remain in the systems at the beginning of the second stage of the reaction.

However, it as to be noted that the total heat released by the reaction (after around 100 hours) is higher for systems with higher gypsum content (Figure 3-28 and Figure 3-29).

3.5.1.2 Parameters controlling the reaction rate during the second stage of reaction

The kinetics of the reaction after gypsum depletion is characterized by an exothermic peak, this means a period of acceleration and a period of deceleration of the reaction rate. Looking more closely to the exothermic peaks that occur after sulfate exhaustion it can be observed that they become broader with increasing gypsum addition. Both acceleration and deceleration are modified by the gypsum content. In order to observe this peak broadening the heat evolution curves have been shifted to align all the exothermic peaks (Figure 3-31).
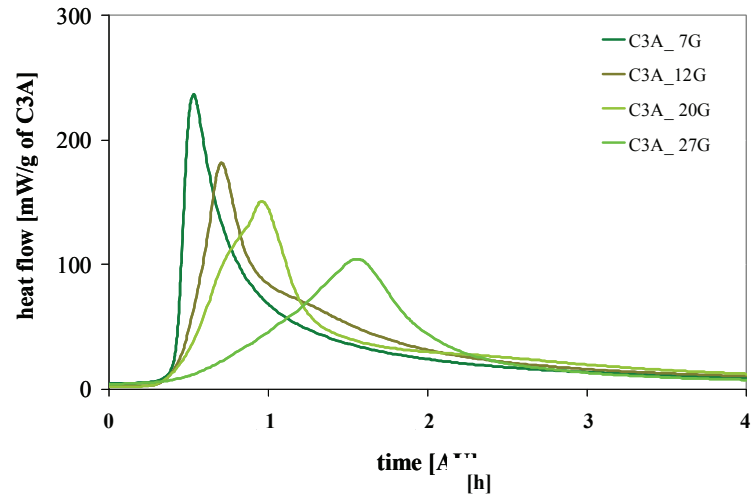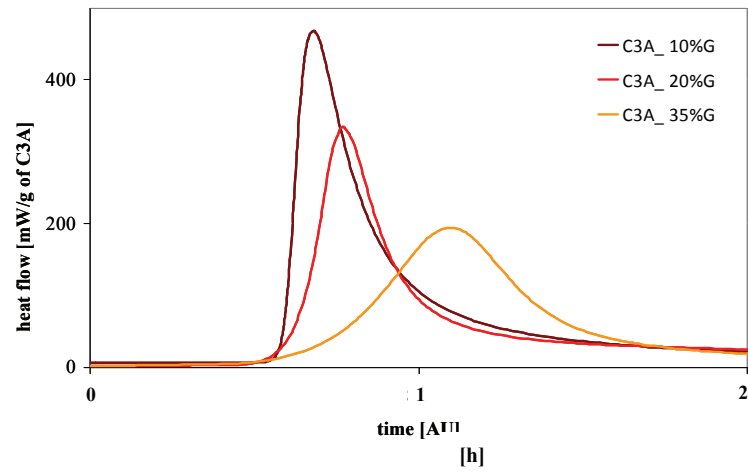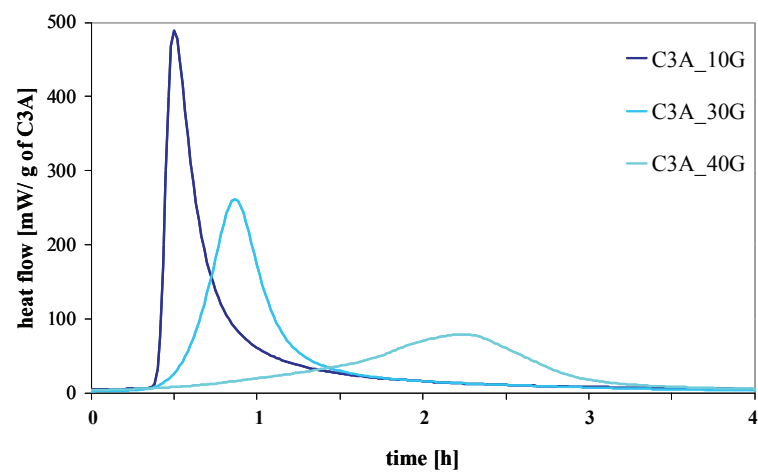
Figure 3-31: Influence of the initial gypsum content on the exothermic peak. Broader peaks were observed with increasing gypsum addition. (The offset of the peaks was shifted to the same time in these plots)

The acceleration period

The acceleration period is characterized by the slope of the exothermic peaks. It can be observed on Figure 3-32 that this slope decreases with increasing gypsum content in the original mix.
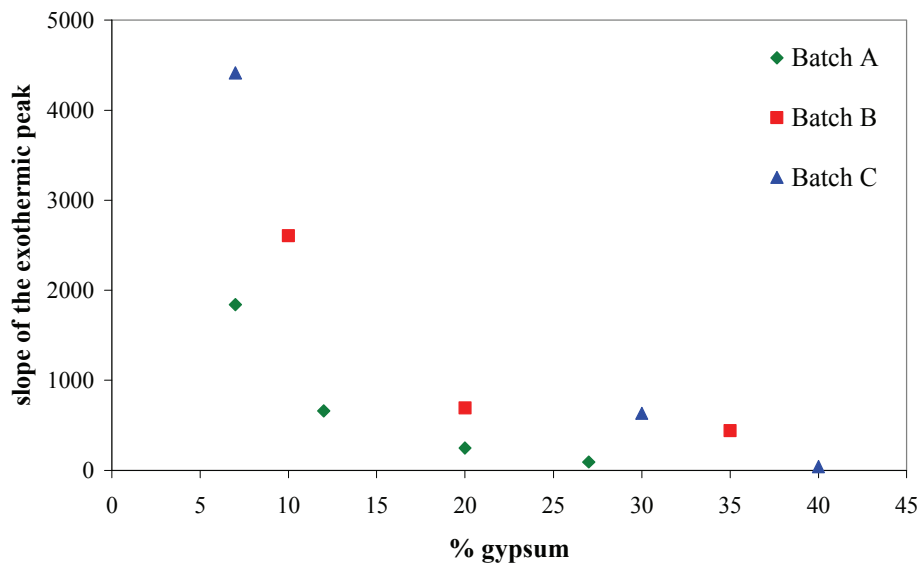
Figure 3-32: Slope of the exothermic peak vs. gypsum content in the original mix

It has to be considered that with increasing gypsum content two parameters that may influence the rate of the reaction during the acceleration period are modified:

- The specific surface area of the C_3A left at the time corresponding to sulfate consumption that decreases with gypsum addition as presented in Figure 3-33. Indeed, for higher gypsum additions the second stage of the reaction starts at higher degree of hydration, therefore the specific surface area of the particles is smaller. The evolution of the specific surface area represented in Figure 3-33 is an out put from the model μic obtained by A.Kumar (LMC) assuming that the specific surface area of the anhydrous powder is the one calculated from the particle size distribution as described in CHAPTER 2.

- The space available for the reaction that decreases also (Figure 3-34) because more ettringite is formed during the first stage of the reaction for higher initial gypsum contents. The space available for the reaction at the beginning of the second stage of the reaction represented in Figure 3-34 was calculated assuming that all the gypsum react with C_3A to form ettringite during the first stage of the reaction. It corresponds to the water left in the systems at this time of the reaction.
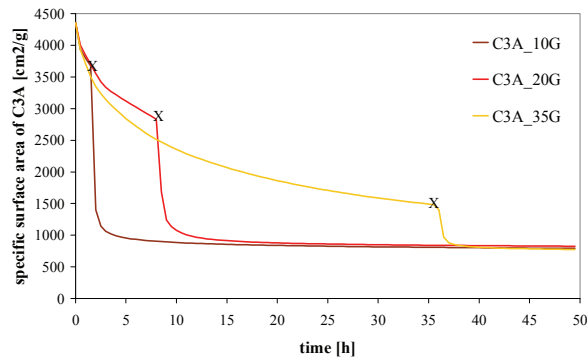
Figure 3-33: Evolution of the specific surface area of C_3A during hydration (Batch B). X=at the time of sulfate consumption: The specific surface area is smaller at the beginning of the second stage for higher gypsum additions. (Output from the model μic)
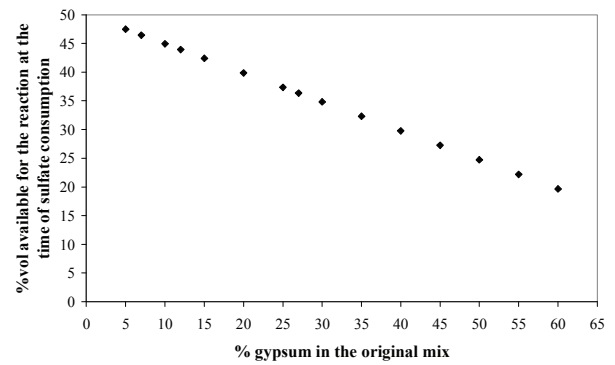
Figure 3-34: % volume available for the reaction at the beginning of the second stage of the reaction vs. initial gypsum content. Less space is available for the reaction during the second stage of the reaction for higher gypsum additions. (Calculated from stoichiometry assuming that only ettringite is formed during the first stage of the reaction).

The role of the specific surface area on the reaction rate during the second stage of the reaction was investigated using C_3A powder sieved in two different and narrow PSDs as represented in Figure 3-35 were the fine (red curve) and coarse C_3A (blue curve) are compared to standard PSD used in this study (black curve).
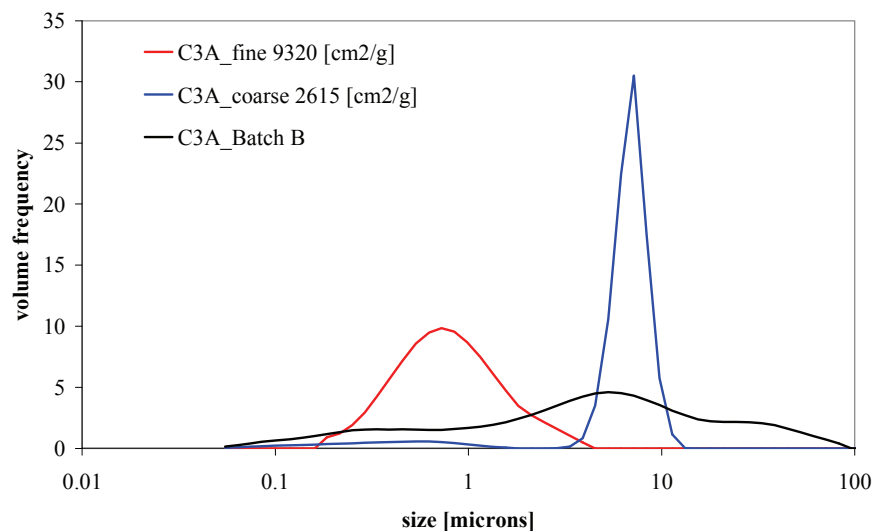
Figure 3-35: Fine (red) and coarse (blue) particle size distribution of the monosized C_3A powders compared to a standard one (black).

The heat evolution curves obtained for these fine and coarse systems with different gypsum additions are reported in Figure 3-36, Figure 3-37 and Figure 3-38.
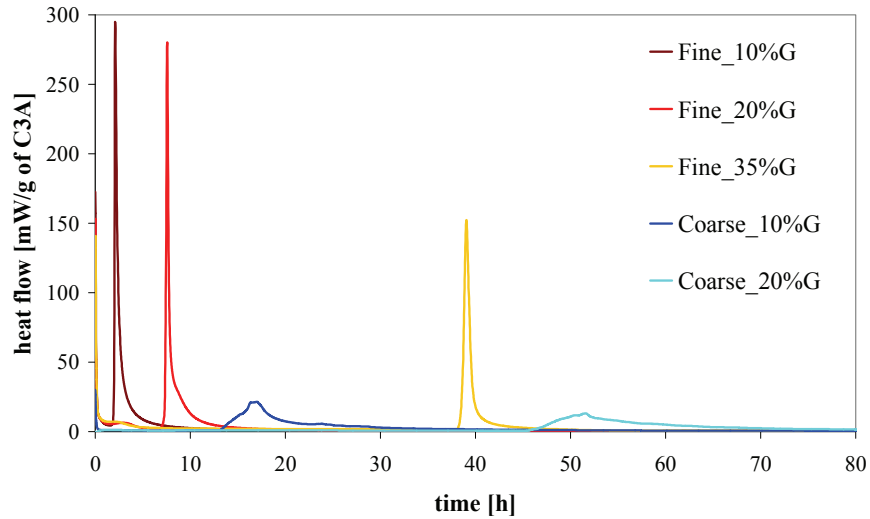
Figure 3-36: Heat evolution curves for monosize C₃A particles. The exothermic peaks are broader for coarser C₃A particles (blue curves).
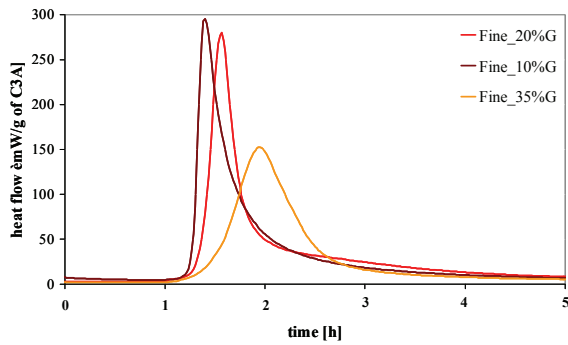
Figure 3-37: Zoom on the calorimetric peaks of fine C₃A (peak shifted)
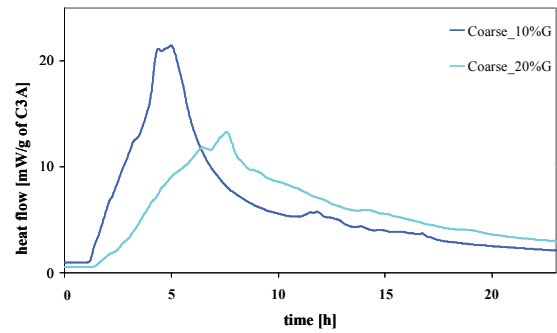
Figure 3-38: Zoom on the calorimetric peaks of coarse C₃A (peak shifted)

The exothermic peaks of the coarser particles are significantly lower, broader and occur later (for a same gypsum addition) than the exothermic peaks observed for finer particles. The slopes of the exothermic peaks during the acceleration period obtained for the coarser C₃A powder are significantly lower than the slopes calculated for the powder composed of fine particles as reported in Figure 3-39.
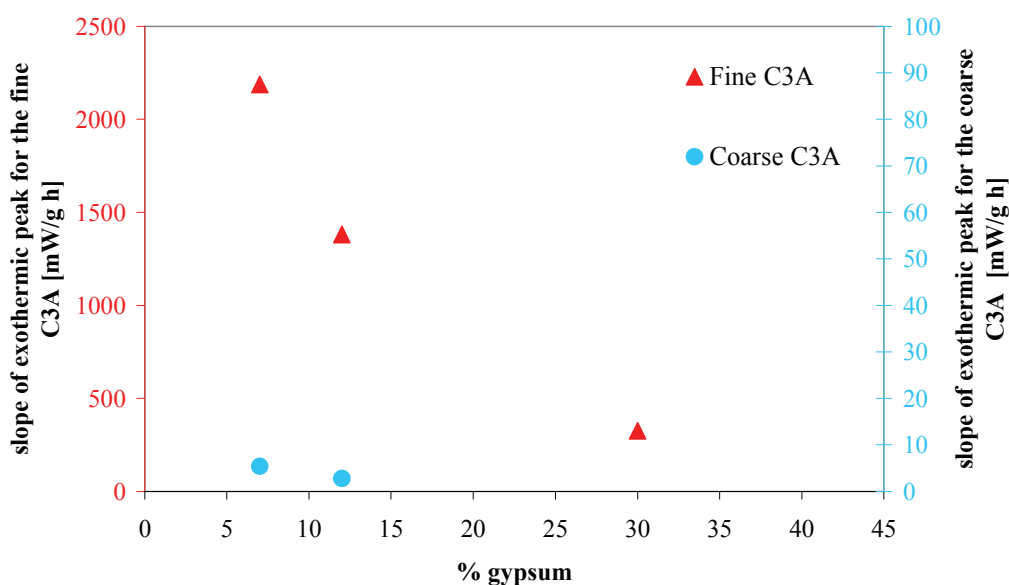
Figure 3-39: Slopes of the exothermic peak vs. gypsum content in the original mix for monosize C₃A particles. The slopes of the peaks for the coarse C₃A powders are significantly lower than the slope calculated for the fine C₃A powders.

These results show the strong influence of the specific surface area of the powder on the reaction rate. As higher gypsum contents implies a higher degree of hydration at the time corresponding to the depletion of gypsum, smaller specific surface area of the remaining C₃A (that lead to slower reaction rate) are observed.

In order to investigate the influence of the space available for the reaction on the acceleration period, the heat evolution curves of samples composed of 88% C₃A (from Batch A) and 12% gypsum with different w/s ratios were monitored. W/S ratios from 0.5 to 2 were investigated. The results are presented in Figure 3-40. The calorimetric peaks were shifted in order to better compare the acceleration periods.
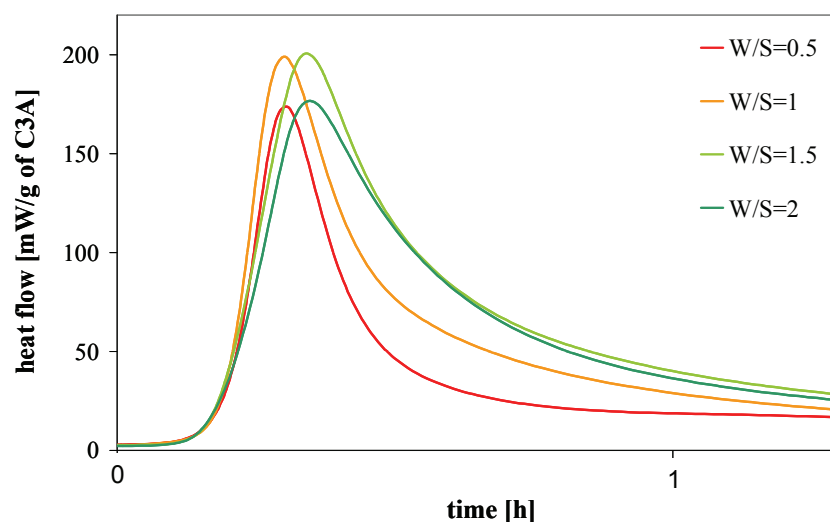
Figure 3-40: Influence of w/s ratio on the calorimetric peaks (Peaks shifted). Samples: C3A_12G (Batch A). The variation of w/s ratio from 0.5 to 2 has only a small influence on the acceleration period but a strong influence on the deceleration period where higher w/s ratios lead to slower deceleration rates.

It can be observed that the change in the space available induced by this modification of w/s ration almost doesn't influence the acceleration period. However it has to be noted that a variation of w/s ratio from 0.5 to 2 for a sample containing 12% gypsum induce only a small variation of the space available for the reaction at the time corresponding to the exothermic peak (+/- 5 %). An influence of the space available for the reaction on the acceleration period can therefore not be excluded with this experiment. Moreover, comparing the results obtained in this study carried out on pastes (w/s =1) to the calorimetric curves obtained by Minard et al. [9] in diluted suspension (w/s ratio = 25) (Figure 3-3) it can be observed that in diluted suspension there is no significant peak broadening with increasing gypsum content. This observation suggests therefore that a significant change in the space available for the reaction has a strong effect on the reaction rate during the acceleration period when hydration occurs in pastes. The diminution of the reaction rate during the acceleration period observed with increasing gypsum content can therefore be attributed to the reduction of the space available for the reaction due to the precipitation of more ettringite during the first stage of the reaction.

Tow parameters controlling the hydration rate during the second stage of the reaction were identified in this study:

- the specific surface are of the reacting C_3A particles.
- the space available for the reaction that depends on the w/s ratio or on the amount of hydrates previously precipitated.

These tow parameters can be resumed in one: the exposed surface area of C_3A. When the exposed surface area of C_3A is reduced (due to smaller specific surface area or due to the contamination of the surface by other hydrates) the reaction rate decreases.

In terms of mechanisms, three possible mechanisms can control the rate of reaction during the acceleration period:

- the dissolution of ettringite
- the dissolution of C_3A
- or the nucleation of AFm phases

The observations previously made do not allow us to clearly identify the mechanism responsible for the kinetics observed in the different C_3A-gypsum systems. However several hypotheses may be formulated:

- Higher reaction rates were observed for systems with low gypsum content (and therefore small amounts of formed ettringite). This observation is not consistent with the hypothesis of the dissolution of ettringite being the rate controlling mechanism as a lower reaction rate should be observed when less ettringite is present in the system.
- The influence of the exposed C_3A surface area on the reaction rate is consistent with the hypotheses of either the dissolution of C_3A or the nucleation of AFm phases being the rate controlling mechanism. Indeed the exposed surface area of C_3A directly influenced the rate of C_3A dissolution and if heterogeneous nucleation of AFm phases is assumed (as for C-S-H nucleation in alite pastes) a smaller exposed surface area will induce a smaller amount of nuclei.

The deceleration period

The deceleration period is also modified depending on the gypsum content of the original mix. It can be observed that the deceleration is slower with increasing gypsum (Figure 3-31).

Two possible parameters may be at the origin of this deceleration and control the rate of reaction during this period:

- A lack of reactant (water or anhydrous phases)
- A lack of space

The microstructural study show that substantial amount of C_3A was still present in the microstructure after several days of hydration. The lack of anhydrous phases can therefore not be claimed to be at

the origin of the deceleration of the reaction rate. Moreover, a slower deceleration is observed for the samples with higher gypsum content that have a higher degree of hydration (and therefore less anhydrous phases) at the time corresponding to the exothermic peak.

The amount of water necessary for the complete reaction depends on the phase assemblage generated and w/s varies between 0.4 and 0.9 depending if 100% of monosulfoaluminate or 100% of hydroxy-AFm are formed. As w/s = 1 was chosen in this study the lack of water cannot be at the origin of the deceleration.

In Figure 3-40 it can be observed the deceleration part is significantly modified by small changes in the space available. Slower decelerations were observed for systems where more space is available for the reaction. This confirms the role of space available for the reaction. A space filling effect as described for example by Bishnoi for alite hydration [25] and Gosselin for calcium aluminate cements [26] due to the impingement of the hydrates can therefore be considered to be rate controlling during the deceleration period of stage 2.

As observed in the microstructural study, the shape of the AFm platelets forms during the second stage of reaction depends on the gypsum content of the original mix (Figure 3-19). Longer platelets are formed when gypsum content is low. The difference in the shape of the AFm platelets is coherent with the difference in the deceleration period observed by calorimetry for the different gypsum additions. As impingement of the hydrates is more probable in systems with low gypsum content where the AFm platelets are longer, a faster and earlier deceleration can be expected.

3.6   Influence of the temperature on the hydration kinetics

Cement hydration is known to be temperature dependent. The Arrhenius theory and the concept of activation energy (Ea):

$$k = \exp\left(-\frac{Ea}{RT}\right)$$

is commonly applied to cement to quantify the sensitivity to temperature of the hydration reaction. The Arrhenius theory is based on simple chemical reaction, therefore the concept of "apparent" activation energy is used in the case of cements since the hydration of cement involves several simultaneous and coupled chemical reactions [27, 28]. However, if one of these reactions is dominant and controls the hydration rate, the determination of the activation energy can provide insights on the rate limiting factor of the reaction. Transport controlled reaction have generally small Ea (< 20 kJ/mol) while for reaction that are surface controlled the Ea is usually higher (> 20 kJ/mol) [29].

The temperature dependence of the hydration of C_3A-gypsum systems has been investigated in the past. Brown and LaCroix [30] reported that the ettringite formation is controlled by a diffusion process with an activation energy Ea of 4,2 kJ/mol. Another study by Tenoutasse reports higher activations energies of 50 kJ/mol [24], that is consistent with the surface controlled theory that explains the slow down of the C_3A reaction in the presence of gypsum by the blocking of the C_3A reaction sites by calcium and sulfate ions. The dispersion of the values reported in the literature can be explained by the method used to calculate the activation energy. While Tenoutasse calculated k at different temperatures from the height of the calorimetric peak, Brown and LaCroix calculated it from a model where the hydration rate was thought to be controlled by a diffusion process.

In the present study the influence of the temperature on the hydration kinetics of C_3A-gypsum systems depending on the gypsum content was investigated. Heat evolution profiles were monitored by isothermal calorimetry at three different temperatures: 20°C, 26°C and 30°C. The results obtained for the three samples of Batch B are reported on Figure 3-41 for the sample C3A_10G, on Figure 3-42 for the sample C3A_20G and on Figure 3-43 for the sample C3A_35G. Due to the highly exothermic reaction at 30°C of the samples C3A_10G and C3A_20G, the maximum of the exothermic peak could not be measured. To ensure a good comparability of the results the three calorimetric measurements were carried out with the same original paste: after mixing the paste was put into three calorimetric vessels, one for each temperature. The heat evolution curves of the experiments carried out at 26

and 30°C show an endothermic peak instead of the usual exothermic dissolution peak. This is a measurement artefact due to temperature of the samples and the entry of fresh air in the channel when the sample was introduced into the calorimeter.

3.6.1 Determination of the activation energy (Ea)

For all the gypsum contents studied, the temperature influences significantly the kinetics of the reaction, accelerating the hydration. The time necessary for gypsum consumption decreases as the temperature increases and the exothermic peak characteristic of the second stage of the reaction occurs earlier with increasing temperature.

The apparent activation energy of both first and second stage of reaction was calculated for the three gypsum additions. Several methods exists to calculate the activation energy of a cementitious system [31, 32]. To determine the activation energy for the first stage of reaction, the method of the equivalent time based on the Maturity Method as described by Carino [31] was used. The part of the cumulative heat evolution curves corresponding to the first stage of reaction were mathematically superposed using the following formula:

$$t_{eq} = \alpha \cdot t$$

Where α is the age conversion factor obtained to superpose the cumulative curves as shown in Figure 3-44. To determine the activation energy for the second stage of reaction the differential calorimetric curves were used and a similar method was used to superpose the slope of the calorimetric peaks:

$$t_{eq} = \alpha \cdot (t + \beta)$$

Where α is the age conversion factor obtained to superpose the slopes of the calorimetric peaks as shown in Figure 3-45 and β is a shift factor used to shift the calorimetric peaks in order to align the peak to help the determination of the age conversion factor. This β factor was not taken into account for the calculation of the activation energy.

The activation energies were then calculated with the following equation where T ref is 293 °K:

$$E_a = \frac{\ln(\alpha) \cdot R}{\dfrac{1}{T} - \dfrac{1}{T_{ref}}}$$

Figure 3-41: Heat flows at three different temperatures for the sample C3A_10G. Due to the limitation of the calorimeter the maximum of the exothermic peak at 30°C could not be measured.
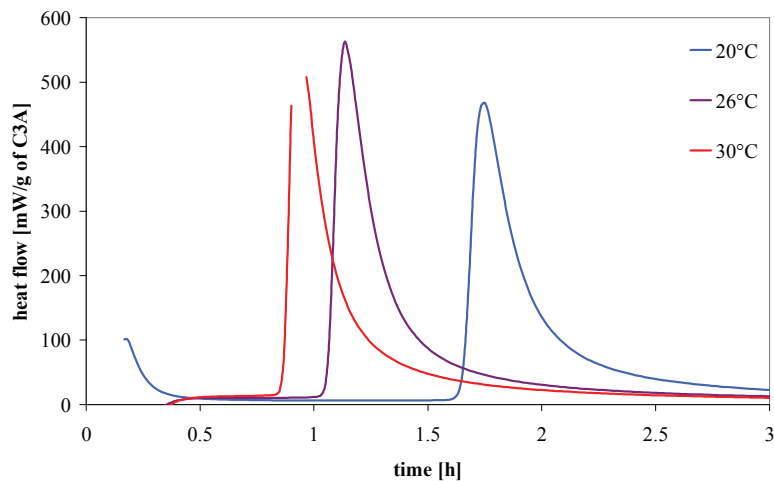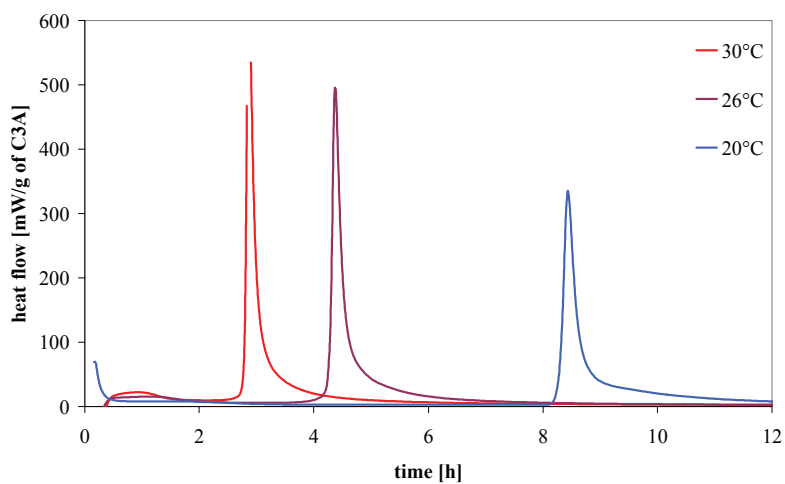

Figure 3-42: Heat flows at three different temperatures for the sample C3A_20G. Due to the limitation of the calorimeter the maximum of the exothermic peak at 30°C could not be measured.
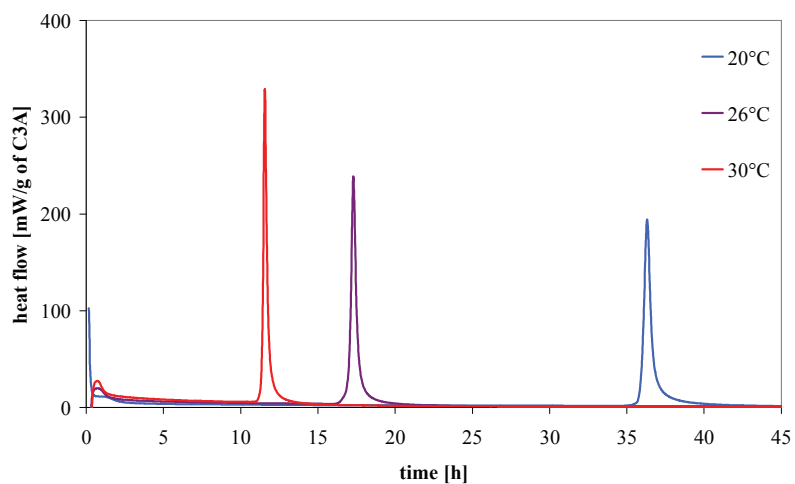
Figure 3-43: Heat flows at three different temperatures for the sample C3A_35G.
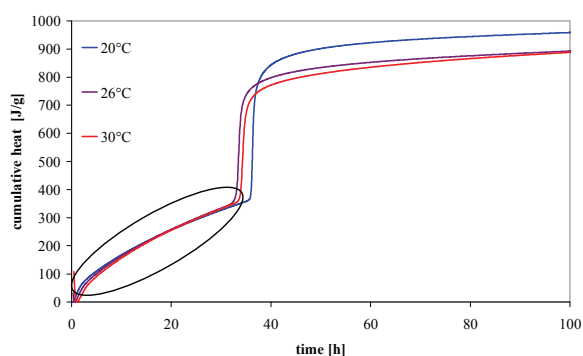
Figure 3-44: Example of superposition of cumulative curves to determine Ea for the first stage of reaction using the equivalent time method.
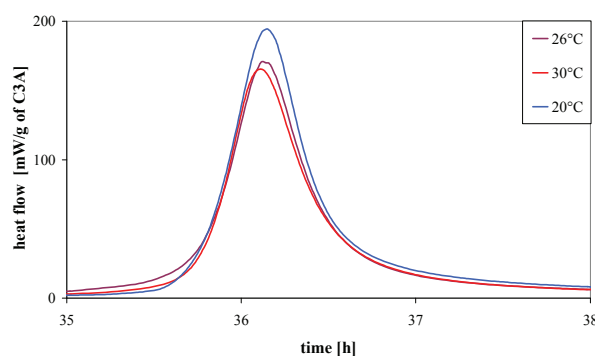
Figure 3-45:Example of superposition of calorimetric peaks to determine Ea for the second stage of reaction using the equivalent time method.

The calculated activation energies for the first and second stages are reported in Table 3-4. The Ea reported are mean values calculated for the two age equivalent factor obtained between 20 and 26°C and 20 and 30°C. The error is the standard deviation.

Table 3-4: Calculated activation energies (Ea).

	Ea 1st stage (kJ/mol)	Ea 2nd stage (kJ/mol)
C3A_10G	44 ± 11	21 ± 12
C3A_20G	79 ± 1	59 ± 8
C3A_35G	80±2	44±9

Relatively high apparent activation energies were obtained for the three gypsum replacements and for both first and second stage of reaction. These high activation energies indicate that the reaction is limited by surface controlled mechanisms [29] in both first and second stage of the reaction.

The difference between the activation energies obtained for the first and second stages may be explained by the adsorption of calcium and sulfate ions on C_3A surface during the first stage of reaction that may play a role in the modification of the Ea. It is interesting to note that the Ea calculated for the first stage of the reaction for the sample C3A_10G that contain a low amount of gypsum is similar to the Ea calculated after the gypsum depletion for the other systems. However it has to be noted that higher standard deviations were obtained for the sample with the lower gypsum

addition, probably due to the fact the first stage of the reaction is very short, especially for high temperature and the measurement may be influenced by the introduction of the sample in the calorimeter. Therefore the temperature may be not perfectly stable during the first minutes of reaction.

3.7   Conclusions on tricalcium aluminate – calcium sulfate systems

The reaction of C_3A and gypsum with water is usually divided in two stages as presented in Figure 3-46. The first stage corresponds to the hydration in the presence of gypsum and second stage begins when sulfate ions in solution are consumed.
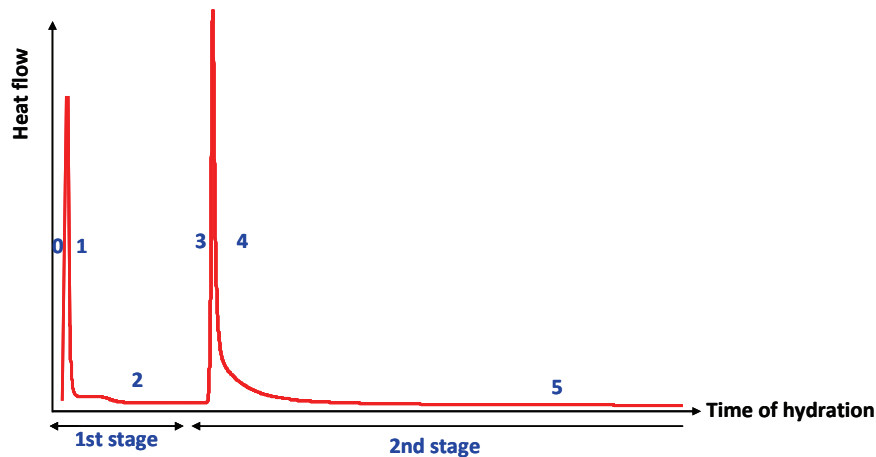
Figure 3-46: Stages of C_3A-gypsum hydration

The first stage is characterized by an acceleration of the reaction (period 0 in Figure 3-46) right after mixing with water that can be attributed to the dissolution of the species. This acceleration is followed by a deceleration (1) and a period of low reactivity (2). This study confirms the findings of Minard et al. [9] on the controlling parameter during this period of hydration. The fact that the hydration rate depends on the specific surface area of the C_3A and the high activation energy calculated, which suggest a surface controlled mechanism, are consistent with the claim that the hydration rate during this period is controlled by the dissolution of C_3A. The duration of the period of low reactivity depends on the gypsum content of the original mix. Ettringite as well as AFm phases [8, 9, 11, 21] are formed during this first stage of reaction.

The second stage of the reaction is also characterized by an acceleration (3) and a deceleration periods (4). The present study shows that the rate of reaction during this second acceleration, which corresponds to the surge in C_3A dissolution after the depletion of gypsum, is largely influenced by the exposed surface area of C_3A. During this period, C_3A and ettringite dissolve to form AFm phases with a chemical composition that suggest the formation of solid solutions between the hydroxy-AFm and monosulfoaluminate (with miscibility gap). The amount of sulfate in the interlayer depends on the initial content of gypsum. It was also shown that the reaction rate during the deceleration period is

controlled by the impingement of the AFm platelets. The study of the microstructure show that the morphology of the AFm platelets depends on the gypsum addition: higher gypsum additions lead to smaller platelets. In the latter case the deceleration in the heat evolution curve was observed to be slower.

The reaction continues then at a slow rate (5) until the reactant runs out. It was observed by SEM images that a dense hydrate (with a similar chemical composition that of the AFm platelets) forms within the grain boundaries. The microstructural development of C_3A-gypsum pastes shows therefore similar features to C_3S and cement hydration with the precipitation of hydrates that fill the space between the grains and the development of a dense product within the original grain boundaries. However, in the case of C_3A-gypsum pastes, the dense "inner" product seems to be less obvious at later ages. A re-crystallization as hydrogarnet or as matrix product can be suggested. When hydroxy-AFm phases were present in the phase assemblage, hydrogarnet was observed at later ages. This last phase was observed to form at the original grain boundaries of C_3A and grow as a shell around hydrating C_3A grains. Hollow hydrogarnet shells were observed where the small grains have completely reacted.

References

1.   Taylor, H.F.W., *Cement Chemistry 2nd edition*. Thomas Telford ed. 1997.

2.   Minard, H., *Etude intégrée des processus d'hydratation, de coagulation, de rigidification et de prise pour un système C3S-C3A-sulfates-alcalins.* Thèse de Doctorat, Université de Bourgogne, 2003.

3.   Jupe, A.C., et al., *Fast in situ x-ray-diffraction studies of chemical reactions: A synchrotron view of the hydration of tricalcium aluminate.* Physical Review B, 1996. 53(22): p. R14697.

4.   Christensen, A.N., T.R. Jensen, and J.C.J.C. Hanson, *Formation of ettringite, Ca6Al2(SO4)3(OH)12.26H2O, AFt, and monosulfate, Ca4Al2O6(SO4).14H2O, AFm-14, in hydrothermal hydration of Portland cement and of calcium aluminum oxide--calcium sulfate dihydrate mixtures studied by in situ synchrotron X-ray powder diffraction.* Journal of Solid State Chemistry, 2004. 177(6): p. 1944-1951.

5.   Mehta, P.K., *Morphology of Calcium Sulfoaluminate Hydrates* Journal of the American Ceramic Society, 1969. 52(9): p. 521-522.

6.   Scrivener, K.L. and P.L. Pratt, *Microstructural studies of the hydration of C3A and C4AF independently and in cement paste.* Proc. Brit. Ceram. Soc, 1984. 35: p. 207-219.

7.   Meredith, P., et al., *Tricalcium aluminate hydration: Microstructural observations by in-situ electron microscopy.* Journal of Materials Science, 2004. 39(3): p. 997-1005.

8.   Hampson, C.J. and J.E. Bailey, *The microstructure of the hydration products of tri-calcium aluminate in the presence of gypsum.* Journal of Materials Science, 1983. 18(2): p. 402-410.

9.   Minard, H., et al., *Mechanisms and parameters controlling the tricalcium aluminate reactivity in the presence of gypsum.* Cement and Concrete Research, 2007. 37(10): p. 1418-1426.

10.   Matschei, T., B. Lothenbach, and F.P. Glasser, *The AFm phase in Portland cement.* Cement and Concrete Research, 2007. 37(2): p. 118-130.

11.   Pourchet, S., et al., *Early C3A hydration in the presence of different kinds of calcium sulfate.* Cement and Concrete Research, 2009. 39(11): p. 989-996.

12.   Bailey, J.E., C.J. Hampson, and J. Bensted, *The Microstructure and Chemistry of Tricalcium Aluminate Hydration [and Discussion].* Philosophical Transactions of the Royal Society of London. Series A, Mathematical and Physical Sciences, 1983. 310(1511): p. 105-111.

13.   Hampson, C.J. and J.E. Bailey, *On the structure of some precipitated calcium alumino-sulphate hydrates.* Journal of Material Science, 1982. 17: p. 3341-3346.

14.   Collepardi, M., et al., *Tricalcium aluminate hydration in the presence of lime, gypsum or sodium sulfate.* Cement and Concrete Research, 1978. 8(5): p. 571-580.

15.   Stein, H.N., *Some characteristics of the hydration of 3CaO .Al2O3 in the presence of CaSO4 .2H2O.* Silic. Ind, 1963. 28: p. 141-145.

16.   Corstanje, W.A., H.N. Stein, and J.M. Stevels, *Hydration reactions in pastes C3S+C3A+CaSO4.2aq+H2O at 25°C.I.* Cement and Concrete Research, 1973. 3(6): p. 791-806.

17.   Corstanje, W.A., H.N. Stein, and J.M. Stevels, *Hydration reactions in pastes C3S+C3A+CaSO4.2aq+water at 25°C. II.* Cement and Concrete Research, 1974. 4(2): p. 193-202.

18.   Corstanje, W.A., W.N. Stein, and J.M. Stevels, *Hydration reactions in pastes C3S + C3A + CaSO4 .2aq. + water at 25°C.III.* Cement and Concrete Research, 1974. 4(3): p. 417-431.

19.   Brown, P.W., L.O. Liberman, and G. Frohnsdorff, *Kinetics of the early hydration of tricalcium aluminate in solution containing calcium sulfate.* Journal of the American Ceramic Society, 1984. 67(12): p. 793-795.

20.   Gupta, P.S., S. Chatterji, and W. Jeffrey, *Studies of the effect of different additives on the hydration of tricalcium aluminate: Part 5 - A mechanism of retardation of C3A hydration.* Cement technology 1973. 4: p. 146-149.

21.   Scrivener, K.L., *Development of the microstructure during the hydration of Portland cement* Ph.D. Dissertation ,University of London, 1984.

22.   Feldman, R.F. and V.S. Ramachandran, *The influence of CaSO4.2H2O upon the hydration character of 3CaO.Al2O3.* Magazine of Concrete research 1966. 18(57): p. 185-196.

23.   Skalny, J. and M.E. Tadros, *Retardation of Tricalcium Aluminate Hydration by Sulfates* Journal of the American Ceramic Society, 1977. 60(3-4): p. 174-175.

24.   Tenoutasse, N. *The hydration mechanism of C3A and C3S in the presence of calcium chloride and calcium sulfate* in *The 5th International Symposium on the Chemistry of Cement* 1968. Tokyo.

25.   Bishnoi, S. and K.L. Scrivener, *Studying nucleation and growth kinetics of alite hydration using µic.* Cement and Concrete Research, 2009. 39(10): p. 849-860.

26.   Gosselin, C., E. Gallucci, and K. Scrivener, *Influence of self heating and Li2SO4 addition on the microstructural development of calcium aluminate cement.* Cement and Concrete Research. 40(10): p. 1555-1570.

27.   D'Aloia, L. and G. Chanvillard, *Determining the "apparent" activation energy of concrete: Ea-- numerical simulations of the heat of hydration of cement.* Cement and Concrete Research, 2002. 32(8): p. 1277-1289.

28.   Kada-Benameur, H., E. Wirquin, and B. Duthoit, *Determination of the apparent activation energy of concrete by isothermal calorimetry.* cement and Concrete Research, 2000. 30: p. 301-305.

29.   Lasaga, A.C., *Kinetic Theory in the Earth Sciences* ed. P.s.i. geochemistry. 1998, Princeton, New Jersey: Princeton University Press.

30.   Brown, W. and P. LaCroix, *The kinetics of ettringite formation.* Cement and Concrete Research, 1989. 19(6): p. 879-884.

31.   Carino, N.J., *Handbook on Nondestructive Testing of Concrete: Second edition, Chapter 5: The Maturity Method*. 2006, Boca Raton, FL: CRC Press.

32.   Poole, J.L., et al., *Methods for Calculating Activation Energy for Portland Cement.* ACI Materials Journal, 2007. 104(1): p. 303-311.

CHAPTER 4   HYDRATION OF ALITE - C$_3$A - GYPSUM SYSTEMS

4.1 Literature review

4.1.1 Alite hydration

Before discussing the interactions between the calcium silicate and calcium aluminate phases that occur during cement hydration and their influence on the hydration kinetics, it is important to introduce what is known about alite hydration. This phase represents up to 70% by weight of the cement and many features of the hydration of ordinary Portland cements are similar to alite hydration. Alite hydration as been extensively studied and many theories exist about its hydration mechanisms. The description of these theories given in this chapter follows the argumentation of Juilland [1].

The reaction of C$_3$S with water leads to the formation of calcium hydroxide (CH, or portlandite) and a poorly crystalline calcium silicate hydrate (C-S-H) as shown in the following equation:

$$C_3S + (3-x+n) H \rightarrow C_xSHn + (3-x)CH$$
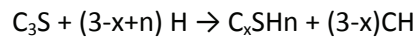
The heat evolution profile of alite hydration can be divided, according to Gartner *et al.* [2], into six time periods or stages corresponding to different regions of the calorimetric curve as presented in Figure 4-1.

Figure 4-1: Division in time period of the heat development monitored by isothermal calorimetry and solution phase analysis of an alite paste. Adapted from [2].

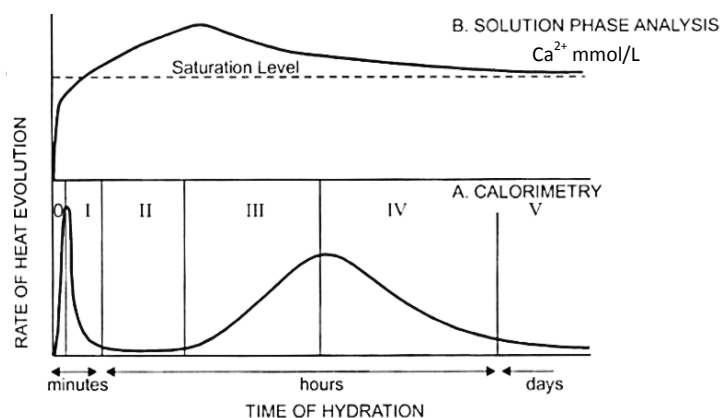**Stage 0, I and II:** the initial fast reaction, first deceleration and induction periods.

The initial exothermic peak is due to dissolution and lasts only few minutes. Following this, there is a deceleration and then a period of slow reaction lasting a few hours. The reasons for this deceleration are quite controversial and several theories have been proposed.

- One of the earliest and still popular theory for the first deceleration period is the formation of a protective layer of hydrates on the C_3S grains that prevents further dissolution [3, 4]. Some authors hypothesized that the hydration reinitiates after the conversion of the primary hydrate into a form more permeable to water [3, 4]. Others suggested that the rupture of this membrane is caused by osmotic pressure [5, 6], but little evidence has been found to support this theory. The strongest indications for the existence of a hydrate layer come from the work of Gartner and Jennings [7] who proposed that is the formation of C-S-H (SI) on C_3S grains that is responsible of the induction period and a solid-state transformation to a less protective form of C-S-H (SII) that leads to the end of the induction period.

- An alternative theory invokes an incongruent dissolution and the formation of a Ca^{2+} double layer close to the negative surface which inhibits C_3S dissolution [8]. In this case, the acceleration period starts when Ca^{2+} ions are consumed from the solution by the precipitation of hydrates [9].

- Several authors proposed that the induction period is controlled by the nucleation and growth of hydrates, CH or C-S-H [10]. Some authors claim that the induction period is due to the poisoning of the CH nuclei by silicates and that the nuclei cannot grow until the level of supersaturation is high enough to overcome this phenomenon [11]. This theory implies that the seeding of cement pastes with CH crystals would shorten the induction period, whereas it has been shown that this in fact prolongs the induction period [12]. For others the induction period corresponds to the nucleation period of C-S-H and ends when the nuclei start to grow. For Garrault and Nonat [13, 14] the nuclei form at the very beginning of the hydration reaction. There is then no true induction period but a continual increase in the rate of C-S-H formation. In this case, the seeding of cement pastes effectively shortens the induction period as shown by Thomas *et al.* [15]. Most nucleation and growth theories can explain the existence of an induction period but do not really address the question of the rapid slowdown of the reaction that occurs in the first minutes of hydration.

- Recently, Juilland et al. [1, 16] applied concepts from geochemistry on the role of crystallographic defects and solution saturation to propose a mechanism that explain the fast

deceleration observed during early hydration of alite. In crystal dissolution theory three dissolution mechanisms of minerals exists: vacancy islands where small pits can nucleate without the help of impurities, etch pits that form at the outcrops of dislocations or other defects and step retreat that takes place at pre-existing roughness [17]. The occurrence of one of these mechanisms depends on the level of undersaturation. Juilland et al. observed the formation of etch pits at defects on alite surface when immersed in pure water, while when lime saturated solutions are used they observed a dominance of smooth surfaces with formation of steps. Therefore they explain the initial slow down of the reaction observed during alite hydration by the dissolution theory: when the level of undersaturation dropped below that needed to provide enough energy for the nucleation of etch pits at dislocations, the rate of dissolution became slow as atoms dissolved only from preformed steps, leading to the deceleration and induction periods. Evidence in support of this was discussed by Juilland et al. from new results but also from the re-examination of results in the literature.

Stage III, IV and V: the acceleration, second deceleration periods and slow reaction periods.

The acceleration period corresponds to the acceleration of the reaction due to massive precipitation of hydrates and leads to the setting and solidification of the cementitious matrix. It is generally accepted that the reaction rate is controlled by the nucleation and growth of C-S-H during this stage. However the mechanism of C-S-H growth remains unclear. Garrault and Nonat [14] suggested that C-S-H clusters form by heterogeneous nucleation at the C_3S surface and then grow by aggregation of units of C-S-H . More recently, Bishnoi [18] suggested that during the acceleration period a loosely packed C-S-H filled a large fraction of the microstructure and the subsequently packing density increases with hydration. Assuming this growth model and using the modeling platform µic, Bishnoi was able to model the acceleration period but more importantly, the transition between the acceleration period and the second deceleration period. The deceleration of the reaction has generally been attributed to the transition to stage V where the reaction rate is controlled by a diffusion regime though a dense layer of hydrates formed around the C_3S grains [2]. However the recent modeling work of Bishnoi showed better coherence between the model and experimental results assuming that a space filling effect (the deceleration of the reaction rate due to impingement between neighboring nuclei) was controlling the reaction rate during this step.

4.1.2   Interaction between the cement phases

Portland cement is composed of calcium silicate (alite and belite), calcium aluminate (C_3A and C_4AF) and calcium sulfate phases (gypsum, anhydrite and hemihydrate). The heat evolution profile of ordinary Portland cements is very similar to that of alite, see Figure 4-2. As in alite pastes a

dissolution peak (peak 1) is followed by an induction period and then a re-acceleration of hydration is observed. Peak 2 is attributed to alite hydration. The differences from the alite calorimetric curve, such as the peaks 3 and 4, come from the presence of the C_3A phase and its reaction with calcium sulfate. These peaks are however not always well defined in the calorimetric curve of OPC. Peak 3 was often attributed to the monosulfoaluminate formation. However, Scrivener [19] suggested that peak 4 is caused by monosulfoaluminate formation and peak 3 is due to a second formation of ettringite.
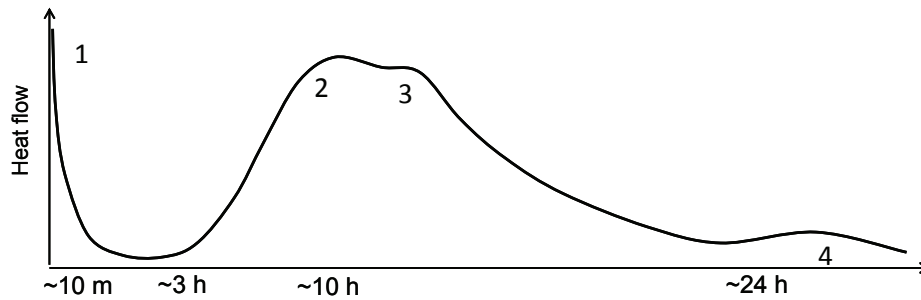

Figure 4-2: Typical calorimetric curve of an OPC. Exothermic peak 1: dissolution of the species. Peak 2: alite reaction. Peak 3: second formation of ettringite. Peak 4: formation of monosulfoaluminate.

In OPC the cement phases do not hydrate in isolation and many chemical and physical interactions between them can change their mechanisms and/or kinetics of hydration compare to the pure systems. In order to understand these interactions, researchers have studied the hydration reaction of model cements made of mixture of cement phases. The most basic mixture of pure phases that react like a cement is composed of three phases: alite, C_3A and gypsum as belite and C_4AF are known to have a minor contribution at early ages.

The first studies on this kind of multi-phase system are reported in the 70's with the studies of Tenoutasse [20] Corstanje *et al.* [21-24], Regourd *et al.* [25] and Hannawayya [26, 27]. Corstanje *et al.* studied by calorimetry model systems composed of 75% C_3A – 25% C_3S with additions of gypsum from 0 to 8%. These systems are far from the composition of real cements where the C_3S, C_3A and gypsum contains are respectively close to 90% - 6% and 4% (if belite and C4AF are not taken into account and the amount of the C_3S and C_3A is renormalized). However, they observed that only the kinetics of C_3A hydration is modified with increasing gypsum content, the C_3S hydration remain unaffected. Tenoutasse studied a more realistic composition (80% C_3S, 20% C_3A and gypsum additions from 0 to 6%). He observed that with low gypsum additions the peak due to C_3A reaction occurs first and that the peak due to the silicate hydration is retarded like the undersulfated cements reported by Lerch [28]. However, when the silicate reaction occurs before gypsum consumption its peak is practically unchanged.

The phase assemblage of model cements was studied by Hannawayya [26, 27]. These studies show that with a typical OPC composition, the phase assemblage of mixed C_3S, C_3A and gypsum is the sum of the phase assemblages observed in pure systems. Hannawayya [26, 27] observed after 7 days by XRD peaks due to the presence of CH and ettringite. As the hydration proceeds, the ettringite reacted with C_3A to form monosulfoaluminate ($C_4A\$H_{12}$) and traces of hydroxy-AFm (C_4AH_{13}) were found. For systems composed of 76%C_3S – 19% C_3A -5% gypsum Regourd *et al.* [25] found by EDS analysis that calcium silico aluminate hydrates analogous to ettringite and monosulfoaluminate could be formed. With higher gypsum content, however, these phases were unstable and converted into calcium sulfoaluminate hydrates.

More recently Minard [29] investigate how the kinetics of alite hydration is modified in cements. To do so, she studied alite hydration in solution containing different ions such as aluminate and sulfate ions. Subsequently systems containing alite with C_3A-gypsum additions were investigated.

- Minard's results in diluted suspension and in pastes show that alite hydration is slowed down in the presence of aluminate ions in the pore solution.
- In the presence of only calcium sulfate the rate of alite reaction is increased but the induction period remains unchanged.
- While the presence of aluminate and calcium sulfate ions in solution influences the kinetics of alite hydration, in the presence of C_3A and gypsum phases, the kinetics of alite reaction remain almost identical in model cements and in pure systems (Figure 4-3).

The effects of the aluminate and calcium sulfate ions in solution on the alite reaction tend to be canceled out in cement pastes since they are consumed by C_3A hydration.
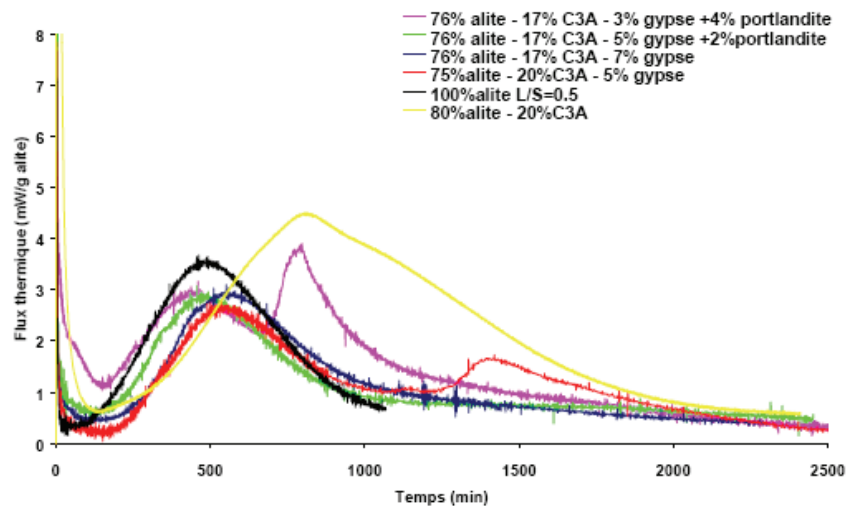
Figure 4-3: Heat evolution profiles of model cement pastes of different composition. The composition of the model cements influences mainly the aluminate reaction. The silicate reaction is almost unchanged. Reproduced from [29].

It is important to note that all the previous studies described here have been carried out on mixtures of alite, C_3A and gypsum powders while in Portland cement, the alite and the aluminate phases are present as polyphase grains. The studies of Di Murro [30] on mixtures of pure phases (monophase grains) and polyphase grains of alite and C_3A mixed with gypsum showed significant differences in the hydration kinetics, mainly that of C_3A, depending on the monophase or polyphase nature of the cement grains. She observed that the calorimetric peak attributed to the C_3A reaction with ettringite to form monosulfoaluminate occurs later in systems composed of monophase grains (Figure 4-4). She explained this feature by the fact that the phase availability is different in monophase and polyphase systems. In polyphase grains, the minor phase C_3A is then better dispersed and present in small amounts in all the cement grains instead of few coarse monophase C_3A grains. Its specific surface is also higher than in monophase systems, leading to a higher reactivity.
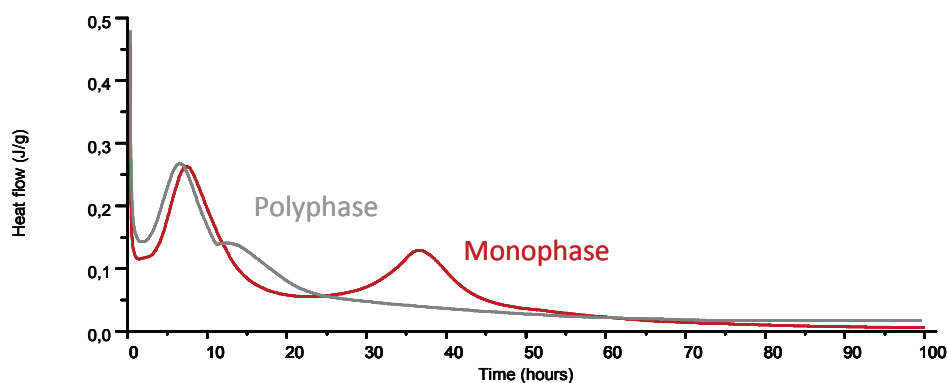

Figure 4-4: Heat evolution and conductivity curves of monophase and polyphase model cement pastes containing 73% alite – 18% C_3A – 9% gypsum. The aluminate reaction is strongly influenced by the monophase / polyphase nature of the grains. Adapted from [30].

80

4.1.3 Microstructure of cementitious materials

C-S-H is the most important hydrate in the microstructure. Two different terms are used to distinguish C-S-H in the microstructure of Portland cement: the "inner" and the "outer" products. The inner product forms within the boundary of the original grains and has homogeneous morphology [31]. The outer product forms in the matrix and has a fibrillar or foil-like morphology [31]. The matrix is a mixture of the four major hydrates: C-S-H, CH, Afm, and Aft. Of these, C-S-H and CH are by far the most abundant (Figure 4-5).
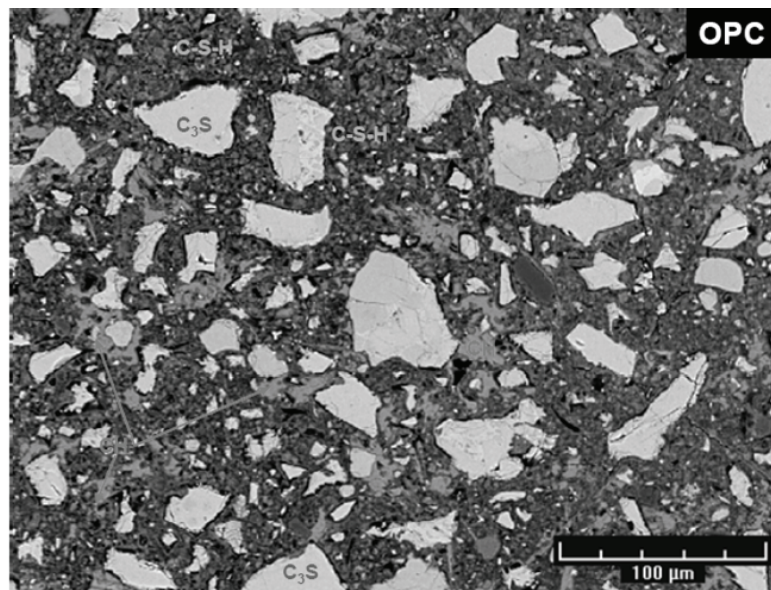

Figure 4-5: SEM – BSE image of ordinary Portland cement at 24h of hydration. Reproduced from [32].

The microstructural development of Portland cement during the hydration reaction was described by Scrivener as presented in Figure 4-6 [19]. Within the first minutes after contact with water, the aluminate part of polyphased cement grains reacts with gypsum and water to form an amorphous aluminate rich gel (now thought to be AFm as discussed in the previous chapter) and ettringite rods. By 10 hours, outer C-S-H is formed on the ettringite rod network leaving a space of around 1µm between the grain and the shell of hydrated product. The formation of a separated shell of hydrates around the hydrating grains is a particularity of the microstructural development of cement pastes. These grains are named after the discoverer as Hadley grains [33, 34].
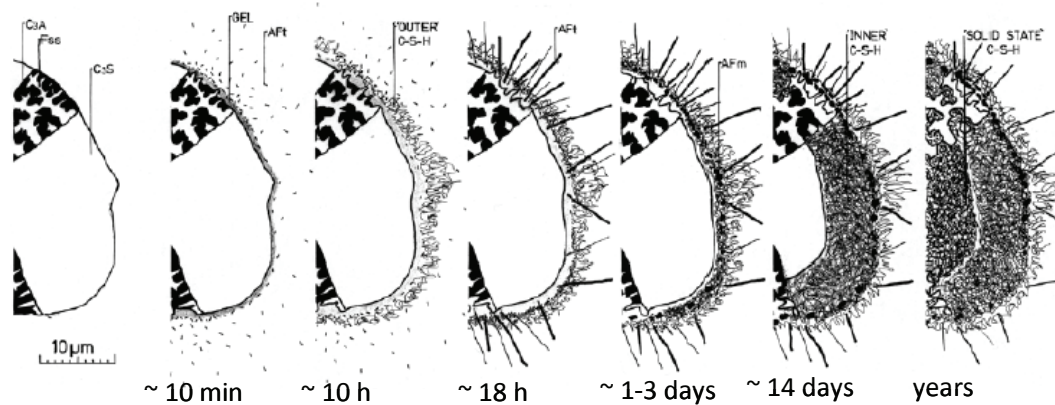
~ 10 min   ~ 10 h   ~ 18 h   ~ 1-3 days   ~ 14 days   years

Figure 4-6: Microstructural development of cement grains. Adapted from [19].

After 18 hours, long rods of AFt are formed from the secondary hydration of C_3A and C-S-H inner product start to form inside the shell. In a microstructure old of around 1 to 3 days, AFm hexagonal platelets, arising from the reaction between the C_3A and the AFt, can be observed. By 14 days, the space between the cement grain and the shell of hydrated product is filled by the inner C-S-H. Remaining anhydrous material reacts slowly up to several years to form more inner C-S-H. Some hollow-shells, where only the shell of hydration product remains after the complete reaction of the cement grain, may be found in the microstructure.

4.1.3.1   Microstructure of alite pastes

The microstructure of alite paste is similar to that of cement, but with some important differences that concern the morphology and the dispersion of portlandite. In OPC portlandite grows with variable shape and deposits everywhere in the matrix, in alite pastes portlandite grows into large CH clusters (Figure 4-7).
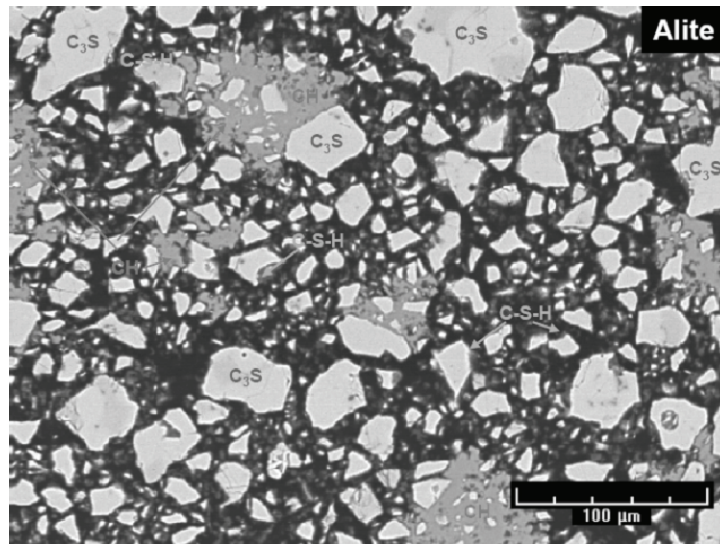
Figure 4-7: SEM image of alite paste at 24h of hydration. The main difference with the microstructures of OPC is the formation of big clusters of CH. Reproduced from [32].

Gallucci and Scrivener [35] studied different model cementitious systems such as alite with and without gypsum addition, alite-C_3A-gypsum systems and OPC. They reported two types of systems from the point of view of CH distribution depending if C_3A was present in the system or not. They observed that CH precipitated preferentially in the vicinity of gypsum grains but it seems that the dispersion of CH in the matrix is strongly related to the presence of aluminate phases.

Another difference discussed between microstructures of cement and alite pastes concerns the formation of Hadley grains. While the abundant occurrence of Hadley grains is reported in cement pastes some early reports stated that Hadley grains do not form in alite pastes [36]. The formation of these grains was associated with the presence sulfate and aluminate phases together with alite [36]. Moreover, the formation of Hadley grains was associated by Scrivener with the polyphase nature of cement grains as she observed close contact between the hydrating grains and the layer of hydrates in model cements made of a mixture of monophase grains of alite, C_3A and hemihydrate. It has to be noted that Gallucci et al. [37] have shown by TEM images that these shells are not empty but filled with C-S-H which has a lower density than the rest of the hydration product. Whether hollow-shells are hollow or contain a low density product does not change the fact that gapped Hadley grains are rarely observed in alite pastes (only for small grains), while their occurrence is quite common in OPC.

However, the recent observations of Kjellsen and Lagerbald [38, 39] seem to challenge the claim that gapped Hadely grains do not occur in alite pastes. They reported the evidence of hollow shells in alite pastes at 24 hours of hydration and the presence of narrow gaps between alite grains and the

hydration product at earlier ages (around 10h of hydration) (Figure 4-8). They state that the hollow shells usually observed at 24h of hydration seem to be the remnant of the small gapped grains seen at early ages. Therefore the hydration mode that leads to the formation of Hadley grains seems to occur in both Portland cement and alite pastes.
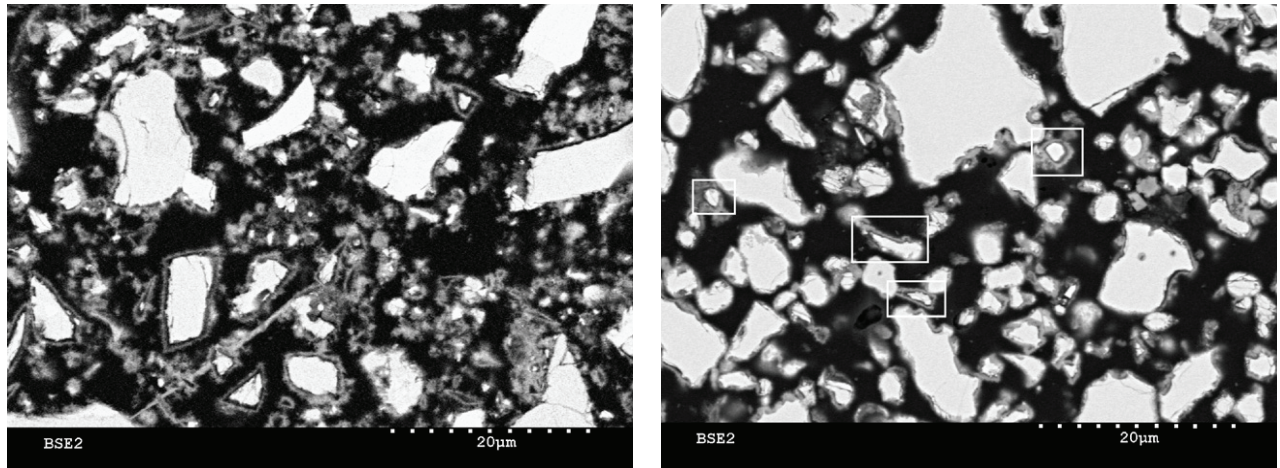

Figure 4-8: SEM images of a cement paste (13h of hydration) (left) and alite paste (13h of hydration) (right). Gapped Hadley grains are observed also in alite pastes but only for the smaller grains and at earlier ages compare to OPC pastes. Reproduced from [39].

4.2 Objectives of the study and experimental plan

The previous chapter described the calcium aluminate – calcium sulfate reaction. The aim of this chapter is to study the interactions of these systems with alite when hydration occurs in multi-phase systems. Indeed, cement hydration is not the simple sum of the reactions of its constituents, but the result of multiple interactions between all the phases. The comprehension of these interactions, is necessary to understand the influence of the cement composition (in particular the amount of C_3A and the sulfate balance), on the microstructural development and hydration kinetics. Such knowledge is crucial for the further development of models such as μic and the development of more sustainable cementitious materials.

For this study, model cements composed of alite, C_3A and gypsum were prepared and their hydration was studied. First, the influence of the composition and the differences between the reaction of individual cement phases when hydration occurs in pure systems or in multi-phase systems were investigated in terms of phase assemblage and microstructural development. Subsequently the kinetics of reaction was studied by isothermal calorimetry. Model cements with different and controlled compositions were investigated. As gypsum controls C_3A hydration it was possible to influence the aluminate reaction and study its interaction with alite depending on the relative time of occurrence of both reactions adding different amounts of gypsum to the model cements, while the alite/C_3A ratio was kept constant at 92/8, which is the typical ratio between alite and C_3A in Portland cement (average calculated based on Rietveld analysis of several Portland cements [40]). Other model cements with different alite/C_3A ratios were also studied. All these systems are called monophase cements as they are made of monophase grains of pure alite, C_3A and gypsum, in contrast to polyphase cements that are made of polyphase clinker composed of both alite and C_3A. Polyphase cements composed of alite/C_3A clinker with different gypsum additions were also prepared to investigate how the monophase or polyphase nature of the cements affects the hydration of the cement phases and if the features observed in monophase systems can also be observed in polyphase systems. Indeed, the dispersion of the anhydrous phases, especially C_3A which is the minor phase, has a significant effect on the hydration kinetics of the model cement as already highlighted by Di Murrro [30] The compositions of the different monophase and polyphase model cements are given in Table 4-1 and Table 4-2.

Table 4-1 Compositions of the monophase model cements

Monophase	wt% alite	wt% C_3A (Batch C)	wt% gypsum (Merck)	wt% Alite/C_3A ratio	wt% C_3A/gypsum ratio
M_2%G	90.20	7.84	1.96	92/8	80/20
M_2.6%G	89.61	7.79	2.60	92/8	75/25
M_3.3%G	88.95	7.73	3.31	92/8	70/30
M_4.1%G	88.23	7.67	4.13	92/8	65/35
M_5%G	87.37	7.60	5.03	92/8	60/40
M_6.2%G	86.34	7.51	6.15	92/8	55/45
M90/10_6.3%G	84.37	9.37	6.25	90/10	60/40
M94/6_3.9%G	90.38	5.77	3.85	94/6	60/40

Table 4-2: Compositions of the polyphase model cements

Polyphase	wt% clinker	wt% gypsum (Merck)	wt% Alite/C_3A	wt% C_3A/gypsum
P90/10_20G	97.56	2.44	90/10	80/20
P90/10_30G	95.89	4.11	90/10	70/30
P90/10_35G	94.89	5.11	90/10	65/35
P90/10_40G	93.75	6.25	90/10	65/35
P_2%G = P92/8_20G	98.04	1.96	92/8	80/20
P_2.6%G = P92/8_25G	97.40	2.60	92/8	80/20
P_3.3%G = P92/8_30G	96.68	3.32	92/8	70/30
P_4.1%G = P92/8_35G	95.9	4.1	92/8	65/35
P94/6_20G	98.52	1.48	94/6	80/20
P94/6_30G	97.49	2.51	94/6	70/30
P94/6_35G	96.87	3.13	94/6	65/35
P94/6_40G	96.15	3.85	94/6	60/40

The x-ray diffraction patterns, the SEM images, particles sized distributions and calculated specific surface areas of the powders are reported in CHAPTER 2.

The research was extended to systems with low gypsum content, so called undersulfated systems. With undersulfated systems, the aluminate reaction to form AFm phases occurs before the alite reaction [28]. The alite peak is then drastically lowered and delayed compare to heat evolution profiles of properly sulfated systems. The reason for renewed interest in the undersulfation problem is that it is sometimes found that commercial cements which are properly sulfated from the point of view of hydration without additives or additions, may behave in an undersulfated manner when used in the field with additives or mineral additions [41]. This behavior leads to problems of improper setting and hardening. It is therefore crucial to understand the reactions concerning the aluminate sulfate balance.

Additional experiments were carried out on alite and C_3A-gypsum systems. Alite-gypsum as well as model systems composed of an inert filler and C_3A-gypsum were prepared as summarized in Table 4-3. The Filler systems have the same composition as the Monophase systems except that alite was replaced by quartz (with a PSD similar to alite) as inert filler. These last samples were prepared in order to study the effect of dilution of the C_3A-gypsum reaction.

Table 4-3: Compositions of the systems prepared for additional experiments

Additional experiments	wt% alite	wt% filler (Quartz)	wt% C_3A (Batch C)	wt% gypsum (Merck)	wt% Filler/C_3A	wt% C_3A/gypsum
Alite_2%G	98			2		
Alite_5%G	95			5		
Alite_10%G	90			10		
F_2%G		90.20	7.84	1.96	92/8	80/20
F_3.3%G		88.95	7.73	3.31	92/8	70/30
F_5%G		87.37	7.60	5.03	92/8	60/40

The experiments carried out on all these samples are summarized in Table 4-4.

Table 4-4: Summary of the model systems and experiments

Samples\ experiments	Kinetics (calorimetry)	Phase assemblage (XRD)	Microstructure (SEM)
M_2%G	@15,20,26 ,30°C		X
M_2.6%G	@15,20,26 ,30°C		X
M_3.3%G	@15,20,26 ,30°C		X
M_4.1%G	@15,20,26 ,30°C		X
M_5%G	@15,20,26 ,30°C		X
M_6.2%G	@15,20,26 ,30°C		X
M90/10_6.3%G	@ 20°C		
M94/6_3.9%G	@15,20,26 ,30°C		
P90/10_20G	@ 20°C		
P90/10_30G	@ 20°C		
P90/10_35G	@ 20°C		
P90/10_40G	@ 20°C		
P92/8_20G	@15,20,26 ,30°C	In-situ at early ages @26°C	X
P92/8_25G	@15,20,26 ,30°C	In-situ at early ages @26°C	X
P92/8_30G	@15,20,26 ,30°C	In-situ at early ages @26°C	X
P92/8_35G	@15,20,26 ,30°C	In-situ at early ages @26°C	X
P94/6_20G	@ 20°C		
P94/6_30G	@ 20°C		
P94/6_35G	@ 20°C		
P94/6_40G	@ 20°C		
alite	@15,20,26 ,30°C		
alite-2%G	@ 20°C		X
alite-5%G	@ 20°C		X
alite-10%G	@ 20°C		X
F_2%G	@ 20°C		
F_3.3%G	@ 20°C		
F_5%G	@ 20°C		

4.3 Evolution of the phase assemblage in multi-phases systems

From previous studies on model cements [26, 27] and OPC it is know that generally the same phases are generated in cements as in pure systems. Alite reacts with water to form C-S-H and CH. C_3A and gypsum hydrates to form ettringite and AFm phases. The aim of this study was to investigate the differences that may exist in the kinetics of formation / dissolution of the phases between the pure and multi-phase system and correlate the evolution of the phase assemblage with the heat evolution profile. We choose to study the four polyphase model cements with an alite/C_3A ratio of 92/8 as these model systems have composition close to that of real cements. The phase assemblage was monitored during the first hours of hydration by in-situ XRD (sampling rate = 14min).

The evolution of the phase assemblage obtained for these four systems are presented in Figure 4-9 to Figure 4-12. As expected the same phases are formed in pure systems and in model cements, the aluminate phase assemblage depends on the gypsum content: low gypsum contents lead to the formation of both monosulfoaluminate and hydroxy-AFm (sample P92/8_20G) while only monosulfoaluminate ($C_4A\$H_{14}$) is formed for higher gypsum contents (samples P92/8_25G, P92/8_30G and P92/8_35G). The sample P92/8_25G showed the kinetics of undersulfated system with the aluminate reaction occurring before the silicate one but had a phase assemblage similar to properly sulfated systems.
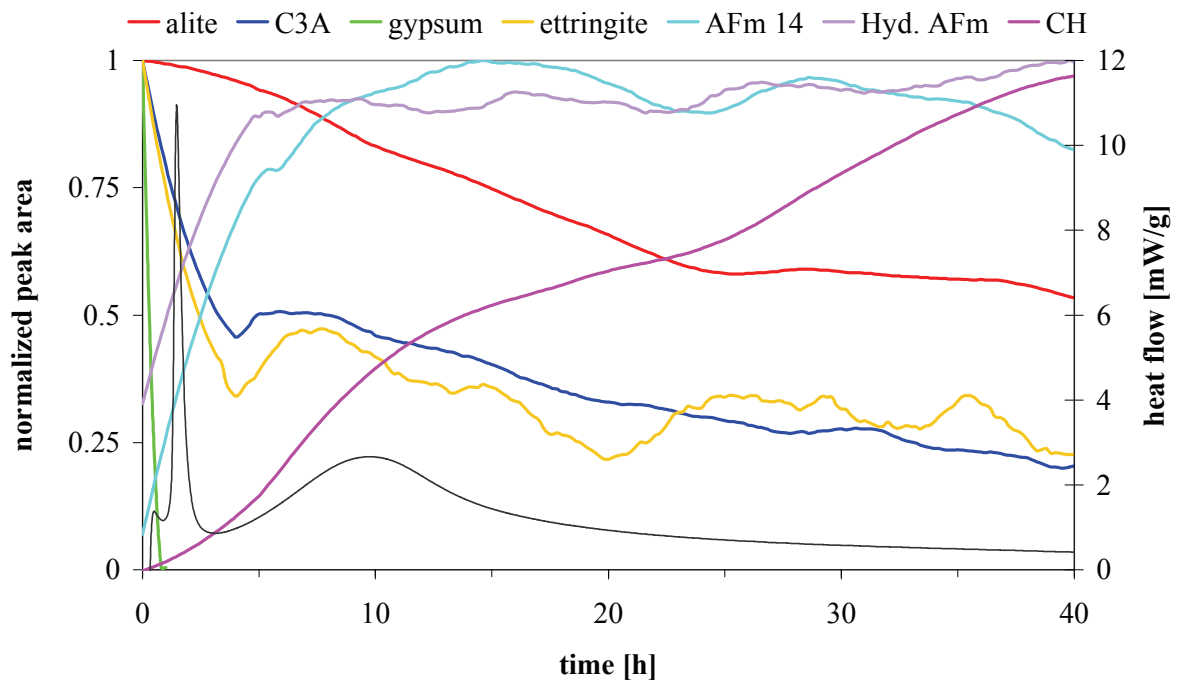
Figure 4-9: Evolution of the phase assemblage and heat flow during the first hours of hydration Sample P92/8_20G (undersulfated system).
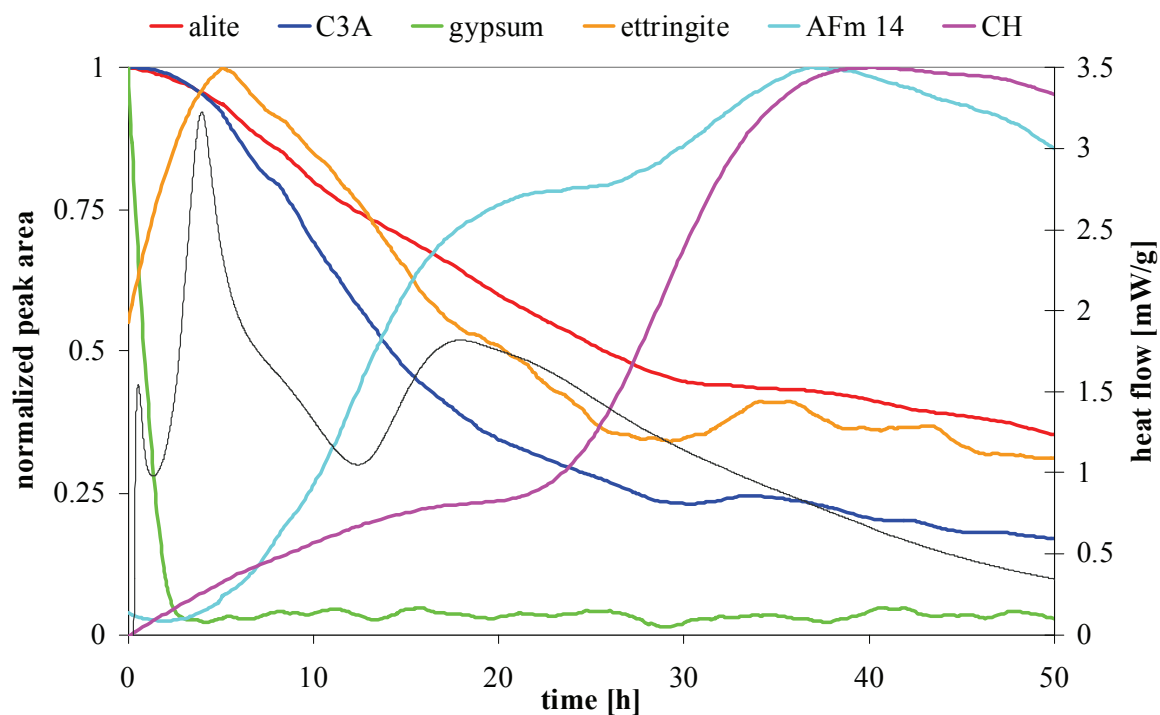
Figure 4-10: Evolution of the phase assemblage and heat flow during the first hours of hydration Sample P92/8_25G (undersulfated systems).
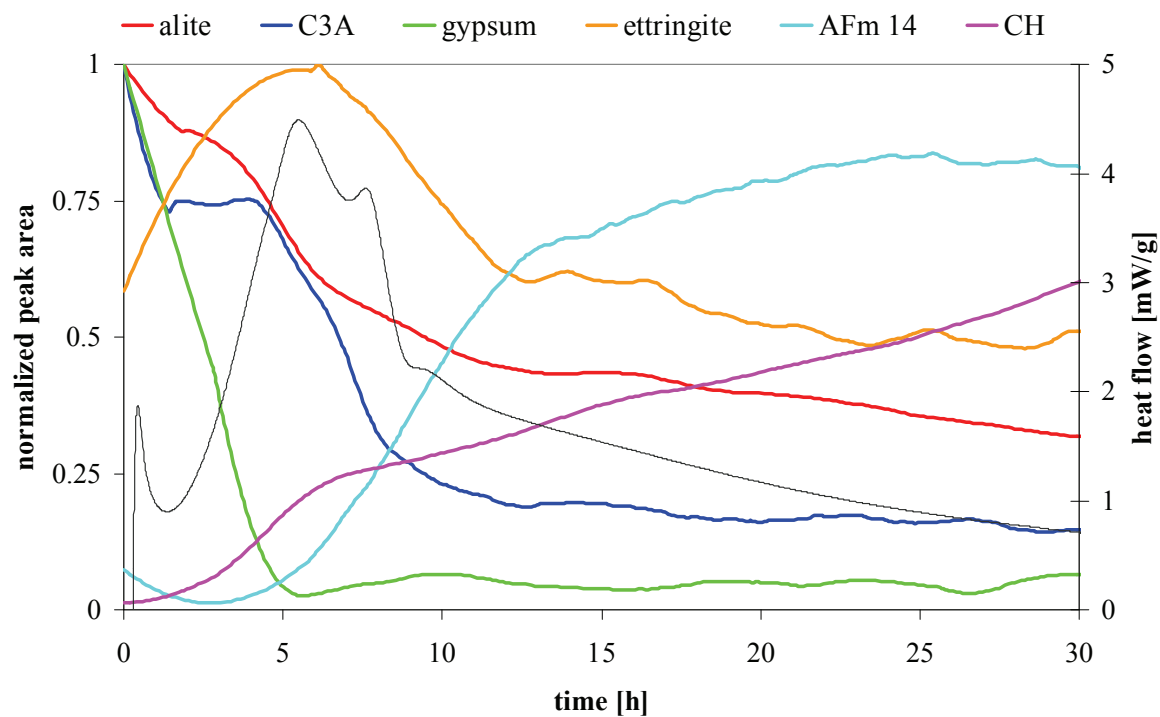

Figure 4-11: Evolution of the phase assemblage and heat flow during the first hours of hydration Sample P92/8_30G (properly sulfated systems)
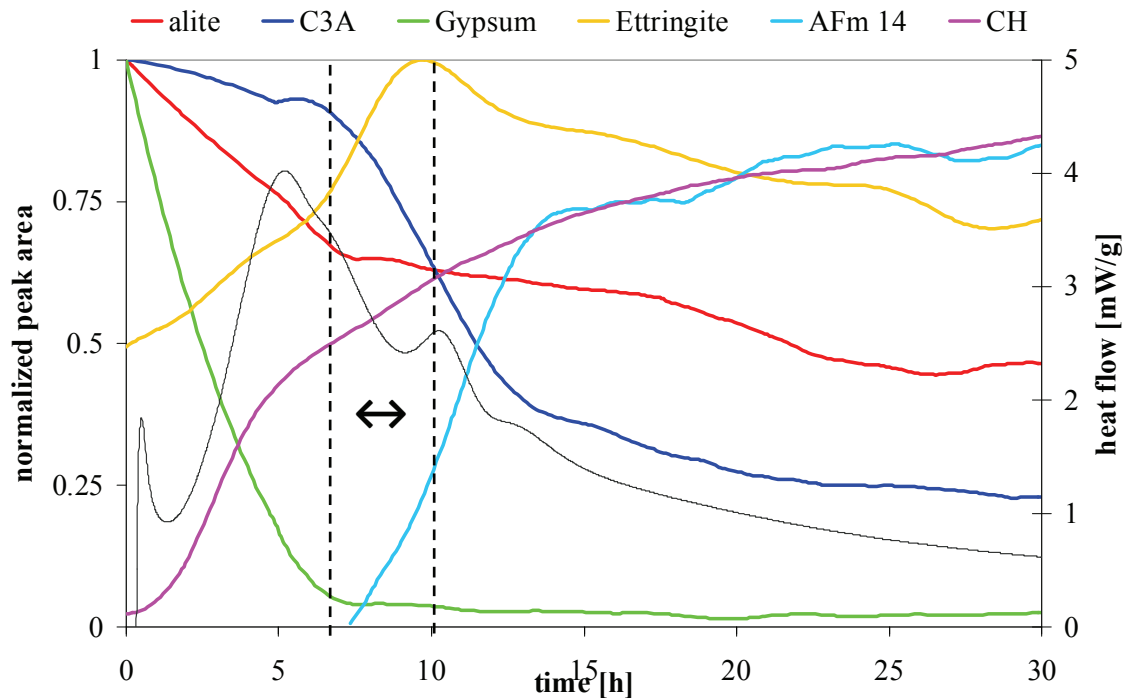
Figure 4-12: Evolution of the phase assemblage and heat flow during the first hours of hydration Sample P92/8_35G (properly sulfated systems). It can be observed that C$_3$A dissolves rapidly after the depletion of gypsum while ettringite continue to form during few hours.

One important difference between the pure and the multi-phase systems can be observed in Figure 4-12 for the sample with the higher gypsum content: while in pure C$_3$A-gypsum systems ettringite start to dissolve immediately after gypsum depletion; in the presence of alite we observed the formation of ettringite even after gypsum consumption. This phenomenon occurs at the time corresponding to the heat development that forms a shoulder on the silicate peak of the calorimetric curve. These results confirm the hypothesis of Scrivener [19] who suggested that this heat development was due to the second ettringite formation. Some of the sulfate adsorbed on C-S-H can react to form more ettringite after gypsum depletion as shown by Gallucci *et al.* [37]. The formation of monosulfoaluminate seems to start right after gypsum depletion. Therefore in model cements we can observe the simultaneous formation of ettringite and monosulfoaluminate for few hours after gypsum depletion. In contrary to the C$_3$A-gypsum system, ettringite is still stable during several hours after the gypsum depletion.

4.4 Influence of the cement composition on the microstructure

As discussed in the literature review there are some differences between the microstructure of OPC and alite pastes. In this section several model systems were studied in order to highlight the origin of these differences. The localization of the hydrates (silicate and aluminate) in the matrix was of particular interest. For this microstructural study, polished sections of model systems of different compositions were prepared and observed by scanning electron microscopy (back scattered electrons).

4.4.1 Portlandite precipitation

It is known that when alite hydrates alone, portlandite precipitates as clusters which grow from a few places in the matrix, whereas in OPC, portlandite crystallizes and grows everywhere in the matrix with variable shape. The results of Gallucci and Scrivener [35] on model systems composed of alite with and without gypsum addition and model cements with monophase and polyphase grains show that the dispersion of CH is mainly due to the presence of calcium- aluminate hydrates in the paste.

In the present study the distribution of portlandite in the microstructure was investigated in model systems of various compositions as presented in Figure 4-13 where they are compared to OPC and alite pastes. The case of the undersulfated cement was of particular interest as it has been less investigated in the past.

Very similar microstructures were obtained for both properly sulfated and undersulfated cements. The dispersion of the precipitates of CH in these systems is closer to the one observed in OPC than the one observed in alite microstructures even though the precipitates seem slightly bigger than in OPC. These observations confirm the hypothesis of Gallucci and Scrivener that it is the presence of aluminate phases more than gypsum that influences the distribution of Portlandite in the microstructure [35]. Indeed, undersulfated systems, where the gypsum is consumed before the beginning of alite reaction, show microstructures similar to the properly sulfated systems from the point of view of CH distribution. No significant difference was observed in the distribution of CH between polyphase and monophase systems.
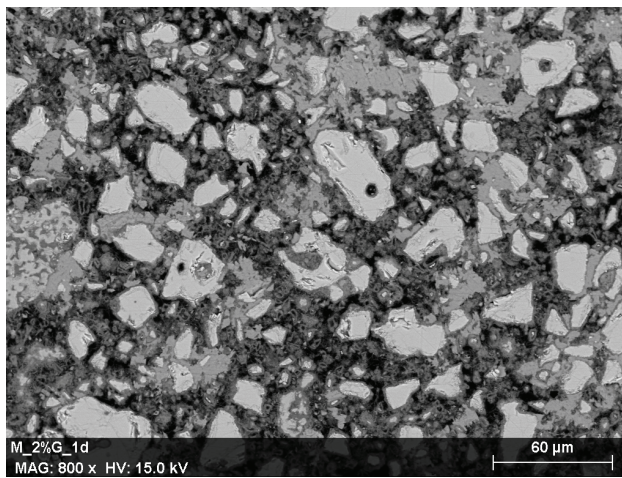
Therefore, if the three main components of cement (alite, C_3A and gypsum) are present, the precipitation of CH is not affected by small changes in the composition of the original mix.
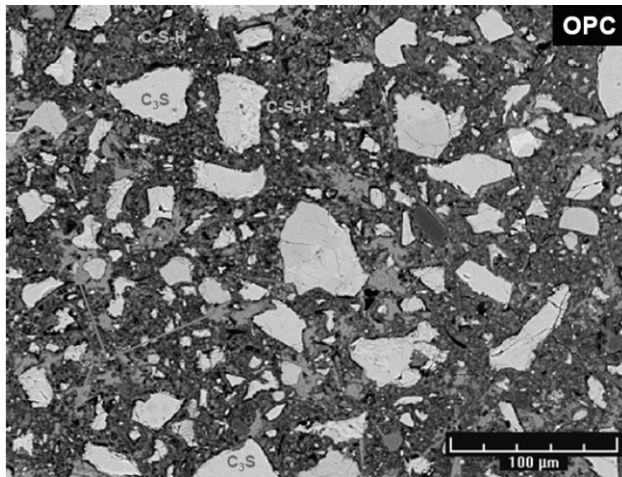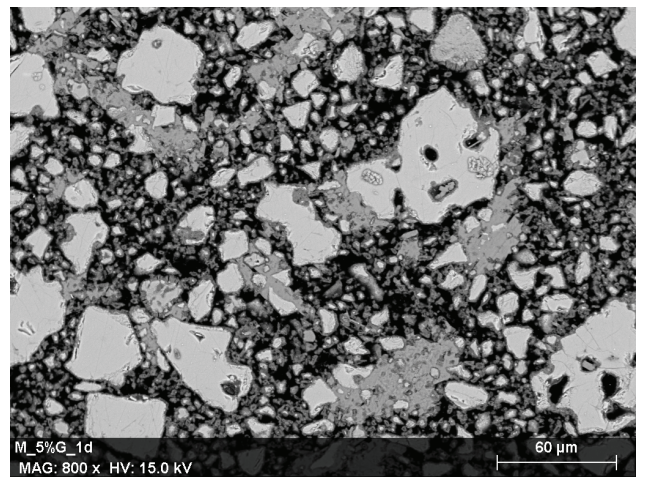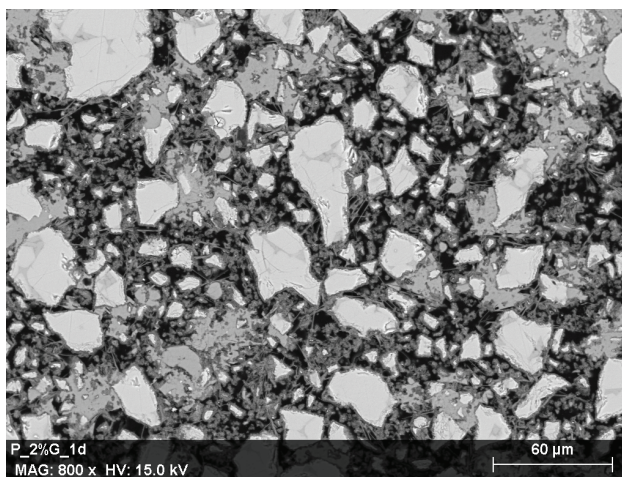
(a) OPC 24h Reproduced from [32].
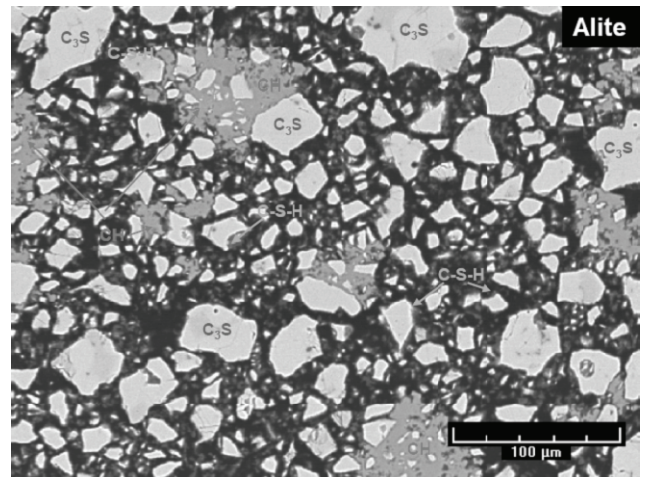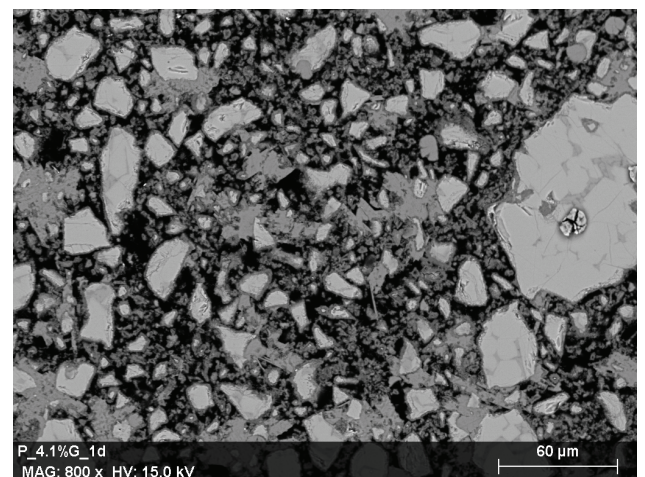
(b) alite 24h Reproduced from [32].

(c) Undersulfated monophase cement 24h

(d) Properly sulfated monophase cement 24h

(e) Undersulfated polyphase cement 24h

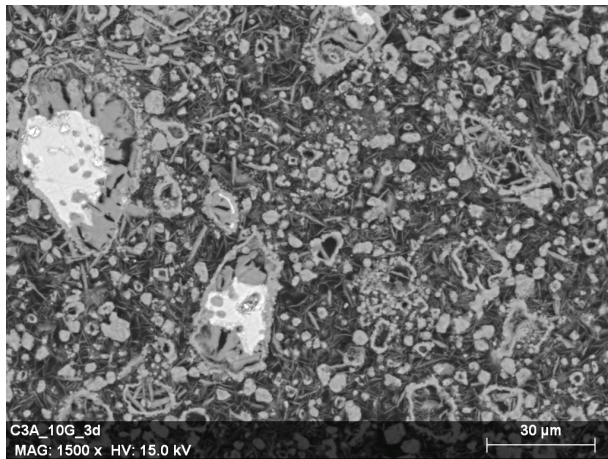(f) Properly sulfated polyphase cement 24h

Figure 4-13: Comparison of CH dispersion in OPC, alite and different model systems. The dispersion of CH observed in model cements is closer to the one observed in OPC than the one of alite. However, the precipitates seem slightly bigger in these model cements than in OPC.

4.4.2 Aluminate hydrates

The distribution of the aluminate hydrates in the microstructure of model cements of different compositions was investigated and compared to the microstructures observed for pure C_3A-gypsum systems (Figure 4-14).

Even though aluminate hydrates were observed everywhere in the matrix it seems that they precipitate preferentially around the C_3A grains in the case of monophase systems, as in the microstructure of pure systems. The main differences between C_3A-gypsum systems and monophase cements are that the dense inner product was not present in the monophase cements as much as in the pure systems and hydrogarnet shells were not observed in model cements even in undersulfated systems after 28 days of hydration.

The distribution of the aluminate hydrates was significantly different in the microstructure of polyphase systems. The hydrates do not precipitated around cement grains but are dispersed in the matrix as in an OPC microstructure. This important difference between the monophase and polyphase systems that was also highlighted by Di Murro [30] is due to the fact that C_3A is present together with alite in all the cement grains in polyphase model cement and OPC while pure C_3A grains are present in monophase and in pure C_3A-gypsum systems. It seems therefore that the difference in the distribution of the aluminate hydrates between the C_3A-gypsum systems and OPC is due to the polyphase nature of the grains.
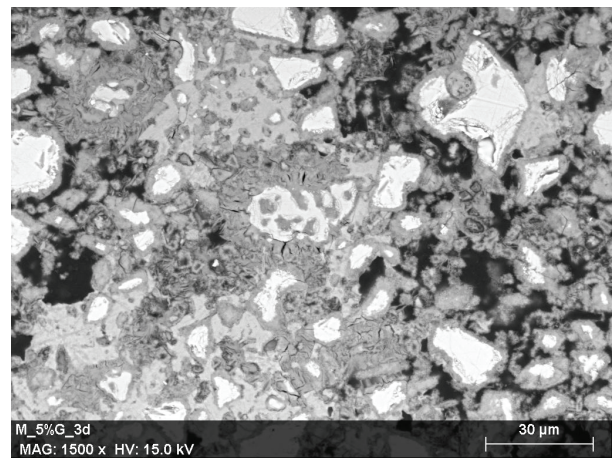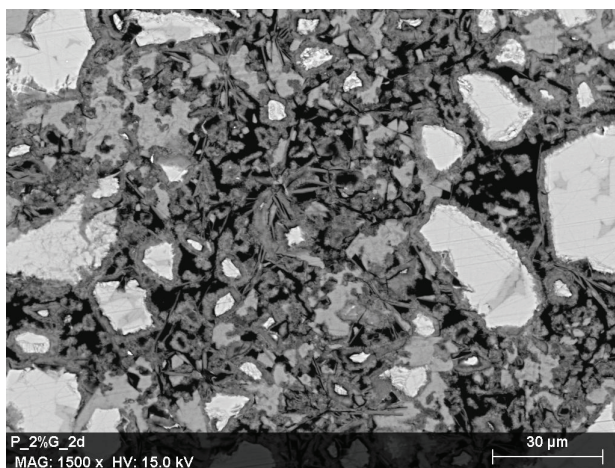
(a) C₃A_low gypsum content (3d of hydration)
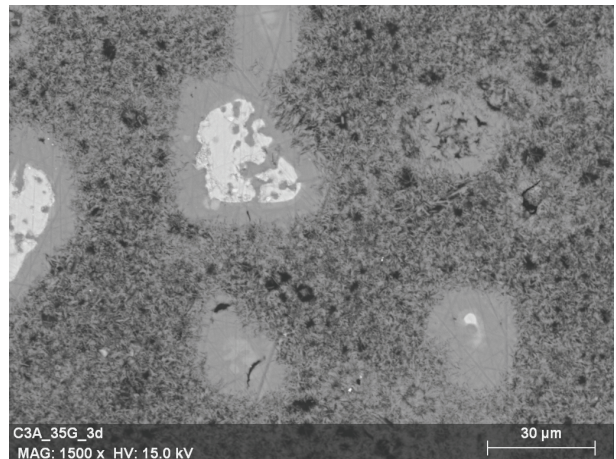
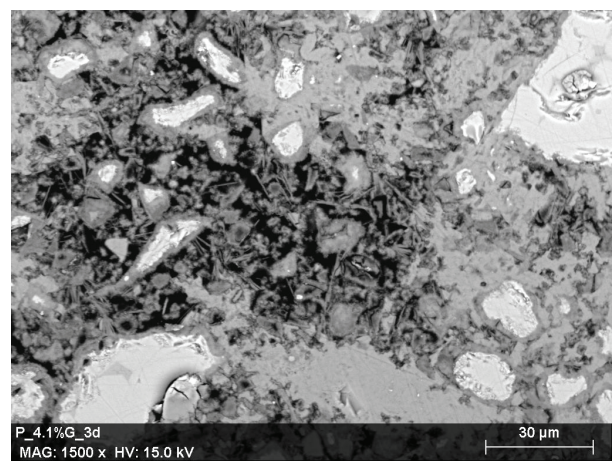(b) C₃A_high gypsum content (3d of hydration)

(c) Undersulfated monophase cement (3d)

(d) Properly sulfated monophase cement (3d)

(e) Undersulfated polyphase cement (3d)

(f) Properly sulfated polyphase cement (3d)

Figure 4-14: Comparison of the distribution of aluminate phases in C₃A – gypsum pastes and in different model systems. The distribution of the aluminate hydrates is significantly different in polyphase systems where the C₃A is present in the alite grains. No hydrogarnet shells where observed when alite is present in the system.

As in pure C$_3$A-gypsum systems the formation of a significant amount of AFm can be observed after the surge in C$_3$A reaction that occurs after the consumption of gypsum (Figure 4-15).
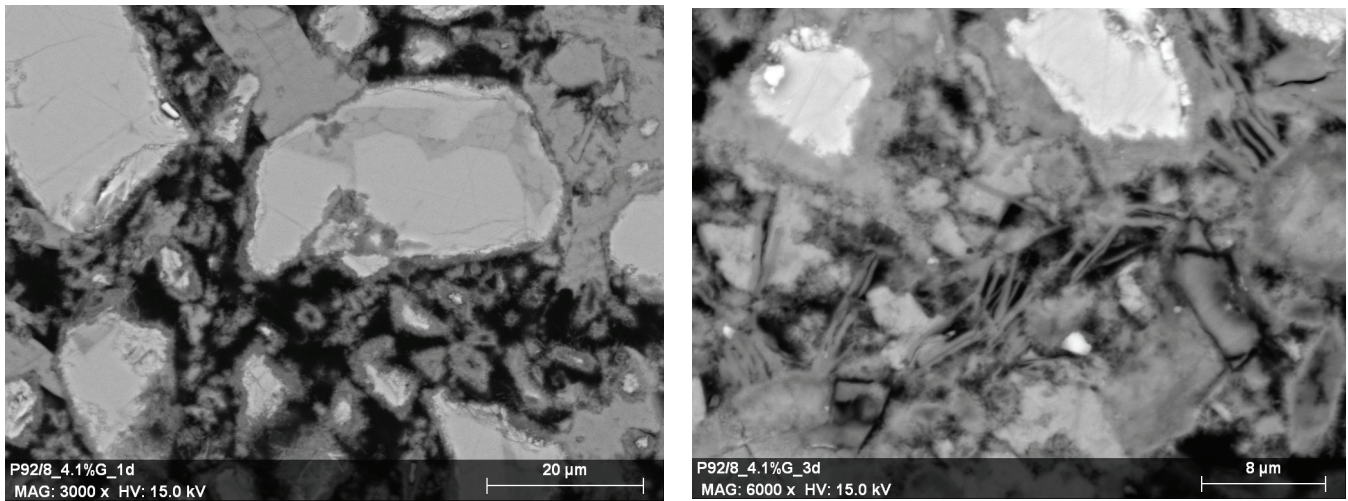
<table>
<tr><td>(a) at 1 day of hydration</td><td>(b) at 3 days of hydration</td></tr>
</table>

Figure 4-15: A densification of the matrix can be observed with the formation of monosulfoaluminate between 1day and 3 days of hydration. Sample: P_4.1%G.

The change in the composition of the finely intermixed outer product (C-S-H with aluminate phases) can be observed by EDS analysis (Figure 4-16). The EDS analysis collected were statistically analyzed and plotted on Al/Ca vs. S/Ca ratio graphs. This representation leads to identification of phases or mixture of phases: when the points lie on the line joining the composition of two phases, we assume that we have a mixture of these phases. For the sample P_4.1%G the change between a matrix composed of C-S-H and ettringite to a matrix composed of C-S-H and monosulfoaluminate occurs between 18h and 24h of hydration. At 24h of hydration both ettringite and monosulfoaluminate are present in the microstructure, at 3 days only AFm hydrates are present together with C-S-H.

However, the transition from a phase assemblage composed of ettringite to AFm as aluminate phases occurs at a slower rate compare to the pure C$_3$A-gypsum system. This is coherent with the XRD measurements previously described that show that ettringite and monosulfoaluminate can co-exist during several hours after gypsum depletion and that the dissolution of C$_3$A and ettringite to form monosulfoaluminate is slower in model cements than in pure C$_3$A-gypsum systems (Figure 4-12 and Figure 3-6). It is also interesting to note in Figure 4-16 that the sulfur content in the mixture of C-S-H and ettringite drop between 15 and 18 hours of hydration. This drop may correspond to the second ettringite formation.
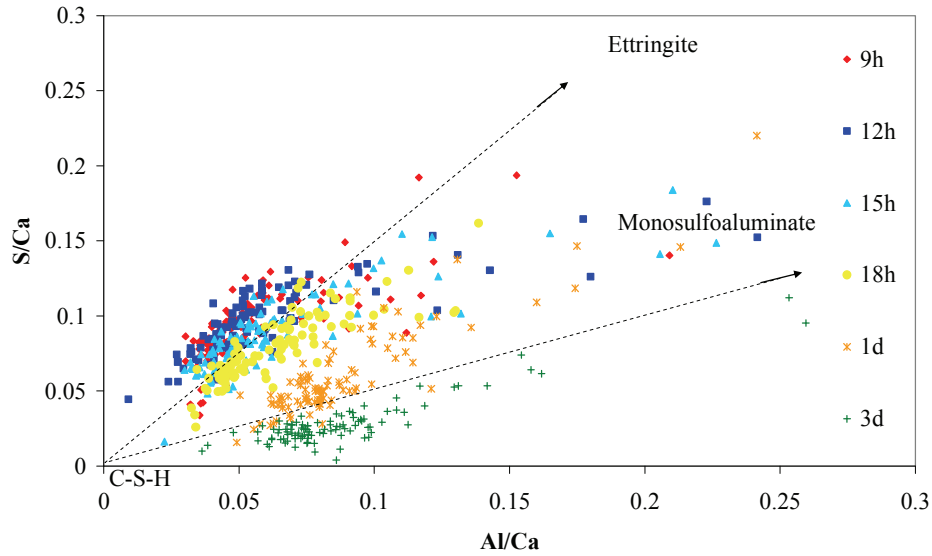
Figure 4-16: Phase assemblage obtained from EDS analyses. As hydration proceeds, the phase assemblage goes from an intermixing of C-S-H and ettringite to C-S-H and monosulfoaluminate. Sample P_4.1%G

(a) Polyphase cement P_2%G (3d of hydration)

(b) Polyphase cement P_2.6%G (3d of hydration)

(c) Polyphase cement P_3.3%G (3d of hydration)

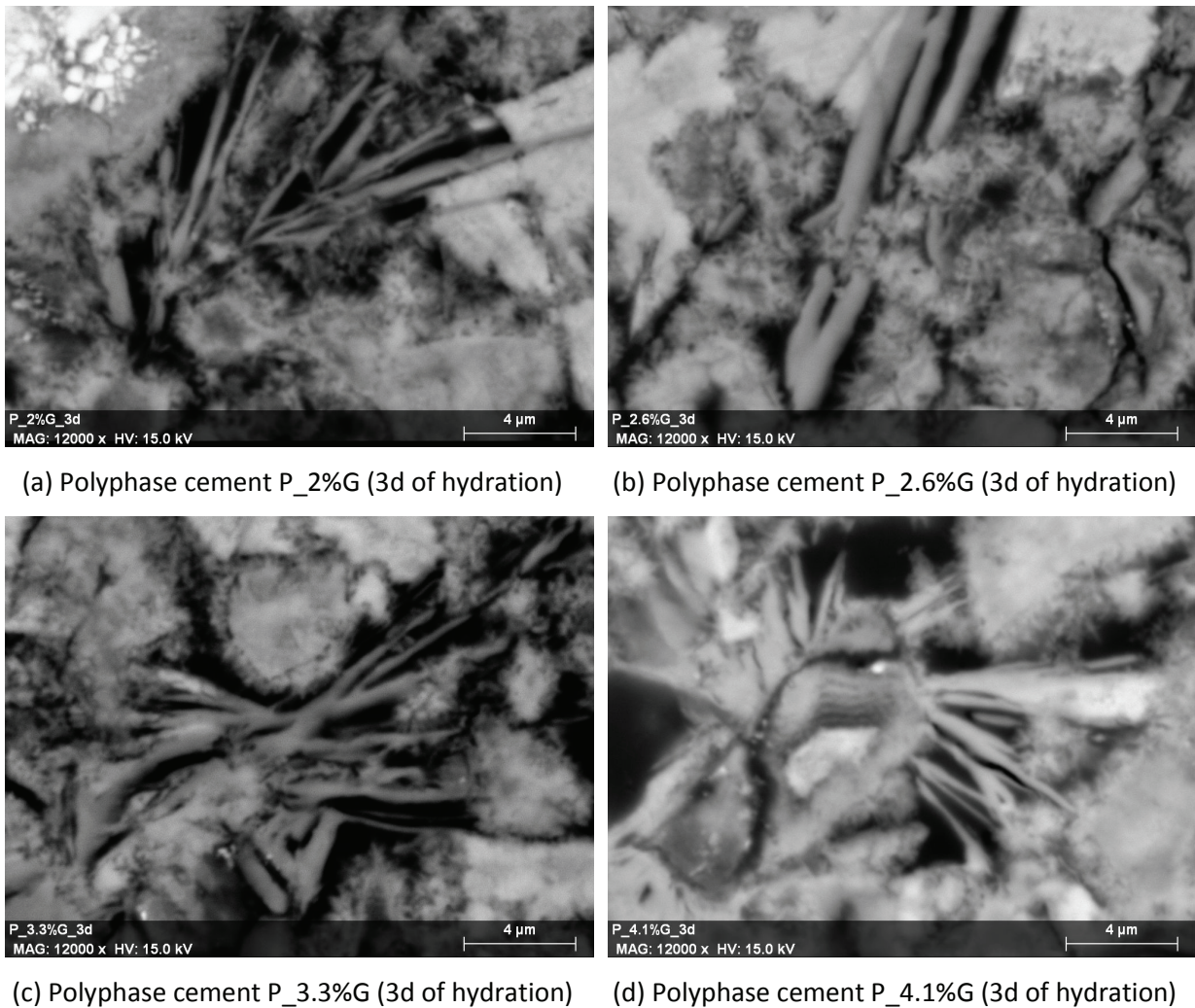(d) Polyphase cement P_4.1%G (3d of hydration)

Figure 4-17: Influence of the gypsum content on the morphology of the AFm platelets in polyphase model cements. Slightly longer AFM platelets were observed in systems with lower gypsum content.

The morphology of the aluminate phases is influenced by the gypsum content in model cement as in C_3A-gypsum systems. It was observed in pure systems that the AFm platelets are longer when the gypsum content is low (Figure 3-19). The same feature is observed for the aluminate hydrates in model cement as reported in Figure 4-17 although the difference is less pronounced than in C_3A-gypsum systems. Longer AFm platelets are present in the microstructure of the undersulfated cement P_2%G while platelets are smaller in the properly sulfated cements P-3.1%G and P_4.1%G. The AFm platelets are particularly massive in the microstructure of the undersulfated cement P_2.6%G that is characterized by a highly exothermic aluminate peak.

4.4.3 C-S-H

The difference in the chemical composition of the C-S-H as well as the occurrence of Hadley grains depending on the cement composition was investigated. C-S-H composition was measured by EDS analysis. The mean S/Ca and Al/Ca ratios of different model systems are reported in Figure 4-19 to Figure 4-22. C-S-H is usually finely intermixed with the aluminate hydrates as can be observed in the S/Ca vs. Si/Ca and Al/Ca vs. Si/Ca graphs presented in Figure 4-18. In order to obtain the S/Ca and Al/Ca ratios of C-S-H the data used for the calculation were restricted to the points that form the cluster of data where the lines between aluminate and C-S-H and CH and C-S-H join (in red in Figure 4-18). A mean value was calculated and the error bars in Figure 4-19 to Figure 4-22 correspond to the standard deviation.
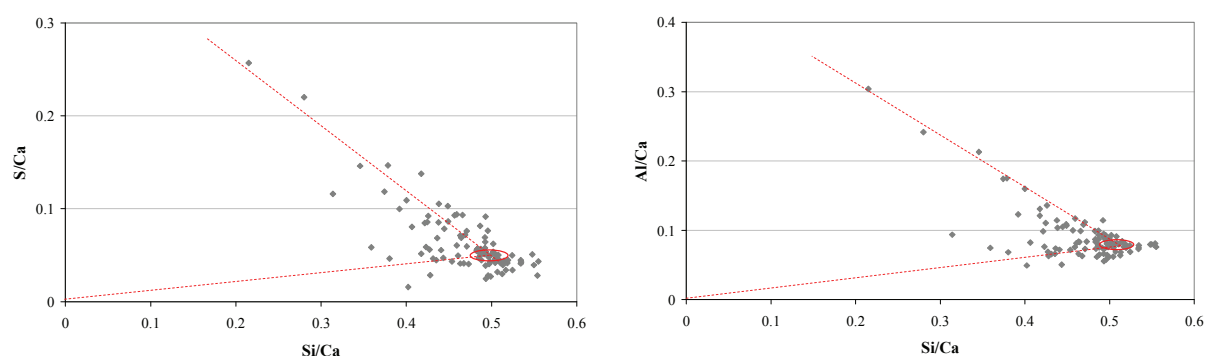

Figure 4-18: Data processing for calculation of S/Ca and Al/Ca content in C-S-H. The data used for the calculation of the chemical composition of C-S-H were restricted to the points that form the cluster of data where the lines between aluminate and C-S-H and CH and C-S-H join.
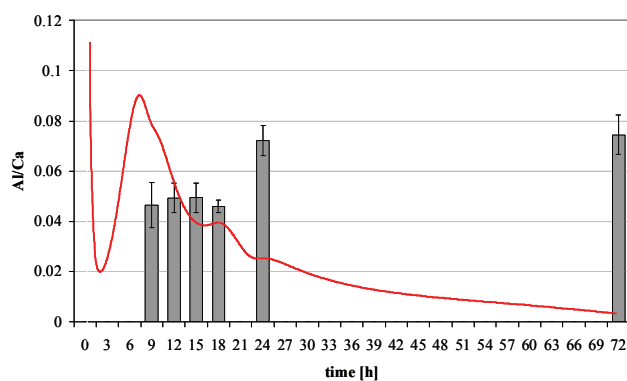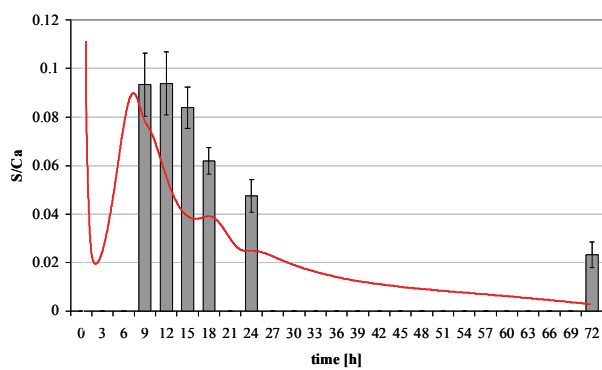
Figure 4-19: S/Ca and Al/Ca ratios of C-S-H of samples P92/8_4.1%G compared to heat evolution profile

Figure 4-20: S/Ca and Al/Ca ratios of C-S-H of samples M_5%G compared to heat evolution profile

Figure 4-21: S/Ca and Al/Ca ratios of C-S-H of samples M_6.2%G compared to heat evolution profile

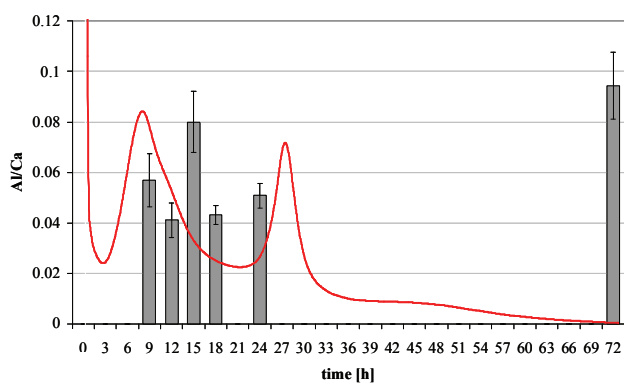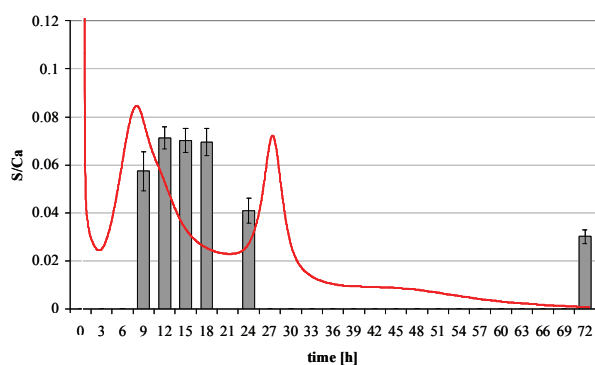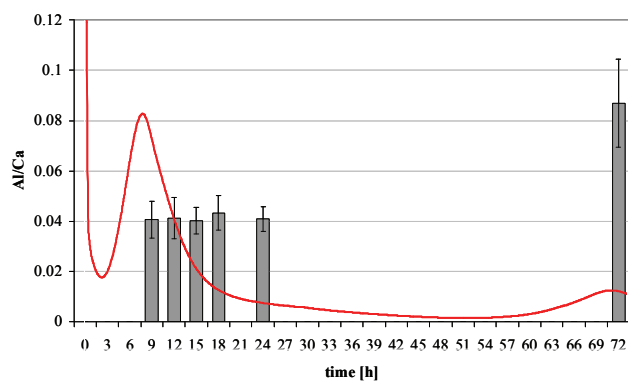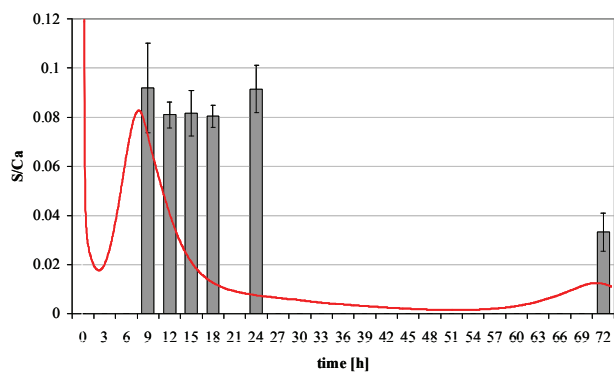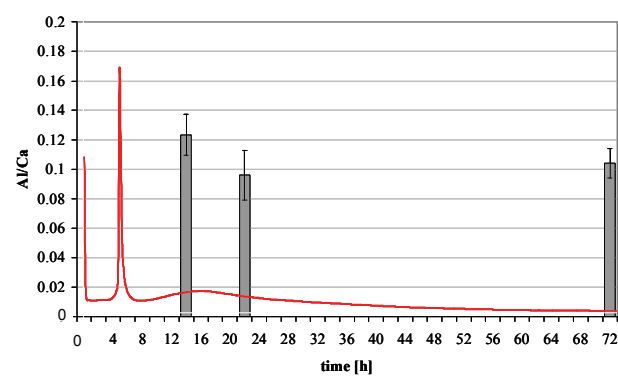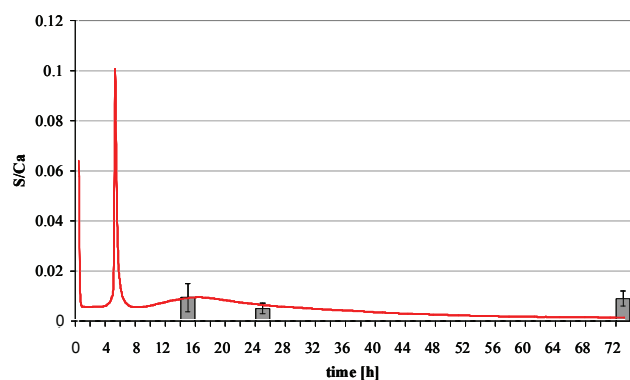**Figure 4-22: S/Ca and Al/Ca ratios of C-S-H of samples M_2%G compared to heat evolution profile**

The main difference in the chemical composition of the C-S-H observed between the model cement comes from the undersulfated or properly sulfated nature of the systems. In properly sulfated systems, when the main reaction of alite occurs when gypsum is still present, a significant amount of sulfate is adsorbed on the C-S-H. However, the sulfate ions that are adsorbed on C-S-H are released as the hydration proceeds. It is hypothesized that these sulfate ions react with C_3A to form more ettringite after the depletion of gypsum. This is the second formation of ettringite as described by Scrivener [19]. This phenomenon occurs in both monophase and polyphase systems. The work of Gallucci et al. [37] on the microstructural development of Portland cements also shows a drop in the sulfate content of the C-S-H shell after gypsum depletion associated with the formation of ettringite within the hydrate shell. Whereas most sulfate ions are released, some remain adsorbed on C-S-H after 3 days of hydration. The gypsum amount that is finally available for the reaction with aluminate phases is then lower than what can be expected from the cement composition. In the case of undersulfated cements, the amount of adsorbed sulfate ions on C-S-H is significantly lower. This occurs probably because all the gypsum is consumed by the reaction with C_3A before the C-S-H growth.

Another important difference in the chemical composition of C-S-H between undersulfated and properly sulfated systems is the Al content of the C-S-H. It is known that the Al ions can substitute Si in C-S-H. In this work it was observed that the Al content of C-S-H tends to increase after the calorimetric peak due to the reaction of C_3A and ettringite to form monosulfoaluminate, because during ettringite formation all the Al ions coming from the dissolution of C_3A are used to form ettringite and are not available in solution. The Al content of C-S-H during the growth period is therefore higher for undersulfated systems.

These differences in the chemical composition at the time of growth of C-S-H may modify the kinetics of the reaction during the growth of C-S-H depending on the composition of the original mix.

The precipitation of C-S-H around anhydrous grains varies also with the cement composition. While in OPC pastes the formation of Hadley grains (both hollow shells and gapped grains) are common, in alite pastes this kind of microstructure is observed only for small grains. For bigger grains close contact between the anhydrous grain and the layer of hydrate is observed. It was suggested that the occurrence of Hadley grains for bigger grains is related to the polyphase nature of the cement grains as is they are usually not observed in monophase systems [36]. In this microstructural study gapped Hadley grains where observed for polyphase systems but also for monophase model cement (Figure

4-23). In this last case gapped Hadley grains were observed only in the microstructure of undersulfated systems.
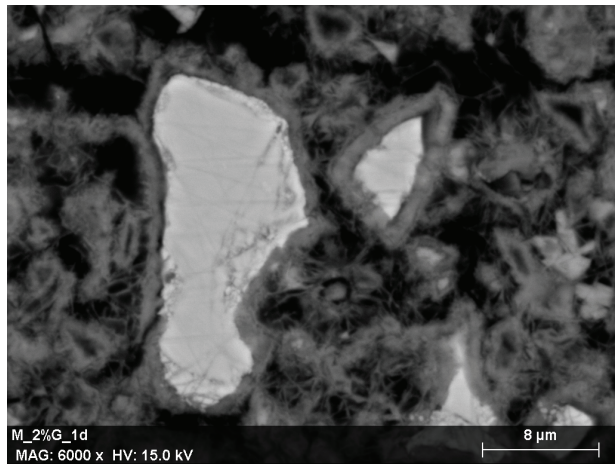
(a) Undersulfated monophase cement 24h
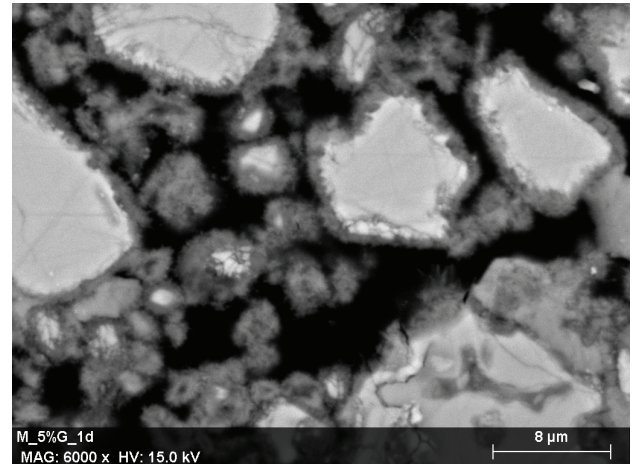
(b) Properly sulfated monophase cement 24h
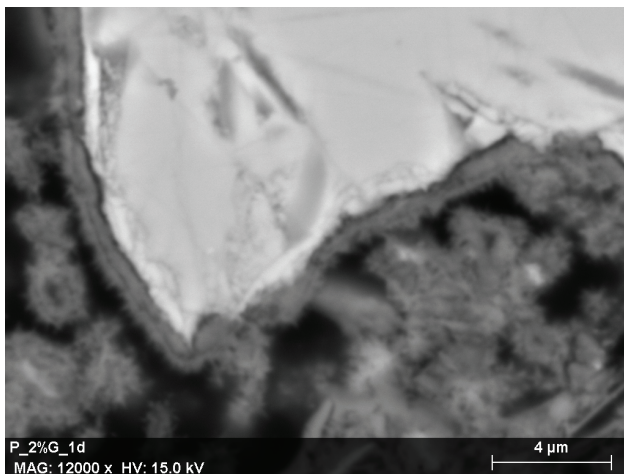
(c) Undersulfated polyphase cement 24h
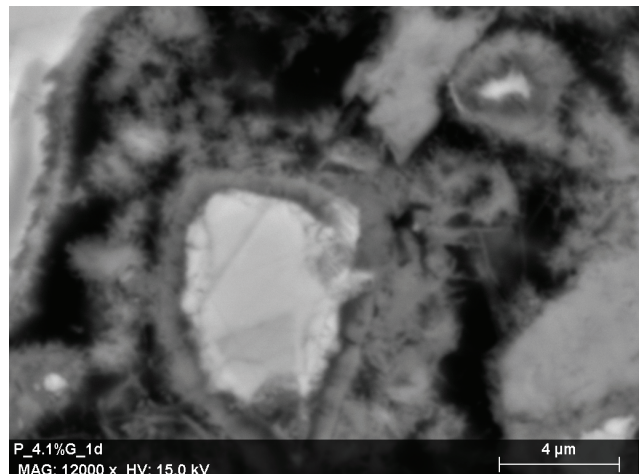
(d) Properly sulfated polyphase cement 24h

Figure 4-23: Comparison of the gapped Hadley grains formed at 24h of hydration for different cement compositions. Gapped Hadley grains were observed also in the microstructure of monophase model cements, but only in the case of undersulfated systems.

No gapped Hadley grains were observed in alite-gypsum microstructures. It can be therefore suggested that the aluminate phases or hydrates (and not only when present as polyphase grains) plays a significant role in the occurrence of such microstructure. It has to be noted however that very small gaps (that are actually not empty but filled with a low density product that can be observed only by TEM [37]) were observed in these model systems compare to OPC pastes. Therefore, it can be suggested that the alkali present in OPC may also play a role in the precipitation of C-S-H.

4.5 Influence of the cement composition on the hydration kinetics

In order to investigate the influence of the cement composition on the overall hydration kinetics, the effect of the interactions between the cement phases needs to be understood. In this section, the difference in reaction kinetics of the individual cement phases when hydration occurs in pure systems and in multiphase systems was studied for several model systems. Their hydration was studied by isothermal calorimetry. The effect of the presence of other phases on alite and C_3A – gypsum reaction were investigated depending on

- the gypsum content (which affect the relative time of occurrence of both reaction)
- the relative amount of both alite and C_3A phases
- the distribution of the anhydrous phases (depending on monophase or polyphase nature of the grains)

4.5.1 Influence of the gypsum content

The heat evolution profiles of model systems with different gypsum additions are presented in Figure 4-24. The gypsum additions of the model cements were chosen to obtain undersulfated cement and properly sulfated cements. Cements M_2%G and M_2.6%G are undersulfated as the characteristic sharp peak of the aluminate reaction after gypsum depletion occurs before the silicate reaction and this later reaction is delayed and its peak lowered compared to properly sulfated systems. The other cements can be called properly sulfated as the aluminate reaction to form monosulfoaluminate occurs after the silicate one. The peak due to aluminate reaction is delayed with increasing gypsum content. This aluminate peak becomes also broader and lower as the gypsum content in the cement increases.
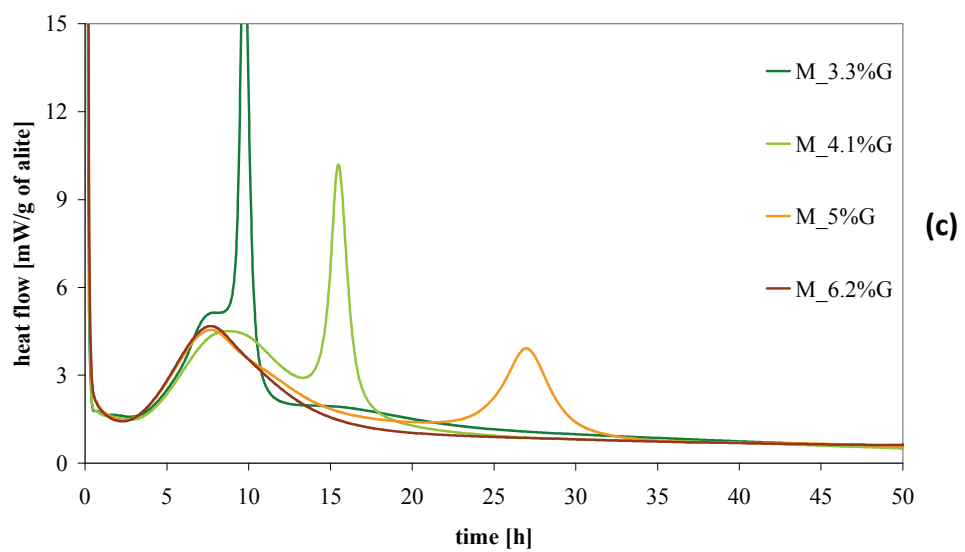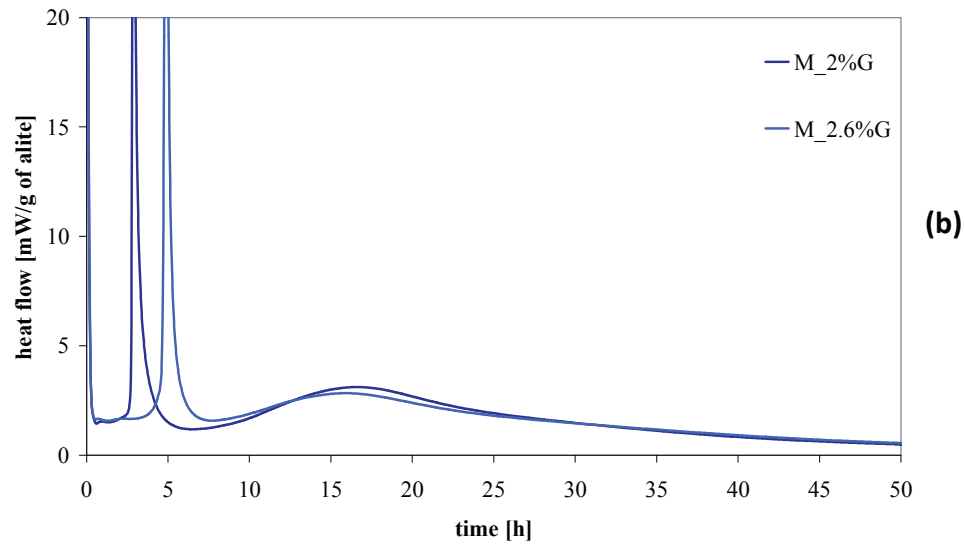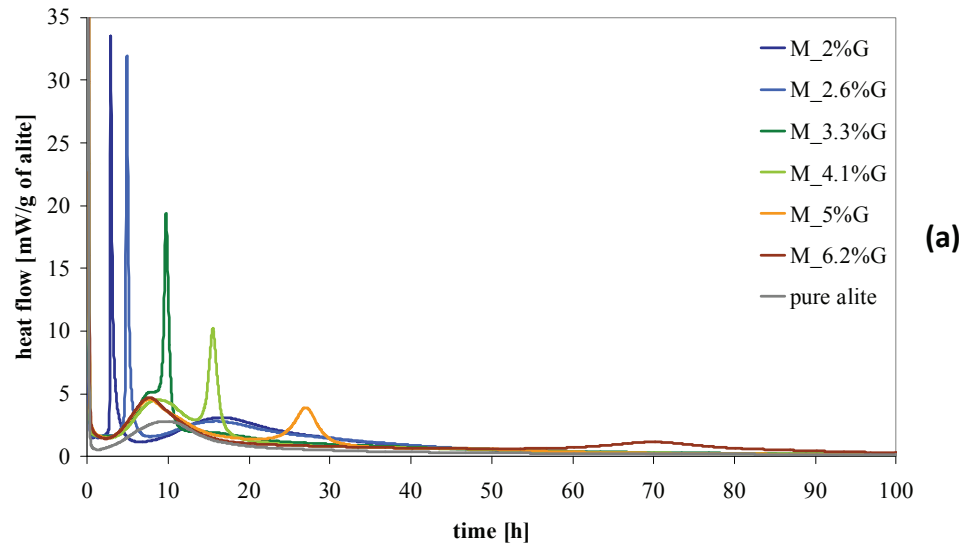
Figure 4-24: (a) Overview of the heat evolution curves for the monophase cements (b) zoom on the undersulfated cements (c) zoom on the properly sulfated cements.

4.5.1.1 Decoupling method for the calorimetric curves of model cements

In order to compare the hydration kinetics of the individual cement phases when hydration occurs in pure or in multi-phase systems, the heat evolution profiles of these model cements were decoupled into alite and C_3A-gypsum contributions. The alite and C_3A-gypsum contributions have been compared to the heat evolution curves of the pure systems to see how the presence of another phase changes the hydration kinetics of the individual cement phases. In the present study we consider the C_3A-gypsum system as a pure system. Previous studies [20, 29] have shown that the effects of C_3A and gypsum on alite reaction are different in 2-phases (alite-C_3A and alite-gypsum) systems than in 3-phases (alite-C_3A-gypsum) systems since C_3A and gypsum react together to form other hydrates. The presence of C_3A and gypsum and their interactions with alite can then not be dissociated in cements.

The method for decoupling the heat evolution curves assumes that the curve of the model cement is equal to the sum of the heat evolution curves for the hydration of the single phases present in the system, adjusted by affine transforms. The heat evolution curves of the pure systems (alite and C_3A-gypsum) were mathematically accelerated (or decelerated) and shifted with an affine transformations in order to obtain, summing them, the best fit with the heat evolution profile of the model cement. This transformation consists of a linear transformation and a translation of the calorimetric curve with the formula:

$$t_i^{'} = \alpha(t_i - \beta)$$

Where: t_i'= transformed time, α = kinetics factor (acceleration), β= shift factor, t_i= original time

With this affine transformation the intrinsic shape of the peak remains unchanged. The area under the curve was also kept constant:

$$Q^{'}_i(t) = \frac{A_o}{A'} Q_i(t)$$

Where: Q_i' = transformed heat released, A_0= area under the original heat evolution curve, A'= area under the transformed heat evolution curve, Q_i' = original heat released

An iterative method developed by Dunant [42] was used to calculate the best fit that could be obtained from a set of given values for the acceleration and the shift of both alite and aluminate reactions. Because the dissolution peak has distinct kinetics and is difficult to measure, it was neglected when carrying out the fits. As this method does not always converge satisfactorily (especially in the case of undersulfated systems) the heat evolution curves of the single phases can be further adjusted using a scaling factor. This second transformation also conserves the shape of the peak, but not the apparent area.
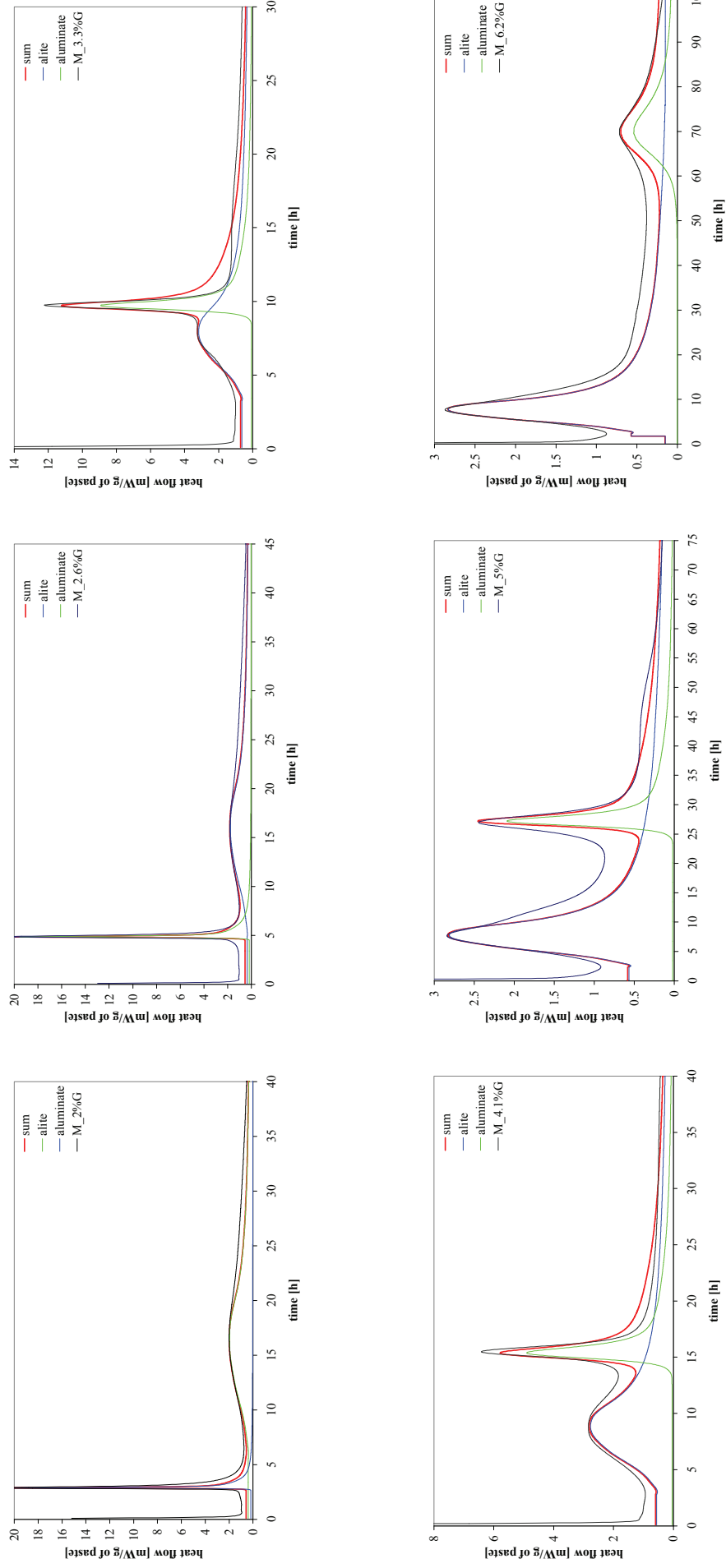
Figure 4-25: Model cements decoupled into alite (blue curves) and aluminate (=C$_3$A-gypsum) (green curves) contributions. The red curves correspond to the sum of the alite and aluminate contributions and the black one is the measured heat evolution profile.

Figure 4-25 shows the six systems with the decoupling into silicate and aluminate contributions to the heat evolution profile. For all the cements studied it was possible to obtain a reasonable fit of the main calorimetric peaks, especially the alite peak, with the sum of the calorimetric curves of the pure systems. This means that the intrinsic shape of the calorimetric peak is the same in model cements and in pure systems and implies that the presence of another phase in the system does not change the fundamental mechanisms of the alite reaction; only the kinetics of the reaction is affected.

4.5.2 Influence of the presence of C_3A-gypsum on the alite hydration

The calorimetric curves in Figure 4-24 show that the alite hydration is modified in different ways depending on the undersulfated or properly sulfated nature of the cement.

The kinetic factor - the acceleration $1/\alpha$ obtained from the decoupling - can be used to quantify the effects of the presence of other phases on the reaction kinetics of the pure systems. The acceleration factors calculated for the alite reaction for the different gypsum additions are reported in Figure 4-26.
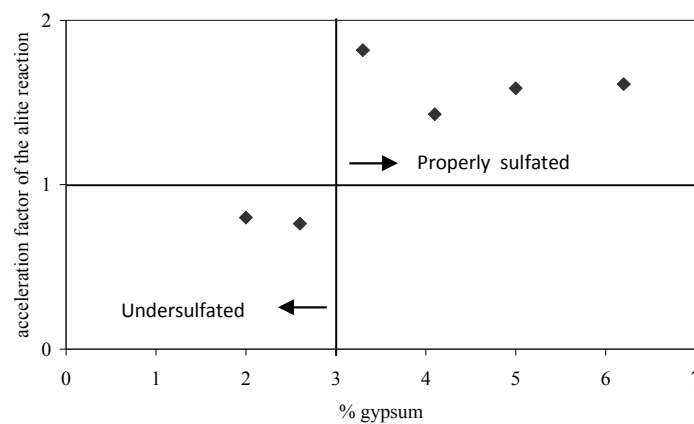
Figure 4-26: Acceleration factors for the alite reaction depending on the gypsum content obtained from the decoupling of the calorimetric curves. Two tendencies depending on the undersulfated or properly sulfated nature of the systems were observed. Alite reaction is accelerated in properly sulfated systems and slightly slowed down in undersulfated systems.

The two different effects of the presence of C_3A and gypsum on the hydration rate of alite depending on the undersulfated or the properly sulfated nature of the cement are clearly highlighted.

In the case of the undersulfated cement, the alite reaction is slowed down slightly during the C-S-H growth period compared to the pure alite system (where the acceleration is equal to 1). The reasons for this are not clear, but two different phenomena can be at the origin of this slow down. There could be an effect on the space for nucleation and growth of hydrates. The reaction of the aluminate phase has already filled the space before the alite reaction and reduces the exposed surface available for nucleation.

Or there could be reaction a "poisoning" of alite by the aluminate ions present in the C-S-H or in solution. Indeed, Minard studied the effect of aluminum ions in solution on the hydration reaction of alite [29]. Her results show that in the presence of aluminum ions the alite reaction is slowed down, probably due to the modification of the C-S-H growth mode when Al ions substitute Si in C-S-H. In the present study, the Al content of the C-S-H of undersulfated systems was measured by EDS analysis at different ages, and compared to the Al content measured in properly sulfated cements. The results are presented in Figure 4-19 to Figure 4-22. These measurements show that the Al content of the C-S-H for undersulfated cement is significantly higher that the content measured in the C-S-H for properly sulfated cements at the time of the main reaction of the silicate phase. This difference in the Al content of the C-S-H may explain the slower reaction observed for undersulfated cements.

It has to be noted that in order to fit the experimental curve of the undersulfated systems, the use of a scaling factor of 1.3 was necessary to obtain a good fit of the alite reaction in the decoupling of the calorimetric curves. This means that the total heat released during alite hydration in undersulfated systems is higher than in pure alite. This phenomenon can be compared to alite-C_3A systems as described by Minard [29] where the alite peak was much more intense in alite-C_3A systems than in plain alite system. Minard suggested that the difference was due to the higher surface available for nucleation and growth of C-S-H due to the affinity of C-S-H with the aluminate hydrates. The same phenomenon, although to a lesser extent, can be evoked in undersulfated alite-C_3A-gypsum systems as similar aluminate hydrates are precipitated. It is however interesting to note in the cumulative heat curves (Figure 4-27), that the overall degree of reaction in all the systems is almost identical from 30 hours of hydration.

Several phenomenon observed in undersulfated systems could be related to what occurs in alite-Al solution and alite-C_3A systems. However, due to the complexity of the interactions in multi-phase systems it was not possible to clearly identify the mechanism that causes the slow down of the reaction.
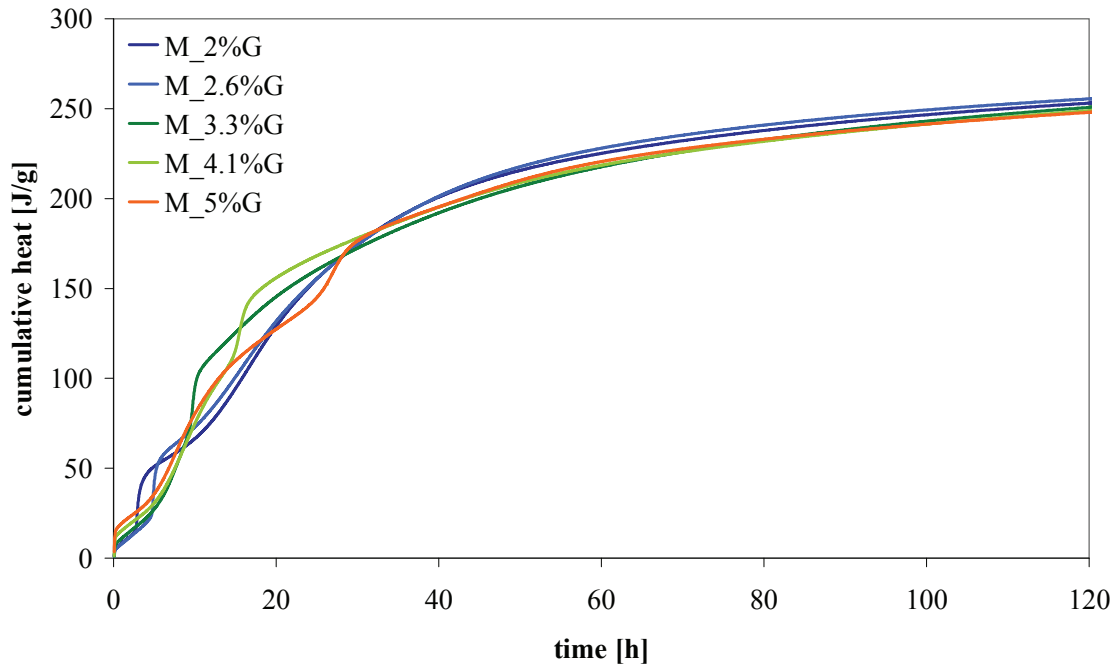
Figure 4-27: Cumulative heat curves of the monophase cements. The overall heat released by the reaction is almost the same for all the systems after 30h of reaction.

In the case of the properly sulfated cements, the alite reaction in model cements is significantly accelerated compared to the pure system. This acceleration may be related to the adsorption of sulfate ions that may modify the growth mode of C-S-H compare to pure alite systems and be at the origin of this acceleration as described by Minard [29].

4.5.2.1 Effect of gypsum alone on alite hydration

Additional experiments were carried out on alite-gypsum systems to investigate the origin of the acceleration of alite hydration in the presence of C_3A and gypsum.

An acceleration of the hydration rate of alite was also observed in systems containing only alite and gypsum (Figure 4-28). The acceleration observed previously in model cements is therefore probably due to the presence of gypsum. This acceleration of the alite reaction in the presence of gypsum was already reported by Minard [29], however she did not report any acceleration in the presence of both C_3A and gypsum as we observed with our samples. On Figure 4-28 it can be observed that the alite peak is significantly accelerated in the presence of only 2% replacement of gypsum. The acceleration is maximal with 5% replacement and slightly decreases for the sample with 10% replacement. This observation agree with the fact that there is probably an optimum of gypsum

content in cement pastes that lead to higher mechanical performances at early ages [2, 28]. The acceleration factors obtained from the decoupling of the calorimetric curves (Figure 4-26) show a maximal acceleration for a gypsum addition of 3.3% of gypsum. This value can therefore be considered as the optimal gypsum addition for these systems.
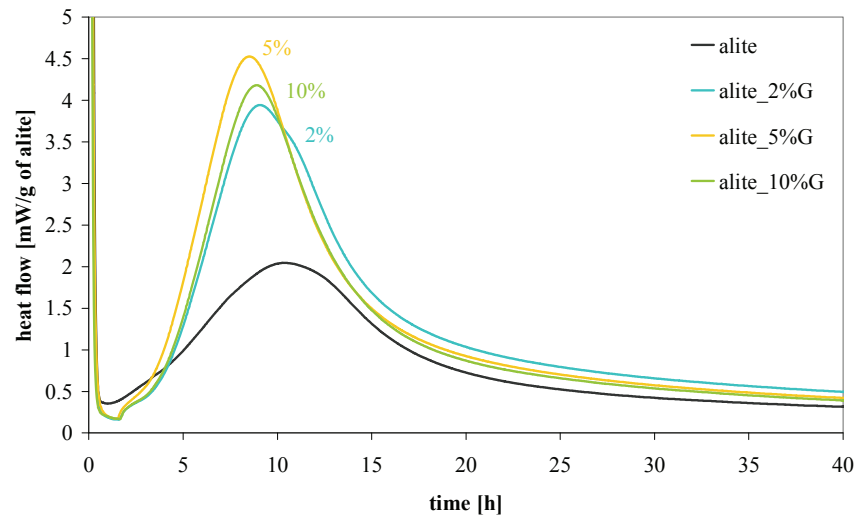
Figure 4-28: Heat evolution curves of alite-gypsum systems. An acceleration of the reaction rate in the presence of gypsum could be observed.

In addition, it can be noted that in Figure 4-28 that whereas the nucleation – growth period of the alite reaction is accelerated in the presence of gypsum, the induction period is longer. The same feature can be observed in the heat evolution curves of the model systems in Figure 4-24.

4.5.3   Influence of the presence of alite on the C_3A-gypsum hydration

Discrepancies were observed between the experimental and calculated curves (Figure 4-25), especially for the properly sulfated model cements. There are more exothermic peaks than the ones obtained summing the contributions of the pure systems. The three peaks that follow the main silicate peak (named S in Figure 4-29) were all attributed to the aluminate reaction since their time of occurrence is influenced by the gypsum content of the cement.

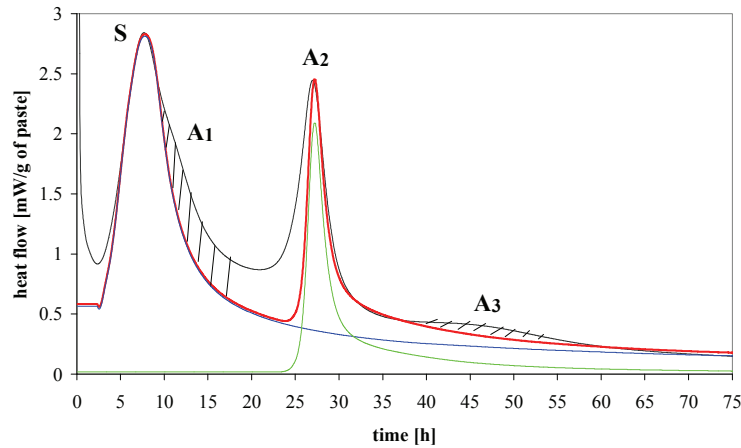**Figure 4-29: Difference between the calorimetric curve of the model cement M_5%G and the sum of the alite and aluminate contributions. Multi aluminate peaks occurs in the presence of alite.**

For pure C_3A – gypsum systems, the heat evolution profile is characterized by only one sharp exothermic peak, while in multi-phases systems three peaks can be attributed to the aluminate reaction. The aluminate reaction is therefore modified in multi-phases systems compare to a pure C_3A-gypsum system, especially in the case of properly sulfated cements.

Aluminate peak 1 (A1 in Figure 4-29) was attributed to the second ettringite formation by Scrivener [19] in 1984. The in-situ XRD measurements on model cements presented in Figure 4-12 show that this peak corresponds to the dissolution of C_3A after gypsum depletion and continuous ettringite formation. While in pure C_3A-gypsum systems ettringite starts to dissolve immediately after gypsum consumption, together with C_3A to form monosulfoaluminate (Figure 3-6), in the presence of alite, continued ettringite formation was observed after gypsum depletion associated with a surge in C_3A dissolution. The chemical analyses of the C-S-H during the first hours of reaction show a decrease of the sulfur content of the C-S-H with time (Figure 4-19). The same feature was also observed in Portland cement by Gallucci *et al*. [37]. Some of the sulfate ions adsorbed on C-S-H can therefore be released to form more ettringite after gypsum depletion. This difference in the evolution of the phase assemblage between the pure C_3A-gypsum systems and the model cements can explain the presence of multiple peaks in the calorimetric curves of model cements.

The peak A2 is the largest aluminate peak that can be compared to the peak observed in pure C_3A-gypsum system. In Figure 4-30 pure C_3A – gypsum systems are compared to the model cements that have the same C_3A/gypsum ratio. Systems where alite was replaced by an inert filler (quartz) are also plotted in these figures.
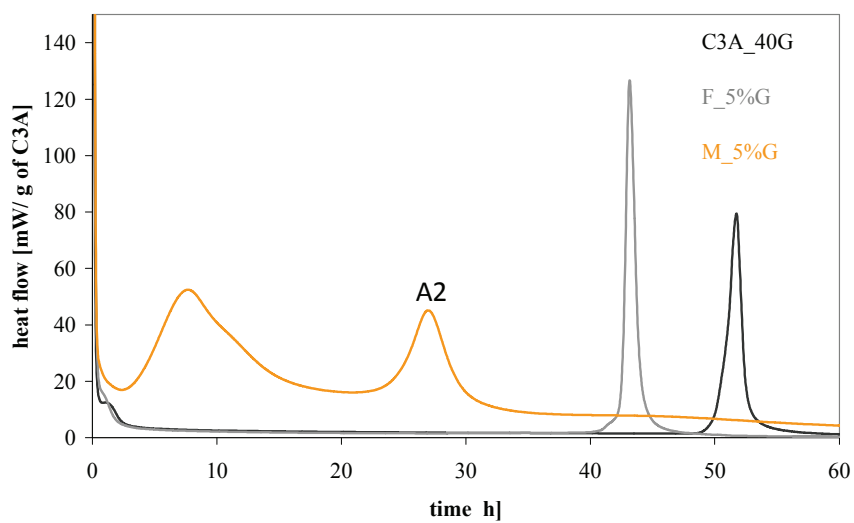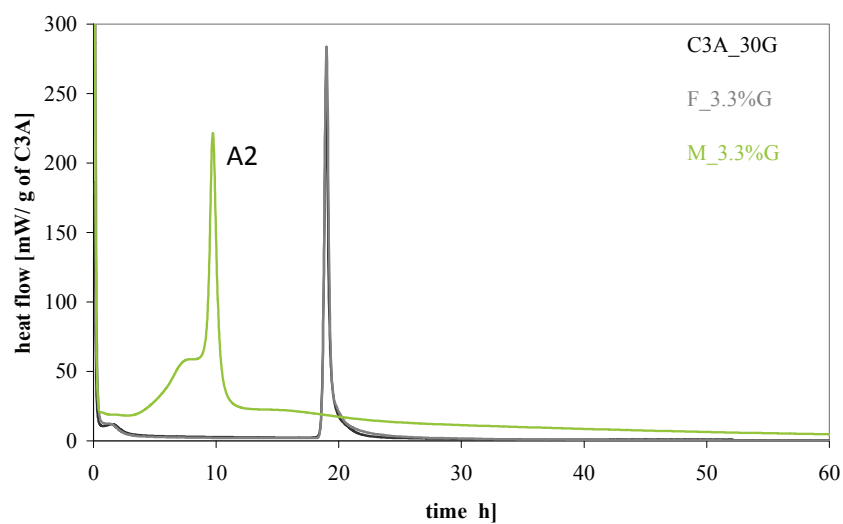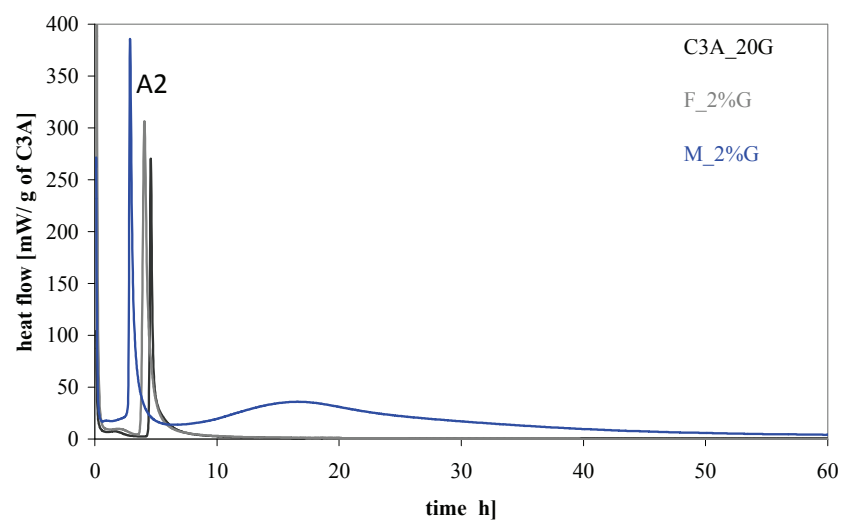
Figure 4-30: Aluminate reaction in pure C₃A-gypsum, Filler- C₃A-gypsum and in alite- C₃A-gypsum systems. The aluminate peak A2 occurs earlier in the presence of alite.

It can be observed that peak A2 appears earlier in model cements than in pure systems for a same C$_3$A/gypsum ratio (Figure 4-31), while the time of occurrence of this peak seems not much influenced by the dilution of the species as it appear almost at the same time in C$_3$A-gypsum systems and in the presence of filler.
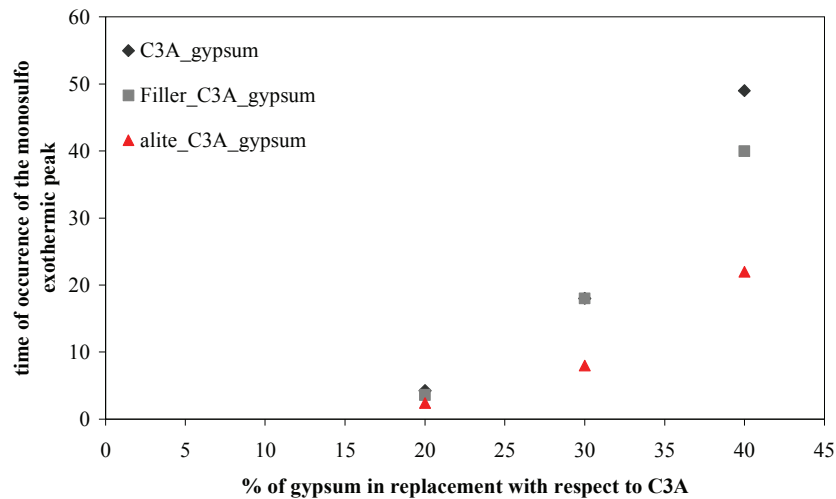
Figure 4-31: Time of occurrence of the A2 peak in model cements and in C$_3$A-gypsum systems. The aluminate peak A2 occurs earlier in the presence of alite.

The difference observed in the presence of alite is probably due to the fact that sulfate ions can be adsorbed on the silicate phases and even though some can be released to form ettringite after gypsum consumption, a significant amount of sulfate remains adsorbed, on C-S-H. Moreover, this peak, which is usually very sharp in pure C$_3$A-gypsum systems, becomes lower and broader with increasing gypsum. The same feature was observed in C$_3$A-gypsum systems but seems to be intensified in the presence of alite. This peak broadening can be attributed to the fact that for properly sulfated systems, the matrix is already filled by silicate hydrates at the time corresponding to this reaction. Plotting the height of the peak vs. volume available in the paste (output of the model μic, (A.Kumar, work in progress LMC)) a linear trend can be observed (Figure 4-32). The space available for the reaction seems therefore to have a significant influence on peak A2.
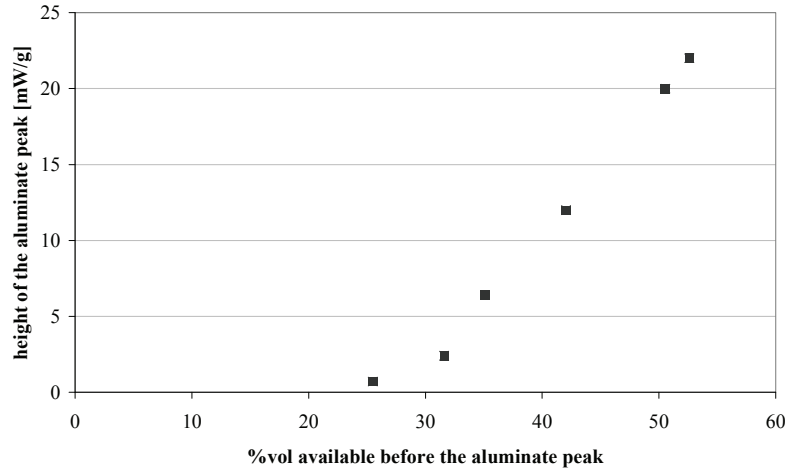
Figure 4-32: A linear trend between the height of the aluminate peak and the volume available for the reaction was observed.

The third peak (A3) is still not clearly explained but it is probably related to the formation of monosulfoaluminate. It is interesting to note that the time of occurrence as well as the intensity of this peak in influenced by the w/c ratio. With increasing w/c ratio (and therefore with increasing space available) this peak tend to occur later and to be lower while the other aluminate peaks occur earlier and are more intense (Figure 4-33).
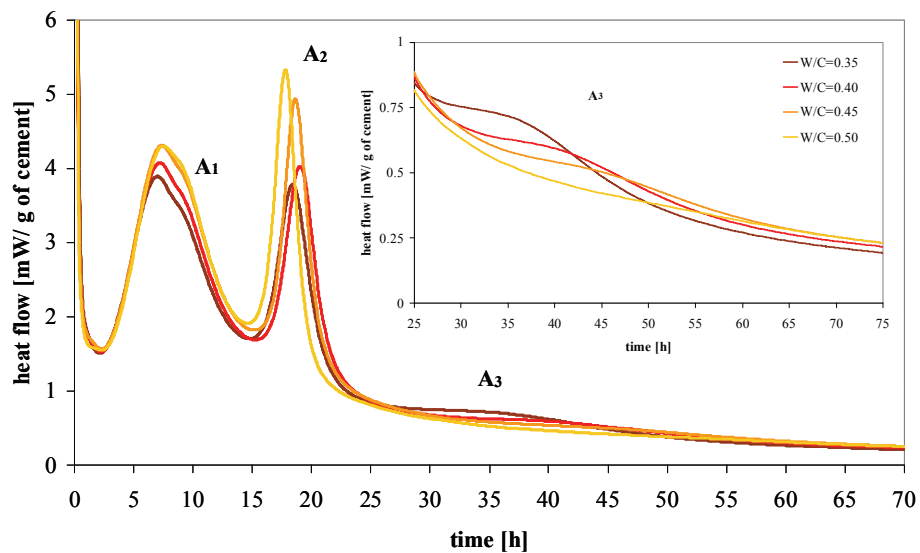
Figure 4-33: Influence of the w/c ratio on the aluminate peaks. Peak A3 is suppressed at higher w/c while the other aluminate peaks are more intense. (Model cement M_5%G)

An aluminate peak with the same behavior was also observed in other systems (CAC [43] and OPC [44]). It is hypothesized that this peak is related to a second formation of monosulfoaluminate. When the w/c ratio is low, not all the monosulfoaluminate can be formed at once due to space constrain. A

113

second formation can occurs later and cause a small exothermic peak. On the contrary when enough space is available for the reaction (higher w/c ratio) the reaction that causes peak A2 is more intense and there is no second reaction that causes peak A3. It is interesting to note that with increasing space available the peak A2 is more intense and sharper. The possible influence of the space constrain on the aluminate reaction seems to be confirmed here.

4.5.4   Influence of the C_3A content

The influence of the alite/C_3A ratio was investigated using model cements with three alite/C_3A ratios but with constant C_3A/gypsum ratio. The heat evolution curves of these monophase model systems are presented in Figure 4-34.
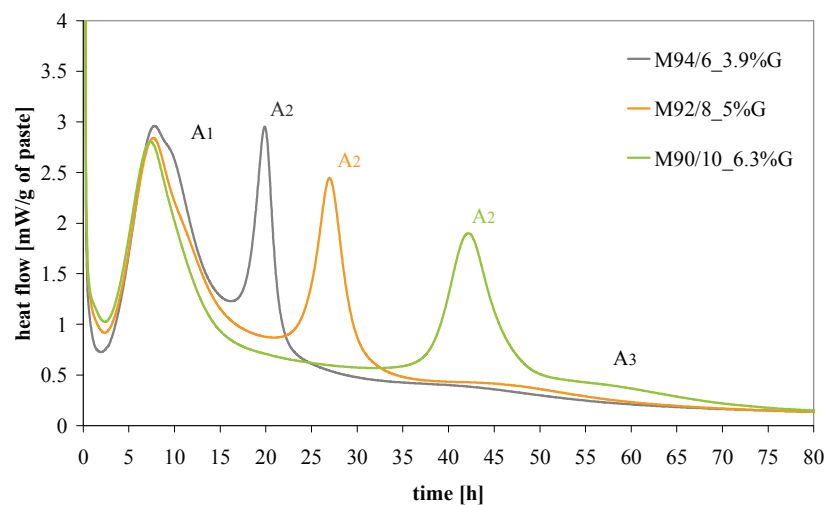
Figure 4-34: Heat evolution curves of model cements with different alite/C_3A ratios. The alite peak is unchanged. The aluminate peak A2 occurs later for higher aluminate and gypsum contents.

These results show first of all that the alite reaction is not influenced by small variations in the C_3A-gypsum content. The aluminate reaction is much more influenced. It can be observed that the time of occurrence of the aluminate peak A_2 does not directly depend on the C_3A/gypsum ratio of the anhydrous mix (that is equal to 60/40 in weight for all the studied systems) but on the total amount of gypsum available for the reaction. It was previously shown that some of the sulfate ions are adsorbed on C-S-H. Therefore, assuming that the same amount of sulfate ion are adsorbed on C-S-H for all the systems, the gypsum available for the reaction directly depends on the total amount present in the anhydrous mix. As observed previously, the aluminate peak becomes lower and broader when the aluminate reaction occurs at later ages. This probably because the space is more and more filled by the calcium-silicate hydrates. It can also be observed that the shoulder on the silicate peak (A_1) is more pronounced for the systems with lower C_3A-gypsum content, but the reasons for this could not be explained.

114

4.5.5 Influence of the dispersion of the phases

The influence of the dispersion of the phases depending on the monophase or polyphase nature of the model cements was investigated by studying the kinetics of hydration of polyphase cements that have the same composition as the monophase cement previously presented. Different alite/C_3A ratios and different gypsum contents were investigated. The heat evolution curves of the polyphase cements are presented in Figure 4-35 for the clinker composition 90%alite/10% C_3A, in Figure 4-36 for the clinker 92/8 and in Figure 4-37 for the clinker 94/6.

The same behavior as for the monophase cements can be observed. With low gypsum content the cements behave like undersulfated cements, with the silicate reaction that occurs after the aluminate one. In the case of properly sulfated cements, the changes in gypsum or C_3A amount influence mainly the aluminate reaction. It is especially interesting to note that the presence of multi exothermic peak for the aluminate reaction is more pronounced in the case of systems with low C_3A content (Figure 4-37).

Comparing the heat evolution curves of monophase and polyphase cements with the same composition in terms of alite, C_3A and gypsum content (Figure 4-38) it can be observed that the monophase or polyphase nature of the cement grains influences mainly the aluminate reaction. The alite reaction is almost unchanged between systems. In the case of properly sulfated cements the same acceleration of the alite is observed in monophase and polyphase cements. The small differences in alite kinetics can be attributed to the difference in the particle size distribution between alite and clinker grains. As the C_3A is the minor phase its hydration kinetics is largely influenced by the availability of the phases. In the majority of the examples presented in Figure 4-38, the aluminate reaction occurs earlier in the case of monophase cements and the exothermic peak is higher and narrower. Di Murro has also observed a difference in the kinetics of reaction of the aluminate phases depending on the monophase or polyphase nature of the model cements [30]. However, her results show a slower reaction in the case of monophase cements, the opposite of what is seen in this study. She explain the faster reaction of the aluminate phases in polyphase cements by the fact that the C_3A is finer and better dispersed when present in all the clinker grains instead of few monophase grains. In the present work the aluminate phases reacts faster in monophase cements. This can be probably attributed to the fact that the synthesized C_3A is especially fine, and finer than the C_3A used in the study of Di Murro and to the coarse gypsum used by Di Murro in her study. The intensity of the aluminate peaks is also modified. Higher peaks are observed in the case of monophase cements.
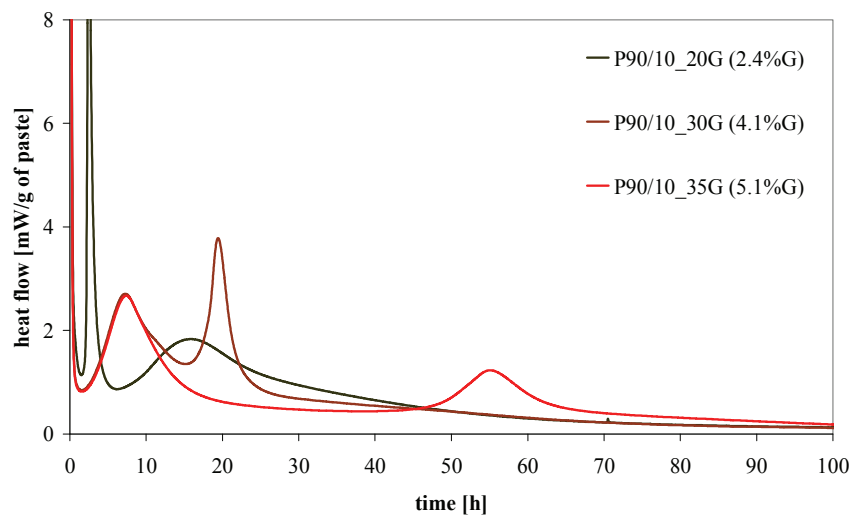
Figure 4-35: Heat evolution curves for the polyphase cements 90/10

Figure 4-36: Heat evolution curves for the polyphase cements 92/8
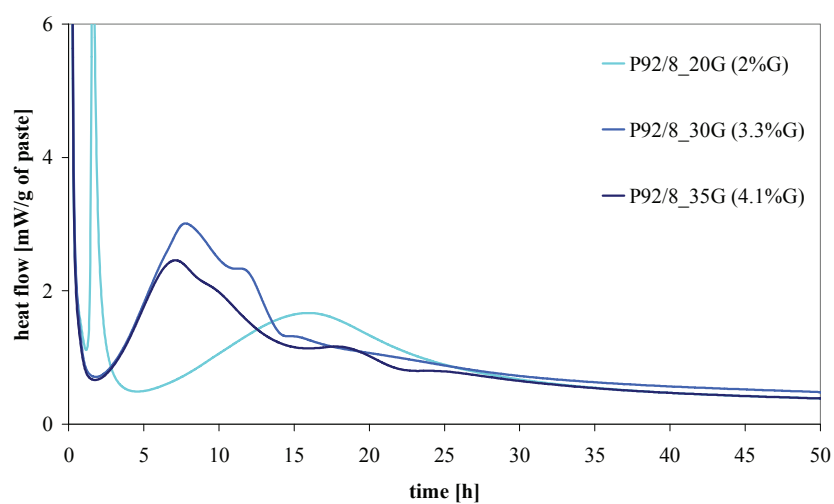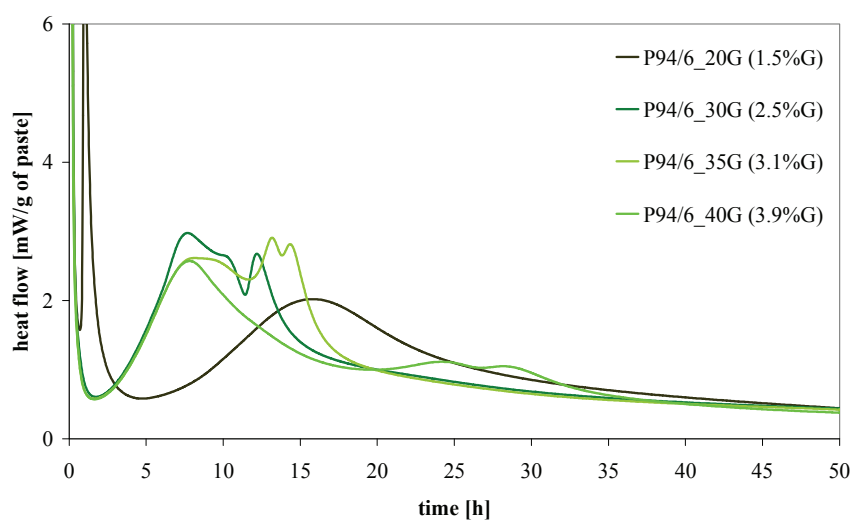

Figure 4-37: Heat evolution curves for the polyphase cements 94/6. The phenomenon of multi-aluminate peak is more pronounced for the clickers with lower C$_3$A content.
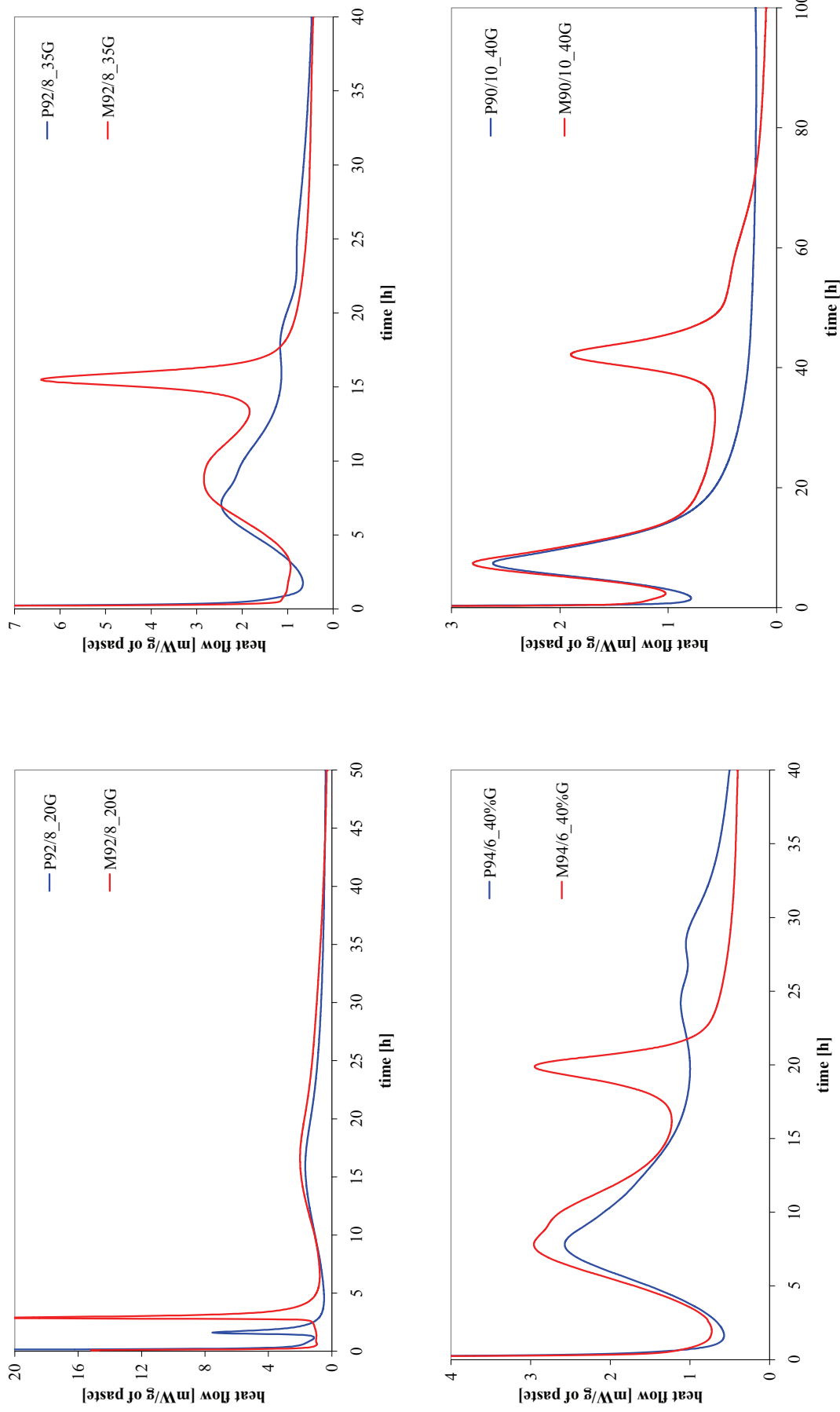
Figure 4-38: Comparison of heat evolution curves of monophase and polyphase cements. The aluminate reaction is strongly influenced by the monophase / polyphase nature of the grains.

4.6   Influence of the temperature on the hydration kinetics

The influence of the temperature on the hydration kinetics of the alite and C_3A-gypsum in multi-phase systems has been investigated on several monophase and polyphase model cements. The scope of this study on temperature effect was to investigate if the alite and aluminate reactions are affected by the temperature in the same way when hydration occurs in pure and in multi-phase systems.

The hydration kinetics of the model cements was monitored by isothermal calorimetry at 4 different temperatures: 15, 20, 26, and 30°C. The calorimetric results obtained for theses model cements are reported in Figure 4-39, Figure 4-40 and Figure 4-41. For all the systems studied, the reactions occur faster with increasing temperature and the peak intensities are higher.

The case of the cement P92/8_2.6%G (Figure 4-41) is particularly interesting. At the reference temperature of 20°C this sample is undersulfated but with an unusual broad aluminate peak and a delayed silicate peak. At high temperature, the heat evolution profile of this sample looks like usual undersulfated cement while at 15°C the aluminate and silicate peaks seems to be overlapped. It can then be thought that at lower temperature this cement may behave in a properly sulfated way. Therefore cements that have a sulfate content just enough to make them reacting like properly sulfated cements at room temperature may behave like undersulfated cement in the field at higher temperature. The cement composition is then not the only parameter that can influence the interaction between the silicate and aluminate phases. The sensitivity of the different clinker phases to the temperature may not be the same, leading to different interactions depending on the temperature.
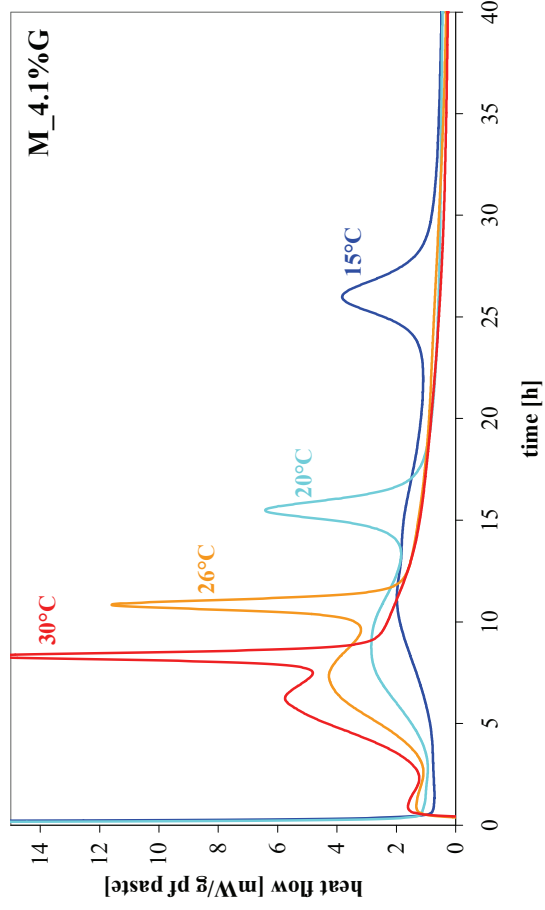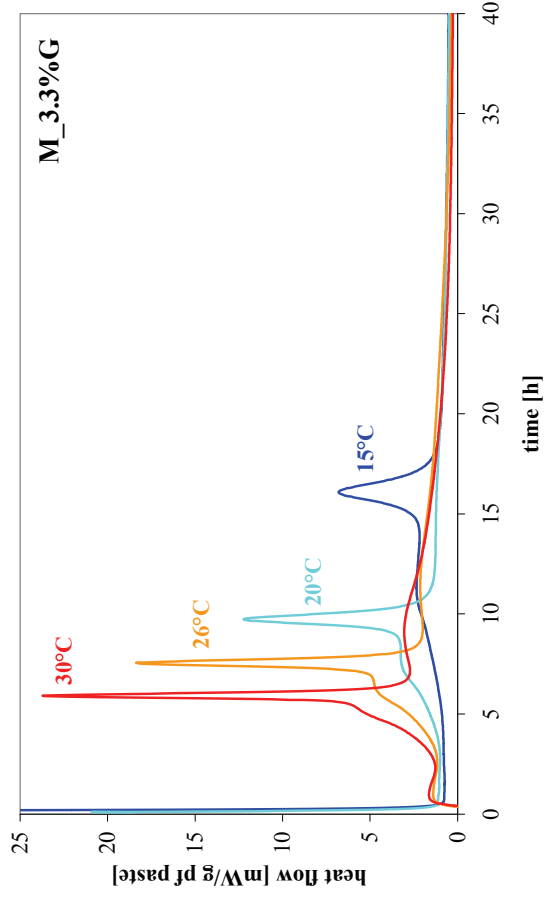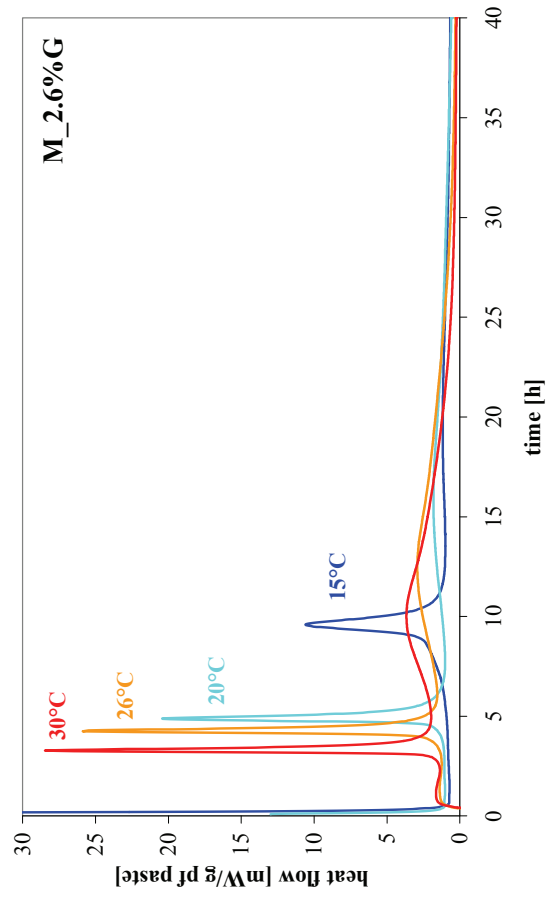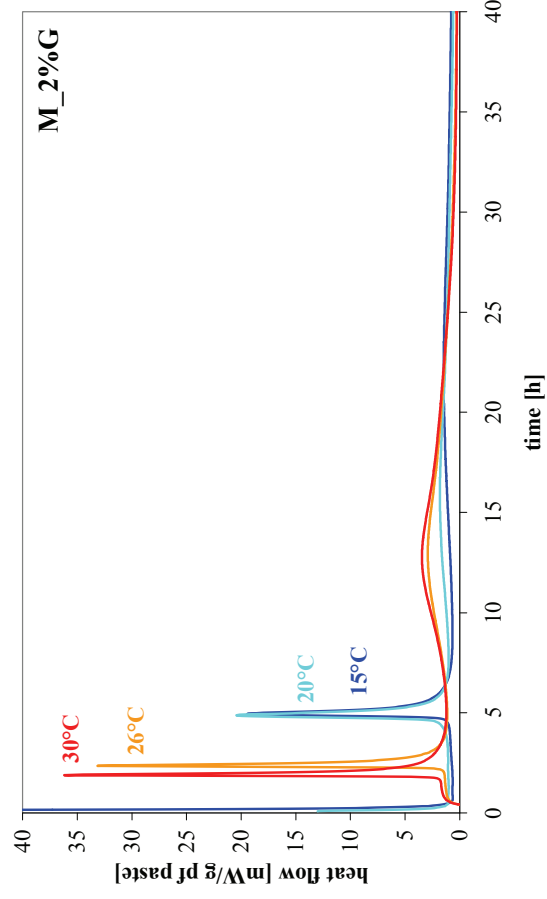
Figure 4-39: Heat evolution curves of monophase cements at different temperatures. The reaction is accelerated with increasing temperature.
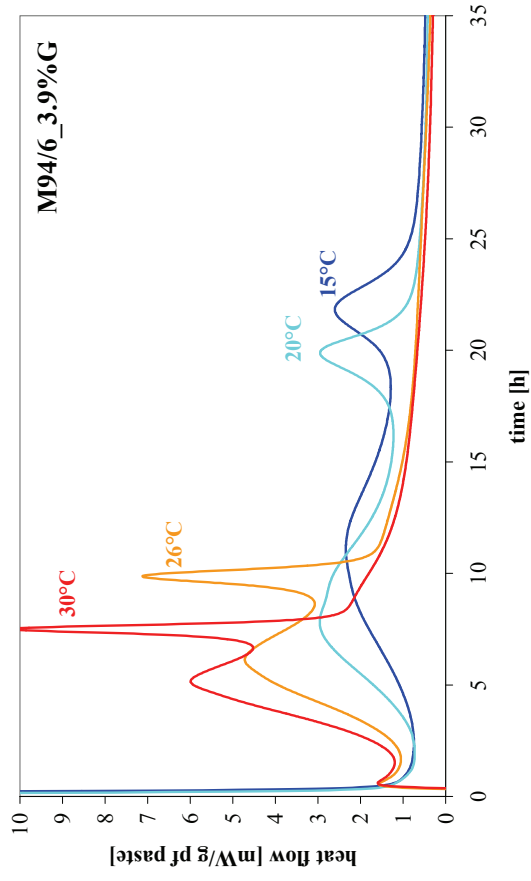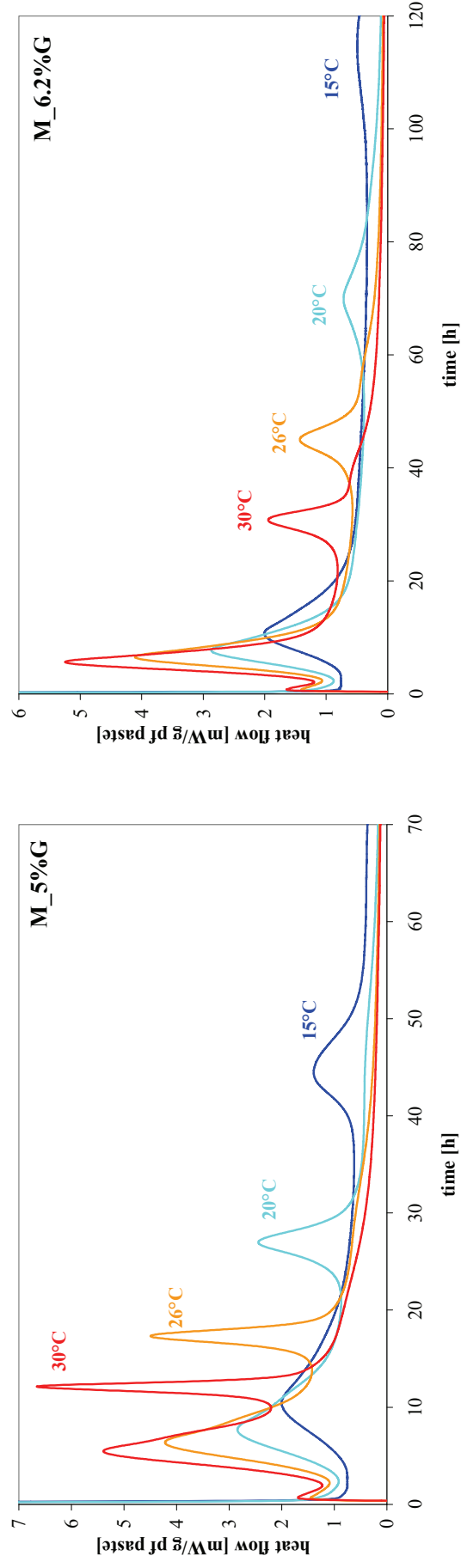
Figure 4-40: Heat evolution curves of monophase cements at different temperatures. The reaction is accelerated with increasing temperature.
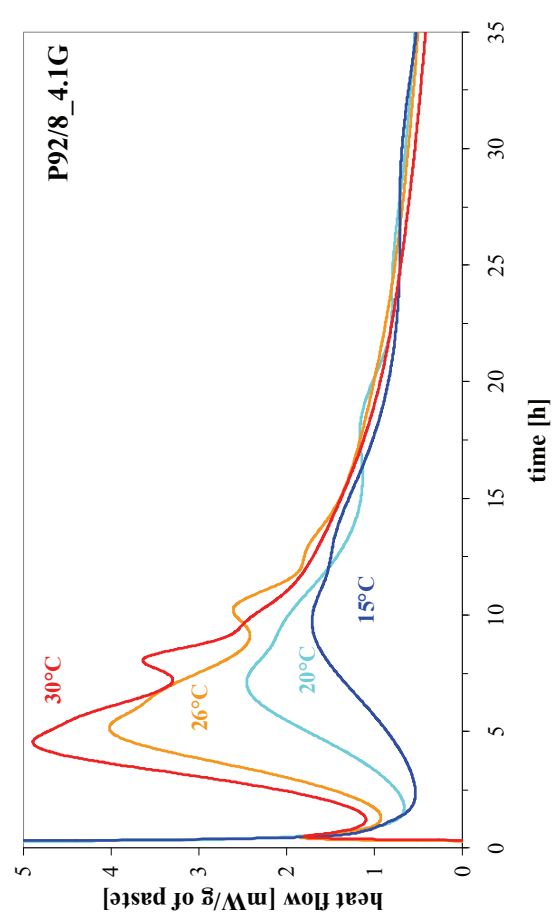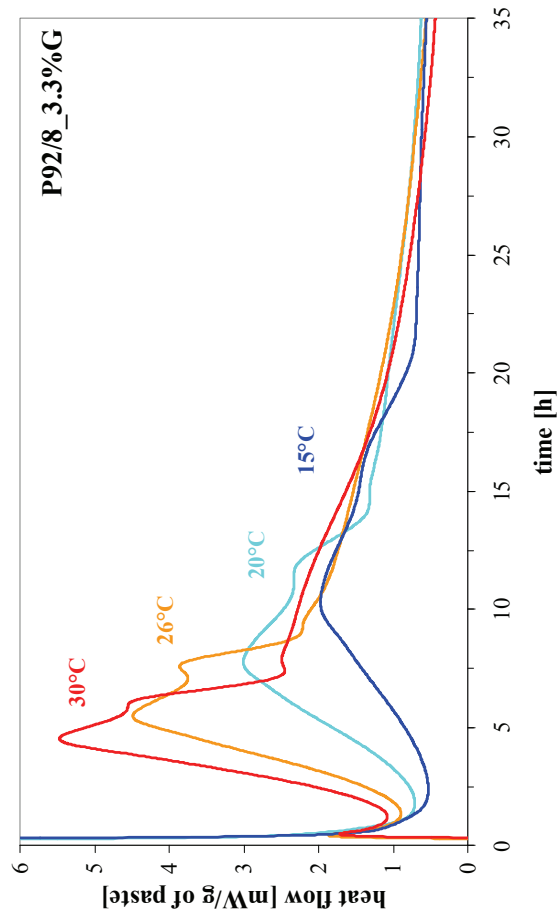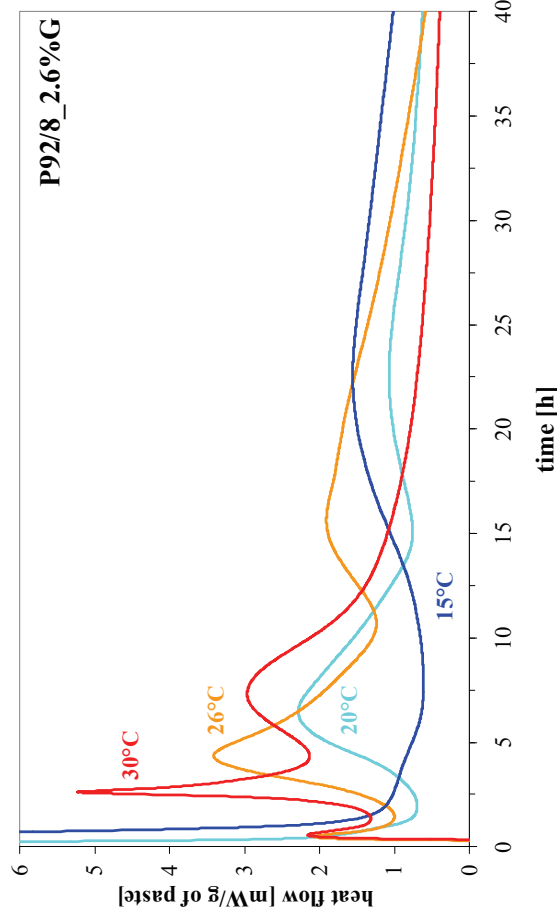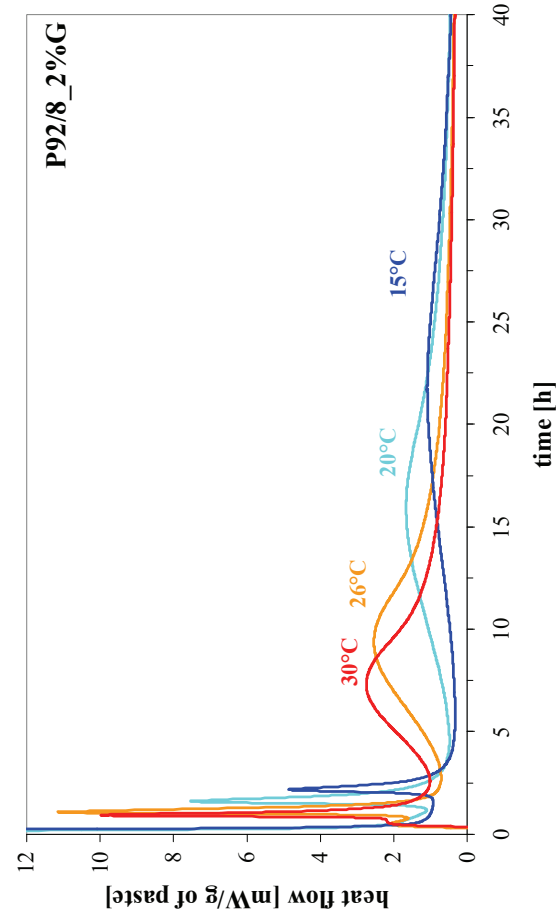
Figure 4-41: Heat evolution curves of polyphase cements at different temperatures. The reaction is accelerated with increasing temperature.

The apparent activation energies (Ea) for the alite and aluminate reactions of all these model cements was calculated with the equivalent time method as described in Chapter 3. The age equivalent factor was obtained by the superposition of the time corresponding to the maximum of the exothermic peak for all the temperature. The calculated activations energies are presented in Figure 4-42 and in Figure 4-43. Ea is the mean value calculated between the three temperatures and the reference temperature of 20°C. The error bar corresponds to the standard deviation.
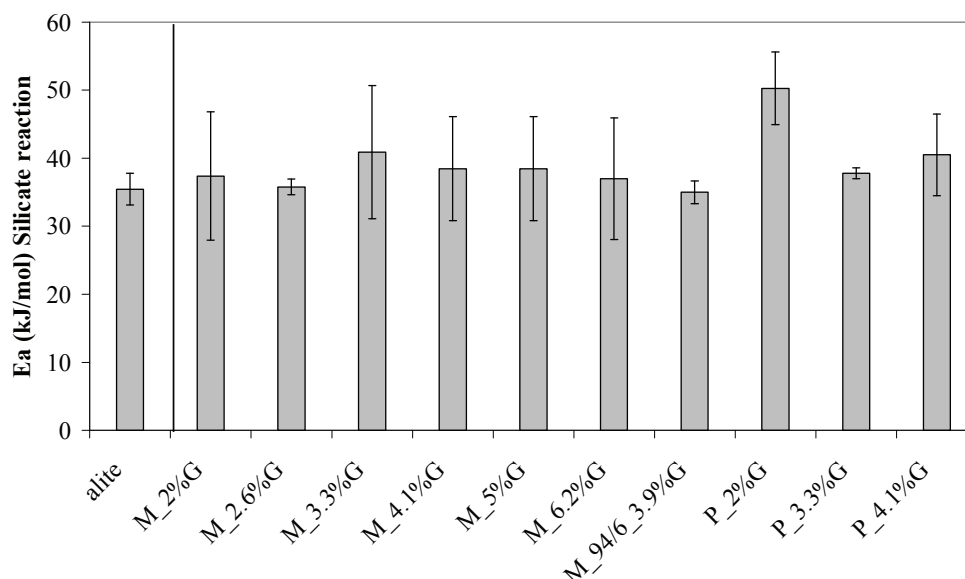
Figure 4-42: Activation energies for the silicate reaction in model cements and in pure alite
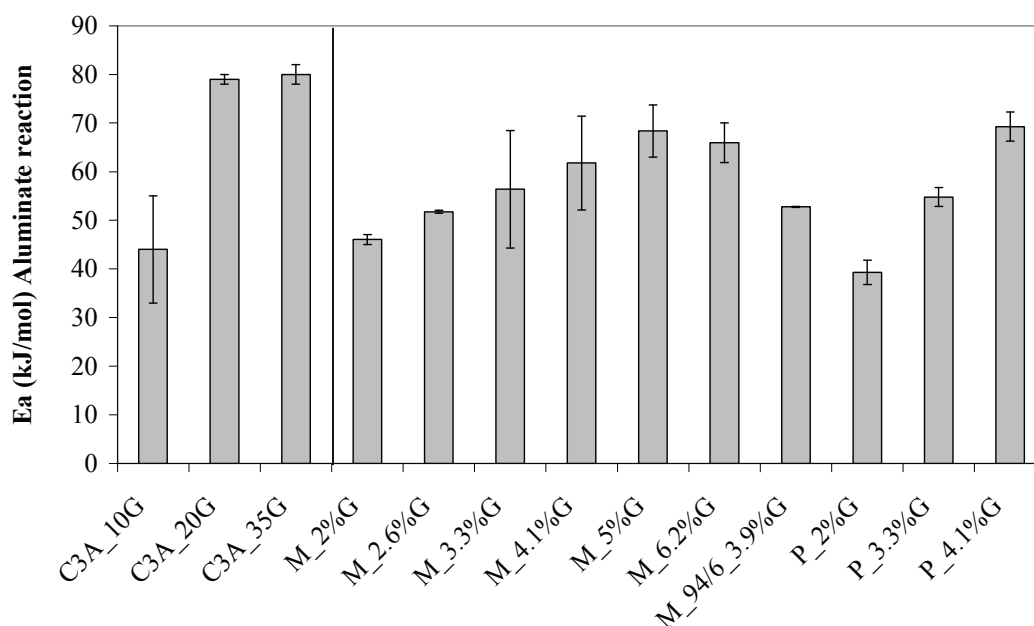
Figure 4-43: Activation energies for the aluminate reaction in model cements and in C$_3$A-gypsum systems. Only the activation energy corresponding to the first stage of C$_3$A-gypsum reaction (ettringite formation) was calculated here.

The alite reaction has a similar Ea in pure and in multi-phase systems. In contrary, the Ea of the aluminate reaction is slightly lower when hydration occurs in multi-phase systems, even though the Ea is still higher than 20 kJ/mol. This means that the fundamental mechanisms of hydration are unchanged in pure C_3A-gypsum and multiphase systems the reaction: in any case the reaction is surface controlled. Moreover, the same trends of increasing Ea with increasing gypsum content are observed in pure C_3A-gypsum and multi-phase systems (except for sample M_2.6%G). The slightly lower Ea obtained from the calorimetric curves for C_3A-gypsum reaction in the presence of alite may be attributed to the space filling effect due to the presence of alite and its hydrates as it has been shown in this work that the reduction of the space available for the reaction seems to strongly influence the aluminate reaction in multiphase systems.

4.7   Conclusions on $C_3S - C_3A -$ gypsum systems

Several changes in the hydration rate of the alite and C_3A-gypsum systems where observed when hydration occurs in multi-phase systems. However this study showed that the fundamental mechanisms of the reactions are unchanged. The same phases are formed and similar activation energies were calculated for the reactions in pure and in multiphase systems. Moreover it was possible to fit the heat evolution profile of the main peaks of the calorimetric curves of model cements summing the alite and C_3A-gypsum contributions modulo affine transforms.

A strong influence of the gypsum content on the overall hydration kinetics of model cement was observed. As calcium-sulfate controls the hydration of C_3A, the time of occurrence of the formation of AFm phases depends on the total gypsum amount of the systems. For the systems that contain low amounts of gypsum, the sulfate ions are consumed before the end of the induction period of alite and the aluminate reaction occurs first. These so called undersulfated systems are not suitable in the field since they lead to flash set and slow strength development. For these systems, the reaction rate of alite was shown to be slowed down during the growth period compare to hydration in plain alite system. The reason for this could not be clearly explained but a poisoning of the alite by Al ions or the effect of the presence of aluminate hydrates on the space available for nucleation and growth of C-S-H can be suggested. When sulfate content is high enough to delay the formation of AFm after the main alite reaction, the system is called properly sulfated. In this case, an acceleration of the rate of alite reaction was observed. This acceleration was attributed to the presence of sulfate ions that modified the kinetics of the reaction.

The C_3A-gypsum reaction was also observed to be subject to change in the presence of alite. Due to the adsorption of sulfates on C-S-H, a second formation of ettringite after the depletion of gypsum occurs. With the correlation of in-situ XRD and EDS analysis, it was shown that most of the sulfates adsorbed on C-S-H can be released after the depletion of gypsum to react with C_3A to form more ettringite. In C_3S-C_3A-gypsum systems ettringite therefore remains stable for several hours after the gypsum consumption and does not dissolve immediately, as in C_3A-gypsum systems.

The microstructural development of the calcium (sulfo) aluminate hydrates is also influenced by the presence of alite. In pure C_3A-gypsum systems AFm phases precipitate in the space between the grains as platelets but also as a denser hydrate that grow inward from the surface. In addition, hydrogarnet was observed to form at the surface of the original C_3A grains. In the presence of alite, the dense "inner" hydrate was less obvious and hydrogarnet shells where not observed.

The microstructural development of the aluminate hydrates is also influenced by the monophase or polyphase nature of the model systems. In polyphase systems the aluminate hydrates were observed to precipitate throughout the matrix, whereas, they were observed mainly around the C_3A grains in monophase systems. This result shows the importance of studying and modeling polyphase systems in order to investigate the microstructural development of cementitious materials.

The heat evolution profile of the C_3A-gypsum reaction is significantly modified in the presence of alite. Three exothermic peaks could be attributed to the aluminate reaction while only one was observed in C_3A-gypsum systems:

- One of these peaks occurs at the time of C_3A dissolution and second ettringite formation after the depletion of gypsum.
- The second one is the main aluminate peak that can be compared to the peak observed in C_3A-gypsum systems. This peak was observed to be broader than the one in C_3A-gypsum systems, probably due to a significant reduction of the space available for the reaction due to the formation of C-S-H and CH.
- The occurrence of the third exothermic peak was attributed to space constrain as it is sensitive to changes in w/c ratio.

Systems with different C_3A contents were also investigated. This work shows that small changes in the C_3A content do not influence the alite hydration. This result is particularly important for the development of new blended cements as two of the main routes for the development of new materials are increasing the mineral additions and the aluminate content in the clinker. However, great care has to be taken to conserve a sulfate amount high enough to avoid the problem of undersulfation. Moreover the influence of the temperature has to be taken into account since this work showed that when systems are sulfated just enough to behave as properly sulfated systems, they may behave in an undersulfated manner in the field, depending on the temperature. This because the C_3A-gypsum reaction is more sensitive to the temperature that the alite one.

References

1.   Juilland, P., et al., *Dissolution theory applied to the induction period in alite hydration.* Cement and Concrete Research, 2010. 40(6): p. 831-844.

2.   Gartner, E.M., et al., eds. *Structure and Performance of cements, 2nd edition, Chapter 3*. Spon Press ed. 2002.

3.   Kantro, D.L., S. Brunauer, and C.H. Weise, *Development of surface in the hydration of calcium silicates. II. Extention of investigations to earlier and later stages of hydration.* The Journal of Physical Chemistry, 1962. 66(10): p. 1804-1809.

4.   Stein, H.N. and J.M. Stevels, *Influence of silica on the hydration of 3 CaO,SiO2* 1964. p. 338-346.

5.   Birchall, J.D., A.J. Howard, and J.E. Bailey, *On the Hydration of Portland Cement.* Proceedings of the Royal Society of London. Series A, Mathematical and Physical Sciences, 1978. 360(1702): p. 445-453.

6.   Double, D.D., A. Hellawell, and S.J. Perry, *The Hydration of Portland Cement.* Proceedings of the Royal Society of London. Series A, Mathematical and Physical Sciences, 1978. 359(1699): p. 435-451.

7.   Gartner, E.M. and H.M. Jennings, *Thermodynamics of Calcium Silicate Hydrates and Their Solutions.* Journal of the American Ceramic Society, 1987. 70(10): p. 743-749.

8.   Skalny, J.P. and J.F. Young, *Mechanisms of Portland cement hydration.* 7th ISCC, 1:II-1/3-II/45, 1980.

9.   Odler, I., *Lea's Chemistry of Cement and Concrete 4th Edition, Chapter 6* ed. Arnold. 1998, London.

10.   Odler, I. and H. Dörr, *Early hydration of tricalcium silicate II. The induction period.* Cement and Concrete Research, 1979. 9(3): p. 277-284.

11.   Tardos, M.E., J. Skalny, and R.S. Kalyoncu, *Early Hydration of Tricalcium Silicate.* Journal of the American Ceramic Society, 1976.

12.   Young, J.F., H.S. Tong, and R.L. Berger, *Compositions of Solutions in Contact with Hydrating Tricalcium Silicate Pastes.* Journal of the American Ceramic Society, 1977. 60(5-6): p. 193-198.

13.   Garrault-Gauffinet, S. and A. Nonat, *Experimental investigation of calcium silicate hydrate (C-S-H) nucleation.* Journal of Crystal Growth, 1999. 200(3-4): p. 565-574.

14.   Garrault, S. and A. Nonat, *Hydrated Layer Formation on Tricalcium and Dicalcium Silicate Surfaces: Experimental Study and Numerical Simulations.* Langmuir, 2001. 17(26): p. 8131-8138.

15. Thomas, J.J., H.M. Jennings, and J.M. Chen, *Influence of nucleation seeding on the hydration mechanisms of tricalcium silicate and cement.* J. Phys. Chem 2009. 113: p. 4327-4334.

16. Juilland, P., *Early Hydration of Cementitious Systems.* Thèse de Doctorat, Ecole Polytechnique Fédérale de Lausanne, 2009.

17. Cabrera, N. and M.M. Levine, *On the dislocation theory of evaporation of crystals.* Philosophical Magazine, 1956. 1((5)): p. 450-458.

18. Bishnoi, S. and K.L. Scrivener, *Studying nucleation and growth kinetics of alite hydration using µic.* Cement and Concrete Research, 2009. 39(10): p. 849-860.

19. Scrivener, K.L., *Development of the microstructure during the hydration of Portland cement* Ph.D. Dissertation ,University of London, 1984.

20. Tenoutasse, N. *The hydration mechanism of C3A and C3S in the presence of calcium chloride and calcium sulfate* in *The 5th International Symposium on the Chemistry of Cement* 1968. Tokyo.

21. Corstanje, W.A. and H.N. Stein, *L'influence du CaSO4.2H2O sur l'hydratation simultanée de C3A et C3S.* Industrie Chimique Belge, 1974. 39(1-6): p. 598-603.

22. Corstanje, W.A., H.N. Stein, and J.M. Stevels, *Hydration reactions in pastes C3S+C3A+CaSO4.2aq+H2O at 25°]C.I.* Cement and Concrete Research, 1973. 3(6): p. 791-806.

23. Corstanje, W.A., H.N. Stein, and J.M. Stevels, *Hydration reactions in pastes C3S+C3A+CaSO4.2aq+water at 25°C. II.* Cement and Concrete Research, 1974. 4(2): p. 193-202.

24. Corstanje, W.A., W.N. Stein, and J.M. Stevels, *Hydration reactions in pastes C3S + C3A + CaSO4 .2aq. + water at 25°C.III.* Cement and Concrete Research, 1974. 4(3): p. 417-431.

25. Regourd, M., H. Hornain, and B. Mortureux, *Evidence of calcium silicoaluminates in hydrated mixtures of tricalcium silicate and tricalcium aluminate.* Cement and Concrete Research, 1976. 6(6): p. 733-740.

26. Hannawayya, F., *X-ray diffraction studies of hydration reaction of cement components and sulfoaluminate (C4A3S) Part IA. Silicates mixed with different components.* Materials Science and Engineering, 1975. 17(1): p. 81-115.

27. Hannawayya, F., *X-ray diffraction studies of hydration reaction of cement components and sulfoaluminate (C3A3) Part 1B. Aluminates mixed with different components.* Materials Science and Engineering, 1975. 17(2): p. 247-281.

28. Lerch, W., *The influence of gypsum on the hydration and properties of Portland cement pastes.* Proceedings of the American Society for Testing and Materials 1946. 46.

29. Minard, H., *Etude intégrée des processus d'hydratation, de coagulation, de rigidification et de prise pour un système C3S-C3A-sulfates-alcalins.* Thèse de Doctorat, Université de Bourgogne, 2003.

30. Di Murro, H., *Mécanismes d'élaboration de la microstructure des bétons.* Thèse de Doctorat, Université de Bourgogne, 2007.

31. Richardson, I.G., *The nature of C-S-H in hardened cements.* Cement and Concrete Research, 1999. 29: p. 1131 -1147.

32. Costoya, M., *Synthesis and Hydration Mechanism Study of Tricalcium Silicate* Thèse de Doctorat, Ecole Polytechnique Fédérale de Lausanne, 2008.

33. Hadley, D.W., *The nature of the paste aggregate interface.* Ph.D. Thesis, Purdue University, 1972.

34. Hadley, D.W., W.L. Dolch, and S. Diamond, *On the occurrence of hollow-shell hydration grains in hydrated cement paste.* Cement and Concrete Research, 2000. 30(1): p. 1-6.

35. Gallucci, E. and K. Scrivener, *Crystallisation of calcium hydroxide in early age model and ordinary cementitious systems.* Cement and Concrete Research, 2007. 37(4): p. 492-501.

36. Scrivener, K.L. and P.L. Pratt, *Microstructural studies of the hydration of C3A and C4AF independently and in cement paste.* Proc. Brit. Ceram. Soc, 1984. 35: p. 207-219.

37. Gallucci, E., P. Mathur, and K. Scrivener, *Microstructural development of early age hydration shells around cement grains.* Cement and Concrete Research, 2010. 40(1): p. 4-13.

38. Kjellsen, K.O. and H. Justnes, *Revisiting the microstructure of hydrated tricalcium silicate--a comparison to Portland cement.* Cement and Concrete Composites, 2004. 26(8): p. 947-956.

39. Kjellsen, K.O. and B. Lagerblad, *Microstructure of tricalcium silicate and Portland cement systems at middle periods of hydration-development of Hadley grains.* Cement and Concrete Research, 2007. 37(1): p. 13-20.

40. Kocaba, V., *Development and Evaluation of Methods to Follow Microstructural Development of Cementitious Systems Including Slags.* PhD thesis, Ecole Polytechnique Fédérale de Lausanne 2009.

41. Sandberg, P. and L.R. Roberts, *Studies of Cement-Admixture Interactions Related to Aluminate Hydration Control by Isothermal Calorimetry,.* Seventh CANMET/ACI International Conference on Superplasticizers and Other Chemical Admixtures in Concrete, SP-217, 2003.

42. Dunant, C., *Internal communication, LMC* 2009.

43. Bizzozero, J., *Dimentional stability of calcium aluminate and sulfoaluminate systems.* Master Thesis, Ecole Polytechnique Fédérale de Lausanne 2010.

44. Chowaniec, O., *Internal communication, LMC* 2010.

CHAPTER 5   CONCLUSIONS AND PERSPECTIVES

The aim of this thesis was to get insight into the hydration reaction of C_3A – gypsum systems alone and in the presence of alite.

5.1 C_3A- gypsum systems

The role of the specific surface area of C_3A as well as the high activation energies calculated for the C_3A-gypsum reaction during the first stage of the reaction suggest that this reaction is surface controlled. These results are in agreement with the findings of Minard et al. [1] that show that the dissolution of C_3A is the rate controlling mechanisms during the first stage of the reaction when sulfate ions are present in solution.

New results were obtained on the second stage of the reaction, when gypsum is depleted.

- It was shown that the dissolution of C_3A and ettringite to form monosulfoaluminate is a rapid reaction that takes place right after the depletion of gypsum. This means that ettringite is not stable rapidly after the depletion of gypsum.
- The second stage of the reaction is characterized by a sharp exothermic peak on the heat evolution profile. The acceleration of the reaction rate was shown to be highly influenced by the exposed surface area of the reacting C_3A particles (which depends on the specific surface area of the C_3A but also on the amount of hydrates that fill the space). The activation energy calculated for the second stage of the reaction are coherent with surface controlled reaction. The deceleration period was shown to be controlled by a space filling effect due to impingement of the AFm platelets. The different deceleration rates observed for different gypsum additions are coherent with the different morphologies of the AFm platelets depending on the gypsum content. Longer AFm platelets, which imply a faster deceleration rate, were observed for samples with lower gypsum additions.
- This study also shows that the chemical composition of the AFm phases that precipitate depends on the gypsum content of the original mix. All the solid solution series (with miscibility gap) between hydroxy-AFm and monosulfoaluminate can form.

- Hydrogarnet was observed at later ages in some systems. This phase precipitated at the original grain boundaries as a rim around the hydrating C_3A grain.

- Finally the formation of a dense hydrate within the C_3A grain boundaries was observed. The presence of this hydrate, which composition is close to the one of the AFm platelets that form in the matrix, becomes less obvious at later ages. A re-crystallization as matrix hydrate or hydrogarnet is hypothesized.

5.2 C_3A- gypsum hydration in the presence of alite

When C_3A-gypsum hydration occurs in the presence of alite, some of the features observed in plain C_3A-gypsum system are subject to change.

- The heat evolution profile of C_3A-gypsum reaction is significantly modified in the presence of alite. Three exothermic peaks that can be attributed to the aluminate reaction could be observed instead of one in C_3A-gypsum systems. This multiplication of the peaks was attributed to the fact that C_3A and ettringite do not dissolve simultaneously and to the reduction of the space available for the reaction due to the presence of C-S-H and CH.

- The dissolution of C_3A and ettringite after the depletion of gypsum occur at slower rate compare to C_3A-gypsum systems. Moreover these dissolutions do not occur simultaneously. This work clearly shows that while C_3A starts to dissolve right after the depletion of gypsum, ettringite continues to form during a few hours. This second formation of ettringite is due to the reaction of C_3A with the sulfate ions that were adsorbed on C-S-H. The analysis of the chemical composition of C-S-H at different ages showed that some of the sulfate ions adsorbed on C-S-H at early ages can be released to form more ettringite after the depletion of gypsum. The shoulder observed on the alite calorimetric peak is associated with this phenomenon.

- As in C_3A-gypsum systems, ettringite is the main aluminate hydrate that forms when sulfate ions are still available and AFm phases (hydroxy-AFm and/or monosulfoaluminate) form afterwards. The morphology of the AFm platelets was also observed to be related to the original gypsum content even though the differences were less pronounced that in C_3A-gypsum systems probably because the space filling is more dominated by the alite products.

- The formation of a dense inner calcium sulfo aluminate product in the presence of alite was less obvious that in C_3A-gypsum systems observed and it was observed only for monophase systems where the aluminate hydrates preferentially form around C_3A grains. Hydrogarnet rims were never observed, even after 28 days of hydration.

- Even though several changes in the hydration kinetics were observed between the C3A-gypsum and the multi-phase systems, this study showed that the fundamental mechanisms of the reaction are unchanged. The same phases are formed and similar activation energies were calculated for the reactions in pure and in multiphase systems

5.3 Effect of the presence of C$_3$A- gypsum on alite hydration

Although alite is the major phase, its hydration kinetics is also modified when hydration occurs in the presence of C$_3$A-gypsum. Depending on the undersulfated or properly sulfated nature of the systems different effects were observed.

- For undersulfated systems, when the aluminate reaction occurs before the alite one, this last reaction is slowed down during the C-S-H growth period compared to the hydration of alite in single phase system.

- In the case of properly sulfated cements the kinetics of alite hydration in the same period is accelerated. A similar acceleration was observed in alite-gypsum systems. Therefore it is hypothesized that the absorption of sulfate ions on C-S-H is responsible for the modification of the kinetics during the nucleation and growth period.

5.4 Perspectives

Concerning C$_3$A- calcium sulfate systems, only the hydration of C$_3$A with gypsum was studied in the present work. As in Portland cement other sulfate sources are present, future works should investigate C$_3$A- hemihydrate and C$_3$A-gypsum-hemihydrate systems. Pourchet et al. showed that the early hydration kinetics of C$_3$A – calcium sulfate is modified depending on the sulfate type added [2]. The formation of the hydrogarnet shell around C$_3$A grains was hypothesized to be related to the formation of Afm phases in the very early ages. As this occurs only in the presence of gypsum[2], the study of the microstructural development of C$_3$A-hemihydrate systems could be therefore of interest.

The role of calcium sulfate on alite hydration was only little investigated in the present study. As understanding the phenomenon of "the optimum gypsum content" is of great interest especially for the development of new ^mix designs, a more complete study on this subject should be considered.

In this thesis, alite-C$_3$A-gypsum systems were investigated. The next step of the study toward real systems should include alkali in the mix design as they are known to strongly influence cement

hydration [3, 4]. Their role on the hydration kinetics and the microstructural development of alite and C_3A-gypsum as well as alite-C_3A-gypsum systems could be another field of major interest.

Finally, investigations of the influence of belite and ferrite phases on the early hydration of alite-C_3A-gypsum systems should be considered.

References

1. Minard, H., *Etude intégrée des processus d'hydratation, de coagulation, de rigidification et de prise pour un système C3S-C3A-sulfates-alcalins.* Thèse de Doctorat, Université de Bourgogne, 2003.

2. Pourchet, S., et al., *Early C3A hydration in the presence of different kinds of calcium sulfate.* Cement and Concrete Research, 2009. 39(11): p. 989-996.

3. Lerch, W., *The influence of gypsum on the hydration and properties of Portland cement pastes.* Proceedings of the American Society for Testing and Materials 1946. 46.

4. Taylor, H.F.W., *Cement Chemistry 2nd edition*. Thomas Telford ed. 1997.

Merci d'avoir eu la patience et le courage de lire jusqu'ici !

AQ

ANNEXE 1 REFERENCES OF THE RAW MATERIALS USED FOR POWDER SYNTHESIS

Table A: References of the raw materials used for powder synthesis

Product	Supplier	Name of the product	Reference number
$CaCO_3$	Merck	Calcium Carbonate pour analyse Reag. Ph Eur (1kg)	1.02066.1000
SiO_2	Merck	Silicon dioxide (5kg)	1.13126.5000
Al_2O_3	Merck	Aluminium Oxide anhydrous (1kg)	1.01095.1000
MgO	Merck	Magnesium oxide (100g)	1.05866.0100
Gypsum	Merck	Calcium sulfate dihydrate 500g	1.02161.0500

A2

Curriculum vitae as of April 2011

Alexandra QUENNOZ   17.11.1982
e-mail : alexandra.quennoz@a3.epfl.ch   Swiss citizenship

EDUCATION

2007-2011: **PhD in Material Science and Engineering**, Ecole Polytechnique Fédérale de Lausanne (EPFL), Switzerland.
- PhD thesis on cement hydration under the supervision of Prof. Karen L. Scrivener (Laboratory of Construction Materials) and supported by the Swiss National Science Foundation.

2005-2007 : **MSc in Material Science and Engineering**, specialization in Structures Energy and Transports, Ecole Polytechnique Fédérale de Lausanne (EPFL), Switzerland
- Master thesis on supplementary cementitious materials, in collaboration with the Universidad Central Las Villas, Cuba.
- Semester projects on nanoparticles for bio/medical applications and composite materials for sport applications.

2002-2005: **BSc in Material Science and Engineering,** Ecole Polytechnique Fédérale de Lausanne (EPFL), Switzerland

1998-2002: **Maturité avec mention**, specialization in Physics and Applied Mathematics, Collège Claparède, Geneva, Switzerland

RESEARCH EXPERIENCE AND TECHNICAL COMPETENCES

Cement hydration: kinetics and microstructural development. Supplementary cementitious materials. Powder synthesis and characterization. Mechanical testing. Scanning and Transmission Electron Microscopy (SEM/TEM): sample preparation and analysis, Energy Dispersive Spectroscopy (EDS), X-ray Diffraction (XRD), Thermogravimetrical Analysis (TGA), Isothermal Calorimetry, Granulometry Laser Analysis

WORK EXPERIENCE

2007-present: **Research assistant** in the Laboratory of Construction Materials, EPFL, Switzerland
- Supervisor for semester projects for undergraduate and graduate students
- Responsible for demonstrating laboratory work to undergraduate students
- Representative teaching assistant at the Teaching Commission of the Material Science and Engineering section

2005 (5 weeks): **Student assistant** in the Laboratory of Construction Materials, EPFL, Switzerland
- Worked on an assigned project: sample preparation for electron microscopy, image analysis

2005 (4 weeks): **Intern at Bobst SA** Département de Mesures et Analyses, Mex, Switzerland
- Worked on an assigned project: mechanical testing of a composite part

LANGUAGES

French: mother tongue
Italian: mother tongue
English: good knowledge in both speaking and writing
German: level A1-A2

SPECIAL INTERESTS

Hiking, running, skiing

PUBLICATIONS

Reviewed conference papers with talk

A.Quennoz, E.Gallucci, K.L.Scrivener, Calcium silicate – calcium aluminate interactions and their influence on cement early hydration, 13th International Congress on the Chemistry of Cement, Madrid, July 2011 (accepted)

Non-reviewed conference papers with talk

A.Quennoz and K.L.Scrivener, *Influence of the gypsum content on the phase assemblage and microstructure of tricalcium aluminate – gypsum pastes*, 30th Cement and Concrete Science, University of Birmingham, September 2010

A.Quennoz, E.Gallucci, C. F.Dunant, K. L.Scrivener, *Decoupling method for heat evolution curves of model cements - Influence of the presence of C3A-gypsum on the alite hydration*, CONMOD 2010, Lausanne, June 2010

A.Quennoz, E.Gallucci, C. F. Dunant, K. L. Scrivener, *Influence of the gypsum amount on the hydration of tricalcium aluminate in C3A-gypsum and in alite-C3A-gypsum systems,* 17.Internationale Baustofftagung, Weimar, September 2009

A.Quennoz, E.Gallucci and K.L.Scrivener, *Hydration of tricalcium aluminate and gypsum alone and in presence of alite*, 28th Cement and Concrete Science, The University of Manchester, September 2008